



**TECHNICAL UNIVERSITY OF CRETE**  
**School of Production Engineering & Management**  
**Dynamic Systems and Simulation Laboratory**

---

# **Real-time traffic control using queue estimation from connected vehicle data**

DIPLOMA THESIS

by

**Sophia Anna Alexaki**

supervisor

**Prof. Markos Papageorgiou**

---

Chania, Greece  
October, 2018

---



Approved by the following examining committee on the October 2, 2018.

Markos Papageorgiou  
Professor, School of Production Engineering and Management  
Technical University of Crete, Chania, Greece

Ioannis Papamichail  
Associate Professor, School of Production Engineering and Management  
Technical University of Crete, Chania, Greece

Anargiros Delis  
Associate Professor, School of Production Engineering and Management  
Technical University of Crete, Chania, Greece

This work is licensed under a Creative Commons Attribution-NonCommercial-ShareAlike 4.0 International license.



# Abstract

Traffic congestion is a critical societal problem that causes an increase in road traffic accidents and environmental pollution as well as waste of time. The aim of this work is to investigate whether the adoption of the new tendency of Internet of things could improve real-time traffic control with the involvement of connected vehicles in the role of the unique detector of the traffic conditions, instead of spot sensors (e.g loop detectors, radars, video sensors etc.).

The first key point of this thesis was the implementation of an algorithm which uses a mathematical approach that achieves real-time queue estimation (in vehicles) in every link of an urban road network, based on connected vehicle measurements. Then, the algorithm was integrated into two real-time traffic control strategies, the Max-pressure algorithm (decentralized control) and the TUC strategy (centralized control) to investigate whether the information from connected vehicles can be considered reliable; and to what extent the percentage of connected vehicles influences this reliability. In order to draw conclusions, the AIMSUN microscopic simulator was used for the urban network of Chania.

Statistical analysis of simulation investigations results showed that the estimation approach leads to reliable queue estimation for all penetration rates tested. Furthermore, as far as it concerns control strategies performance after the integration of connected vehicle approach; it turned out that TUC strategy could work efficiently by taking information from connected vehicles while Max-pressure algorithm which uses second by second measurements to take second by second decisions cannot work properly for low penetration rates of connected vehicles because of the limited real-time information.



# Acknowledgements

The completion of this thesis would not have been possible without the time, support and dedication of the people involved from the beginning of my undergraduate life.

First of all, I would like to express my sincere gratitude to my supervisor Prof. Markos Papageorgiou for the opportunity he gave me to study the field of traffic management, for sharing with me his immense knowledge in this field and for his valuable guidance during the planning and development of this research work. Moreover, I am thankful to Prof. Ioannis Papamichail and Doc. Manolis Diamantis for their constant help and support during the development of this research work. I would also like to thank Prof. Anargiros Delis for being member of my thesis committee.

Special thanks to my labmates and especially Typaldos Panagiotis for their willingness to offer me their help and for the beautiful moments and discussions we had the past year. My tremendous gratitude goes to my family for their love and support in all areas, but mainly for encouraging me to discover and follow my dreams.

Last but not least, I would like to thank my friends and all the people who stood by me, filling these years with beautiful moments and inspiring me to improve myself.

*To my beloved mother, my first and most faithful supporter.*

Sophia Anna Alexaki,

Chania, October 2, 2018



# Contents

<b>1</b>	<b>Introduction</b>	<b>7</b>
1.1	Mobility and Traffic Control Systems . . . . .	7
1.2	Intelligent Transportation Systems and Adaptive Traffic Control Systems . . . . .	8
1.3	Connected Vehicles . . . . .	8
<b>2</b>	<b>Urban Traffic Control Features</b>	<b>10</b>
2.1	The Necessity of Traffic Control . . . . .	10
2.2	Urban Traffic Control Notions and Ways . . . . .	12
<b>3</b>	<b>Real-Time Traffic Control Strategies</b>	<b>14</b>
3.1	Centralized and Decentralized Control Structures . . . . .	14
3.2	Adaptive Traffic Control Strategies . . . . .	15
3.3	Max-Pressure Algorithm . . . . .	15
3.3.1	Max-Pressure Introduction . . . . .	15
3.3.2	Max-Pressure Mathematical Formulation . . . . .	16
3.4	TUC Strategy . . . . .	17
3.4.1	TUC Introduction . . . . .	17
3.4.2	Split Control Mathematical Formulation . . . . .	18
3.4.3	Cycle Control Mathematical Formulation . . . . .	19
<b>4</b>	<b>Real-Time Queue Estimation</b>	<b>21</b>
4.1	Real-Time Estimation of Traffic State . . . . .	21
4.2	Detector Scenario . . . . .	22
4.2.1	Max-Pressure Algorithm . . . . .	22
4.2.2	TUC Strategy . . . . .	22
4.3	Connected Vehicle Scenario . . . . .	23
<b>5</b>	<b>Simulation Environment</b>	<b>28</b>
5.1	Simulation Environment . . . . .	28
<b>6</b>	<b>Queue Estimation Results</b>	<b>32</b>
6.1	Characteristics and Assumptions . . . . .	32
6.2	Parameter Calibration . . . . .	33
6.3	Statistical Evaluation . . . . .	38
6.3.1	Estimation of the Queue Tail Location . . . . .	38
6.3.2	Estimation of Link Vehicle Accumulation Downstream of Queue Tail . . . . .	44

<b>7</b>	<b>Control Strategies Results</b>	<b>54</b>
7.1	Introduction . . . . .	54
7.2	TUC Strategy . . . . .	54
7.3	Max-Pressure Algorithm . . . . .	57
7.4	Strategies Comparison . . . . .	60
<b>8</b>	<b>Epilogue</b>	<b>61</b>
8.1	Conclusions . . . . .	61
8.1.1	Conclusions for Chapter 6 . . . . .	61
8.1.2	Conclusions for Chapter 7 . . . . .	61
8.2	Future Work . . . . .	62
	<b>Bibliography</b>	<b>63</b>
	<b>Appendix A</b>	<b>66</b>
	<b>Appendix B</b>	<b>107</b>

# Chapter 1

## Introduction

### 1.1 Mobility and Traffic Control Systems

Since the beginning of the human species and during its evolution and organization in social clusters, land transport has been a vital factor for its survival, the extension of its domination to the earth, but also for the improvement of quality life he seeks. People with the purpose of transporting goods and moving their own have created a whole transport technology industry that began with the discovery of the wheel (Mesopotamia 3500 BC) and continues to advance up to today, reaching the creation of autonomous vehicles.

Since the second half of the previous century population growth and trade globalization have created the need for more, denser urban centers and interconnections through road networks. At the same time, the rapid technological progress of the automotive industry has triggered an increase in the supply and demand of private means of transport developing a chaotic and complex transport network, which requires regulatory factors of high know-how and complexity in order to be functional.

Traffic control, consists the supervision of the movement of people, goods, or vehicles to ensure efficiency and safety [1]. Some of the most common traffic control system components are operational procedures, rules and laws, and physical devices (e.g. signs, markings, and traffic lights). As the above definition denotes, the crucial part of traffic control is to ensure the efficiency of mobility around different networks in a way witch diminish accidents. Although a traffic control process must be designed in a way that respects its crucial purposes, its efficiency depends not only on the proper design but also on operators compliance and right decision making.

The first attempts to regulate traffic with traffic lights, before traffic was regulated by the police, dates back to December 1868 in London with the first manually operated traffic light. In 1912, a traffic control device was placed on the top of a Paris tower on the Rue Montmartre and Grande Boulevard, which also operated manually. In the same year, Lester Wire, a police officer in Salt Lake City invented the first electric lights while the first interconnected traffic system was installed in 1917 in Salt Lake City, with six connected intersections controlled simultaneously from a manual switch. Some years later, in March 1922 the automatic control of interconnected traffic lights (via automatic timers) operated in Houston, Texas. Over the course of time and the evolution of computers and communication systems, traffic control has also evolved, resulting in the operation of computerized traffic control systems that began in the 1950s and prevail to the present [2].

## 1.2 Intelligent Transportation Systems and Adaptive Traffic Control Systems

ITS (Intelligent Transportation Systems) has been developed since the early 1970s, constituting a global technological trend that establishes a fully effective real-time and accurate information management system. Intelligent Transportation Systems (ITS) is a broad range of diverse technologies applied to transportation to make systems safer, more efficient, more reliable and more environmentally friendly, without necessarily having to physically alter existing infrastructure [3]. The range of technologies involved includes sensor and control technologies, communications, and computer informatics and cuts across disciplines such as transportation, engineering, telecommunications, computer science, finance, electronic commerce and automobile manufacturing.

In many cases, ITS have evolved into Adaptive Traffic Control Systems (ATCS) that employ actuated control through the use of detection and surveillance devices over a central communications network. The primary objectives of ATCS are to adjust traffic signal patterns to meet estimated traffic demand, communicate vital information to traffic engineers and motorists and respond to traffic congestion resulting from crashes or backups [4].

Information technology plays a critical role in efficiency of Adaptive Traffic Control Systems. Generally, real-time traffic information comes from point sensors or Global Positioning System (GPS) receivers. Spot sensors such as loop detectors, radars, video sensors, magnetometers etc. allow the extraction of accurate real-time information of the traffic state. However the information they provide is only point-based information on traffic conditions, which does not represent the total reflection of a traffic state and in order to be more accurate about the realistic measures (such as the speed) over a link of a network, a large quantity of sensors must be installed. Nevertheless the installation of many spot sensors is not practical due to high costs of installation and maintenance [5].

## 1.3 Connected Vehicles

Nowadays most vehicles have built-in GPS or GPS devices, allowing IoT technology to contribute to signal traffic control. Back in 1999 the British technology expert Kevin Ashton introduced the term “Internet of Things” (IoT) to illustrate the function of a system in which different physical objects could be connected to the Internet by sensors. Therefore “Internet of Things” (IoT) is not a new tendency, companies have been using sensors and networks in order to provide a steady stream of information about where devices are, how they’re being used, their condition, and the state of their environment for more than 20 years [6].

In our days, IoT has become very popular due to specific factors such as progress in the field of mining and data analysis and the economic way of disseminating data. On the one hand, the development of many ways to store and process large volumes of data such as cloud and the amelioration of techniques to analyze these data allows the data to be well exploited. On the other hand the extensive technological progress in mobile devices and applications and the broad availability of wireless connectivity permit us to spread data information easily and without significant cost [6]. As a

result of all the above, Internet of things is extremely convenient and efficient in practice.

The IoT has a great impact on transportation field in many ways. Internet of things application extends to the vehicle, the infrastructure and to the driver, via dynamic interaction of all these components of a transport system, achieving inter and intra vehicular communication, smart traffic control, smart parking, electronic toll collection systems, logistic and fleet management, vehicle control as well as safety and road assistance. As far as it concerns the traffic management, IoT via “connected vehicles” may be the key of progress on the upcoming traffic signal control. The common use of point detectors for real-time traffic control, permits the identification of vehicles at specific locations, as a result significant measures which act as parameters on traffic signal control algorithms can only be estimated or completely unknown. With connected vehicles, signal systems would be able to use data transmitted wirelessly from in-vehicle sensors in equipped vehicles to the signal controller, overcoming the problem of getting limited information about measures significant for real-time traffic control strategies, such as vehicle speeds, positions, arrival rates, rates of acceleration and deceleration, queue lengths, and stopped time.

# Chapter 2

## Urban Traffic Control Features

### 2.1 The Necessity of Traffic Control

From the second half of last century, the phenomenon of traffic congestion is well identified. The sharp augmentation of mobility needs has led to the maximization of vehicles in networks. Traffic congestion appears when too many vehicles attempt to use a common transportation infrastructure with limited capacity. In the best case, traffic congestion leads to queuing phenomena (and corresponding delays) while the infrastructure capacity (“the server”) is fully utilized. When a network presents this kind of traffic state, we refer to under-saturated conditions. In the worst (and far more typical) case, traffic congestion leads to a degraded use of the available infrastructure (reduced throughput). An over-saturated link prevents the traffic movements at the upstream intersection to cross, even though they have the right of way (green signal). This is a waste of resources (waste of green time) that contributes to an accelerated increase of congestion due to vehicles trapped in the upstream links, which leads to blocking of further upstream intersections, increased waste of green time, and so forth. This vicious circle frequently leads to gridlocks in network cycles with devastating effects for the traffic flow in extended urban areas. Although traffic congestion is triggered by the sharp increase in demand on an urban network, the inefficient traffic control process may extend this phenomenon, so it is necessary for traffic control strategies to act properly and to prevent the downgrading of the network and the infrastructure [7].

The traffic congestion causes excessive time delays, high fuel costs and a significant environmental burden. Therefore, it is important the existence of efficient traffic control both on urban roads and on motorways (in Greece the problem is mainly in urban networks) in order to achieve the optimal way of human and goods mobility saving time and money, avoiding environmental pollution and ensuring safety in the network. The efficiency of traffic control depends on the quality of the employed control methodologies, so the development of reliable traffic control strategies is a major social need and requires great responsibility.

The figure below illustrates the control loop, which identifies the traffic control process and the interconnection of the elements involved. The next paragraph tries to figure out the main flow of the control loop, which is presented at Figure 2.1, [8].

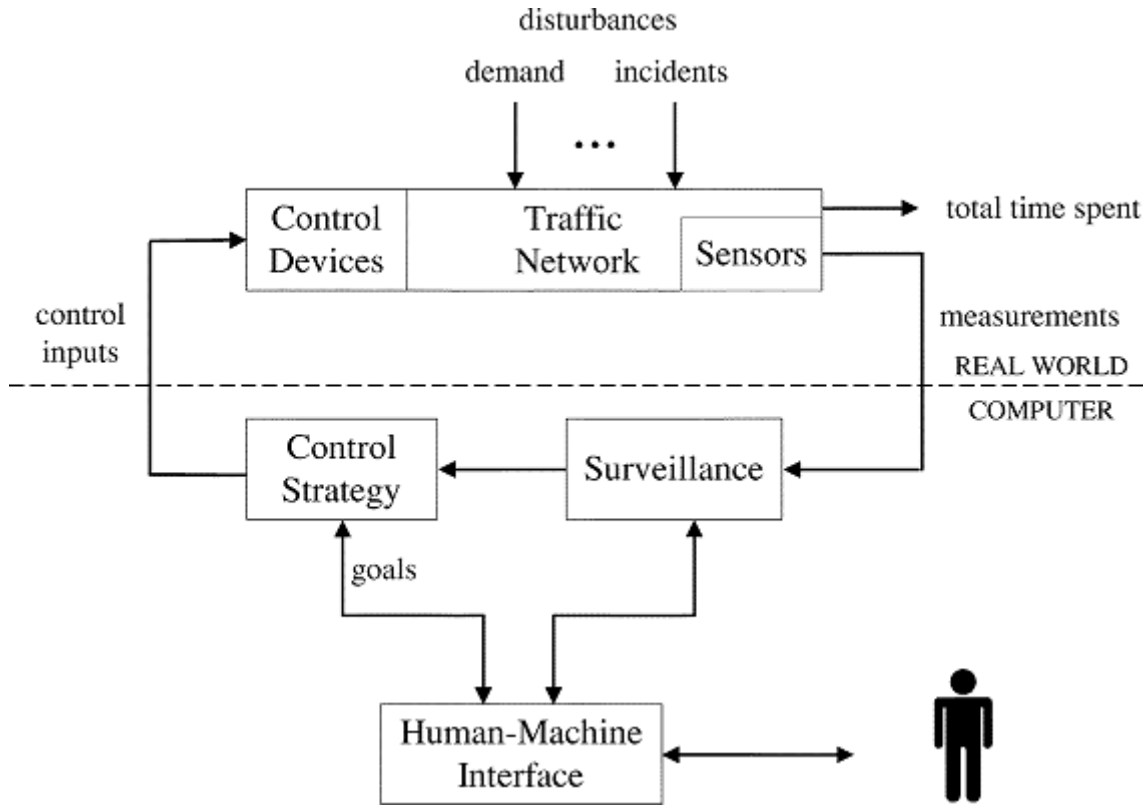


Figure 2.1: The traffic control loop

A traffic network is characterized by some independent measures, called disturbances such as the demand or the incidents, which may possibly be measurable (e.g. demand), detectable (e.g. incident) or predictable over a future time horizon. Disturbances is the first input information we need to know in order to design a control strategy. The next necessary input information is real world measurements about vehicles significant measures such as the average speed or vehicle position. This kind of information may be obtained by sensors or in our case study by connected vehicles. In the case of measurements coming from sensors, the next important stage of control loop is surveillance. The task of the surveillance is to enhance and to extend the information provided by suitable sensors (e.g. inductive loop detectors) as required by the subsequent control strategy and the human operators [7]. In an automatic control system, after the important input information is selected and evaluated, it is integrated in the control strategy algorithms. Obviously, the control strategy is the principal part of control loop which provide control devices e.g. the traffic lights, with the suitable information of orders or control inputs, such as the green times for all the stages of all intersections. In case control strategy is not practiced by algorithms but by a human operator, we have a manual control system. The most common indexes of performance of the control loop are the total time spent by all vehicles in the network, the mean delay, the mean density or even the mean speed measured in the network over a time horizon. Summarily, the kernel of the control loop is the control strategy, whose task is to specify in real-time the control inputs, based on available measurements, estimations and predictions, so as to achieve the prespecified goals (e.g. minimization of total time spent) despite the influence of various disturbances [7].

## 2.2 Urban Traffic Control Notions and Ways

Nowadays, traffic lights at intersections consist the main tool of traffic control in urban networks, pursuing safety and optimal network operation. Below are some definitions of basic features of urban traffic control [7].

- An intersection consists of a number of approaches and the crossing area.
- An approach may have one or more lanes but has a unique, independent queue. Approaches are used by corresponding traffic streams (veh/h).
- Traffic Capacity is the maximum sustainable flow rate at which vehicles reasonably can be expected to traverse a point or uniform segment of a lane or roadway during a specified time period under given roadway, geometric, traffic, environmental, and control conditions; usually expressed as vehicles per hour.
- A saturation flow is the average flow crossing the stop line of an approach when the corresponding stream has right of way (r.o.w.), the upstream demand (or the waiting queue) is sufficiently large, and the downstream links are not blocked by queues.
- Compatible streams are two streams which can safely cross the intersection simultaneously else they are called antagonistic.
- A signal cycle is one repetition of the basic series of signal combinations at an intersection; its duration is called cycle time.
- A stage (or phase) is a part of the signal cycle, during which one set of streams has r.o.w.
- Constant lost (or inter-green) times of a few seconds are necessary between stages to avoid interference between antagonistic streams of consecutive stages

There are four factors that can be appropriately regulated in a traffic control strategy.

- Stage specification: For complex intersections involving a large number of streams, the specification of the optimal number and constitution of stages is a nontrivial task that can have a major impact on intersection capacity and efficiency.
- Split: This is the relative green duration of each stage (as a portion of the cycle time) that should be optimized according to the demand of the involved streams.
- Cycle time: Longer cycle times typically increase the intersection capacity because the proportion of the constant lost times becomes accordingly smaller; on the other hand, longer cycle times may increase vehicle delays in under-saturated intersections due to longer waiting times during the red phase.

- Offset: This is the phase difference between cycles for successive intersections that may give rise to a “green wave” along an arterial; clearly, the specification of offset should ideally take into account the possible existence of vehicle queues.

There are many performance criteria in order to evaluate traffic control strategies (e.g. total travel time, delay, density), in this work it was used criteria of delay and density.

- Delay: The average additional travel time experienced by a vehicle with reference to a base travel time (in this work, the free-flow travel time) per unit distance. It is measured in sec/km.
- Density: The average number of vehicles that occupy one kilometer of road space, expressed in vehicles per kilometer.

Control strategies employed for road traffic control may be classified according to the following characteristics: the collection time of control measurements and the width of the application space. Therefore, on the criterion of the time range of input measurement collection, we consider the fixed-time strategies and traffic-responsive strategies. The fixed-time strategies are derived off-line by use of appropriate optimization codes based on historical constant demands and turning rates for each stream for a given time of day (e.g. morning peak hour). Unlike previous category of strategies, traffic-responsive strategies make use of real-time measurements (typically one or two inductive loops per link) to calculate in real-time the suitable signal settings. As far as it concerns the space of application of traffic control strategy, we consider that isolated or decentralized strategies are applicable to single intersections while coordinated or centralized strategies consider an urban zone or even a whole network comprising many intersections [7].

# Chapter 3

## Real-Time Traffic Control Strategies

### 3.1 Centralized and Decentralized Control Structures

In general, a global or centralized control problem can be viewed as a simple level and simple objective method [9]. By simple level, it is meant that there is a complete system and a single controller. By simple objective, it is meant that the controller computes all the control inputs in a single optimization problem. This framework may also be extended to include systems that have many subsystems and then the control action for each such subsystem depends entirely on the centralized controller [10].

Although the centralized control is suitable for small-scale systems resulting in global system performance, when considering large-scale systems such as transport networks and traffic networks, a centralized control structure results in high computational requirements and increasing communication overhead as it has to collect all the inputs distributed across the large system and generate control actions for the whole system. An other disadvantage of centralized control is that it lacks scalability. Furthermore, in case of failures in the system, this structure offers no graceful degradation. Many times the difficulties resulting from a centralized approach can be overcome considering decentralized control schemes for controlling large-scale systems.

In decentralized control, the global control is distributed across many independent, loosely coupled subsystems. The local controller computes the control inputs using local measurements and optimizes local dynamics. In this control structure, the decomposition of system leads to simpler controller structures. By using local controllers, the computational burden, data gathering, and storage requirements are much lower. When local controllers do not have any conflicting actions, we can combine the series of local solutions to obtain an overall solution. However, in practice, independence among the local controllers is unrealistic and thus the resulting global solution will be sub-optimal [10].

## 3.2 Adaptive Traffic Control Strategies

Over the years the design of adaptive signal systems has received considerable attention and development. The first traffic responsive urban network control strategies were introduced in the 1980s with the first field implementations of the British SCOOT [11], and the Australian SCATS [12]. These well known and widely used traffic responsive control systems are based on heuristic optimization algorithms [13]. Both SCOOT and SCATS decide on incremental changes of splits, offsets, and cycles based on real time measurements [14].

Other optimization methods are OPAC [15], PRODYN [16] and RHODES [17], which are all based on dynamic programming and the rolling-horizon optimization scheme [13]. These strategies do not consider explicitly splits, offsets and cycles. They formulate the traffic-responsive urban control problem as a combinatorial optimization problem, and they employ exponential complexity algorithms to solve for a global minimum [14]. Furthermore an other advanced model-based strategy is CRONOS [18]. Like the other mentioned optimization methods, CRONOS does not consider explicitly splits, offsets and cycles, but unlike them, it employs a heuristic global optimization method with polynomial complexity which allows for simultaneous consideration of several junctions, albeit for the price of specifying a local minimum [14]. In addition, TUC system, see Section 3.4, has been successfully implemented in several large networks in Europe and South America [13].

All the aforementioned systems have a centralized nature; in order to apply one of these systems, the information from all intersections must be collected and transmitted to a central location (i.e. Traffic Management Center). However there are also local controllers as Max-pressure algorithm, see Section 3.3, which are much easier to implement as they only use the measurements around a certain area of interest [13].

## 3.3 Max-Pressure Algorithm

### 3.3.1 Max-Pressure Introduction

The Max-pressure controller is a decentralized algorithm which stems from communication network control and considers signal control as a resource allocation problem. The algorithm achieves to stabilize the network and maximize its throughput within a real time traffic control process. More specifically, vehicles are considered customers served by a specific number of servers. Servers can not function at the same time as they represent the different stages of a junction. The main purpose is to schedule server activation to maximize the number of served clients and therefore the performance of the system.

Some parameters and conditions of a signalized network differ from those of a telecommunication system, so the original algorithm has been modified to be operationally implemented. More specifically, some modifications are due to the fact that in a signalized junction switching from a stage to the next causes inter-stage lost times, hence too frequent switching should be avoided. Further possible differences include the fixed stage sequence, as well as the existence of upper and lower bounds for the stage duration in signal control systems [19].

The basic model of Max-pressure algorithm demands information about the mean

turn ratios and saturation rates and local information about the queues on each intersection. In contrast to other predictive control models the Max-pressure algorithm does not depend on any knowledge of mean current or future demands, the demand has only to be in certain limits. Different variations of Max-pressure basic method can be applied depending on the appropriate infrastructure [13].

### 3.3.2 Max-Pressure Mathematical Formulation

In all different variations of Max-pressure so as the one implemented in this work, the control variables are the effective green time  $g_{n,j}(k_n)$  of each stage  $j$  of all intersections  $n$  of the urban network, where  $k_n = 0, 1, 2 \dots$  is the control discrete-time index. Max-pressure algorithm's main function is to determine the effective green of every stage at all intersection in a way that stabilize the network. The algorithm in order to decide the effective green for each stage attaches a pressure in every stage of every node, giving priority on the stage with the maximum pressure.

The formulation adopted here is proposed in [19] and it is based on the approach proposed in [13] with some modifications that have proved to be beneficial for the algorithm application at Chania urban network. In particular, this version of the algorithm fully respects the predetermined sequence of stages to avoid confusion of the driver as well as the minimum and maximum allowable green time limits (3.1). At this version of the algorithm we assume no standard signal cycle, with other words the signal cycle is developed dynamically after the application of Max-pressure. To apply the algorithm, the pressure of each junction approach must first be calculated (3.2). The principal parameter that determines the pressure can be either the current queue in vehicles or the current number of vehicles in the corresponding link. In this application of the algorithm, the pressure of each approach depends to the expected queues in vehicles, which are normalized in relation to the storage capacity of the approach (first term of Equation (3.2)). To avoid waste of green time due to potential downstream blockage caused by queue spillovers at output links, if in output links the queue is high enough the approach pressures are reduced by an amount equal to a percentage of the pressure of the output links (second term of Equation (3.2)) In our case if the pressure of an output link is more than 0.85 (which means 85 % occupancy) we reduce the pressure of the current link by 10% of this downstream pressure. Finally, the pressure of each signal stage is calculated as the sum of the pressures of all approaches that receive right of way during this stage, and the resulting stage pressures are used to make a control decision (3.3). The next paragraph presents all the above in a mathematical way.

The urban network is represented as directed graph with links  $z \in Z$  and nodes  $n \in N$ . For each signalized intersection  $n$ , the sets of incoming approaches  $In$  and outgoing  $On$  links are defined. The signal control plan of node  $n$  is based on a fixed number of stages that belong to the set  $F_n$ , wherein  $u_j$  denotes the set of links that receive right of way at stage  $j \in F_n$ . The basic equations of the algorithm are shown below. The first one represents the constraint about minimum and maximum limits of allowable green time,

$$g_{n,j,min} \leq g_{n,j}(k_n) \leq g_{n,j,max}, \quad j \in F_n \quad (3.1)$$

while the second one represents the pressure of incoming links of each node during the control cycle  $k_n$ , under the condition of maximum output links pressure.

$$p_z(k_n) = \begin{cases} \left\lceil \frac{x_z(k_n)}{x_{z,max}} 0.1 \sum_{w \in 0_n} \frac{\beta_{z,w} x_w(k_n)}{x_{w,max}} \right\rceil S_z, & \text{if } p_w(k_n) \geq 0.85 \\ \left\lceil \frac{x_z(k_n)}{x_{z,max}} \right\rceil S_z, & \text{otherwise} \end{cases} \quad (3.2)$$

where  $z \in I_n$ ,  $x_{z,max}$  is the storage capacity of incoming link  $z$  (in vehicles),  $x_z(k_n)$  is the queue length of link  $z$  during the control cycle  $k_n$ ,  $\beta_{z,w}$  is the turning movement rates  $S_z$  is the saturation flow of link  $z$ ,  $x_{w,max}$  is the storage capacity of outgoing link  $w$  (in vehicles) and  $x_w(k_n)$  is the queue length of outgoing link  $w$  during the control cycle  $k_n$ . Finally, last equations represent the pressure of each signal stage  $j$  of each intersection,

$$P_{n_j}(k_n) = \max \left\{ 0, \sum_{z \in u_j} p_z(k_n) \right\}, \quad j \in F_n \quad (3.3)$$

where the term  $\sum_{z \in u_j} p_z(k_n)$  refers to the sum of pressures of all incoming links of node  $n$  [13].

In this work, the algorithm uses as input information 1 second time-step measurements of expected queues, in vehicles. The control decision concerns either a short extension, 2 seconds, of the current active stage or the activation of the next step of the sequence. However, extension of the current active stage is only granted if the current green time does not exceed its maximum permissible value, while at the same time, either it has been found to be the maximum-pressure stage, or its initial calculated pressure (at the beginning of the stage activation) has not decreased more than a predetermined percentage (e.g. 35%). This latter condition is used to avoid frequent step changes that contribute to the unnecessary increase in delay due to lost times between stages. In case an active stage is not extended, the next stage is activated at its minimum permissible green time. Then the whole process is repeated so that a new control decision is taken, in order to make a new control active stage or after the minimum green time of the next stage, whichever has been decided [19].

## 3.4 TUC Strategy

### 3.4.1 TUC Introduction

The traffic-responsive urban control (TUC) strategy, was developed by Diakaki, Papageorgiou and McLean, in 1999 as part of an integrated traffic control system for corridor networks within the European Telematics Applications in Transport project TABASCO (Telematics Applications in BAvaria, SCotland, and Others) [14].

The strategy is based on a store-and-forward modelling of the urban network traffic proposed by Gazis and Potts in 1963, and the linear-quadratic (LQ) regulator methodology. TUC approach designs (off-line) and employs (on-line) a multi-variable regulator for the traffic-responsive co-ordinated urban network control in a systematic and generic way [14].

Although traffic-responsive urban network control strategies have been introduced since 1980s, most of them are not suitable for saturated traffic conditions,

which are quite widespread during peak hours in modern cities, because they fail to consider the downstream traffic conditions in their real-time decision-making at individual junctions. In addition, there is generally a lack of efficient, genuinely and systematically coordinated control strategies applicable to large-scale networks. Given the above, TUC has been developed to tackle the problem of traffic-responsive network-wide signal control, particularly under saturated traffic conditions [14].

However, when demands and queuing are low, TUC's split decisions are close to the utilized fixed plans. Thus, its performance depends on the quality of these plans, which need to be the appropriate for the considered traffic load. To circumvent the need for good fixed-time plans, the hybrid variant of the TUC strategy was developed, whereby signalized junctions are controlled by a real-time Webster-type demand-driven strategy as long as traffic conditions are undersaturated; while a switching to the original TUC is effectuated when traffic conditions are close to saturation [20]. An other proposed solution to this problem is an additional actuation control at the local junction level [21]. These two methods need inflow and outflow measurements respectively. In this thesis we do not use either of them because we suppose there is no use of detectors in the network.

TUC consists of three distinct but interconnected modules [19],[22].

- Split control: The aim is the minimization of the risk of oversaturation and queue spillback, through the appropriate manipulation of the green splits at signalized junctions for given cycle times and offsets. The methodology used is based on the linear-quadratic (LQ) regulator theory of automated control.
- Cycle control: It is effectuated through a simple, feedback-based algorithm (P-Regulator) that modifies the network cycle time so as to adapt the cycle duration to the currently observed maximum saturation level in the network.
- Offset control: It is effectuated through the application of a decentralized feedback control law that modifies the offsets of the main stages of successive junctions along arterials, so as to create “green waves”, taking into account the possible existence of vehicle queues.

### 3.4.2 Split Control Mathematical Formulation

The main idea when using store-and-forward models for road traffic control is to introduce a model simplification that enables the mathematical description of the traffic flow process without use of discrete variables. This is of paramount importance because it opens the way to the application of a number of highly efficient optimization and control methods (such as linear programming, quadratic programming, nonlinear programming, and multivariable regulators) with polynomial complexity, which, on its turn, allows for coordinated control of large-scale networks in real time, even under saturated traffic conditions [7].

The basic methodology employed by TUC for split control is the formulation of the urban traffic control problem as a Linear-Quadratic (LQ) optimal control problem based on a store-and-forward type of mathematical modeling. The control objective is to minimize the risk of oversaturation and the spillback of link queues by suitably varying, in a coordinated manner, the green-phase durations of all stages at all network junctions around some nominal values without affecting neither the

offsets nor the cycle times. The LQ-approach leads in a straightforward way to the following multivariable control law [22]

$$g(k) = g^N - Lx(k) \quad (3.4)$$

where  $k$  is the discrete-time index for each cycle,  $g$  is the vector of the green times for all stages of all considered junctions,  $g^N$  is the vector of their nominal values,  $L$  is the control matrix, and  $x$  is the vector of numbers of vehicles  $x_z$  within the network links  $z$  that approach the considered signal-controlled junctions. The control matrix  $L$  depends on the specific network characteristics (topology, staging, saturation flows, and turning rates), but was found in simulation investigations to have very low sensitivity with respect to reasonable variations of the involved traffic parameters (turning rates and saturation flows) [22]. The calculation of  $L$  is the straightforward outcome of the LQ problem formulation and may be very time-consuming for large-scale networks. However, this calculation is carried out off-line (at the lab) once per application network, while the on-line (i.e. real-time) calculations are limited to the execution of Equation (3.4) with a given constant control matrix  $L$  and state measurements  $x(k)$ . After the application of Equation (3.4), a simple low-cost algorithm [22] applies any existing constraints (e.g. cycle constraints and minimum permissible green times), to the obtained values of  $g$ . Moreover, in case that no nominal values are available for utilization in Equation (3.4), two alternative formulas that eliminate the need of nominal values  $g^N$  are available for employment [22]. Given the split decisions of this part of the TUC strategy as well as the input that this part has received from the Cycle and Offset Control parts, complete network-wide signal settings including cycle, split and built-in offsets are available for implementation, at the end of Split Control.

### 3.4.3 Cycle Control Mathematical Formulation

One of the ways to influence traffic conditions via traffic lights is through the modification of cycle time. Note that one single cycle time is considered here for a whole network in order to enable junction coordination via suitable offsets. Considering the aforementioned remarks, the objective of cycle control should be to increase the junctions capacities as much as necessary to limit the maximum observed saturation level in the network.

The feedback algorithm for cycle control comprises the following three steps [22]:

- A pre-specified  $p$  percentage of network links with currently maximum load  $\sigma(k) = x_z(k)/x_{z,max}$  is identified and the corresponding loads are averaged to provide the average maximum load  $\sigma(k)$ .
- The network cycle is calculated from the feedback control law (P-regulator)

$$C(k) = C^N + K^c(\sigma(k) - \sigma^N) \quad (3.5)$$

where  $C^N$  is a nominal network cycle time (e.g. equal to the minimum admissible cycle  $C_{\min}$ );  $\sigma^N$  is a nominal average load (e.g. equal to zero); and  $K^c$  is a control parameter, the value of which affects the intensity of the control reactions. After the application of Equation (3.5), the calculated cycle time is constrained within the range  $[C_{\min}, C_{\max}]$ , if necessary, to become feasible,

where  $C_{\min}$  and  $C_{\max}$  are the minimum and maximum permissible cycle times, respectively.

# Chapter 4

## Real-Time Queue Estimation

### 4.1 Real-Time Estimation of Traffic State

It is generally recognized that one of the most effective ways to reduce congestion on urban networks is through adaptive traffic signal control [23]. An adaptive system is superior to a fixed-time system as it responds in real-time measurements, creating more realistic control plans and thus more efficient.

The adaptive traffic signal control differs from fixed-time signal control in the use of real-time traffic information instead of fixed historical traffic data. Commonly, traffic detection technologies use spot sensors or Global Positioning System (GPS) receivers. As far as concerns spot sensors, loop detectors and magnetometers are widely used and provide controller with information about traffic speed, volume and presence of vehicles. Although traditional sensors are well understood by industry professionals and preferred, the installation and maintenance of inductive loops and magnetometers are typically much more expensive and invasive than more modern detection technologies as they require cutting and patching of pavement. Besides detectors installed in the roadway, many transportation agencies have incorporated radar, infrared, ultrasonic and acoustic traffic detection devices into their actuated control systems. In addition to providing traffic speed, volume and presence, sensors installed above the roadway can also provide vehicle classification and multiple lane coverage. Therefore, the use of this kind of sensors is superior to the inductive loops and magnetometers, preventing unnecessary damage to the pavement, facilitating the maintenance and increasing the coverage area. However, this kind of sensors are typically more sensitive to inclement weather when compared to detection devices installed in the roadway [4]. Generally all spot sensors major disadvantage is that they can only provide point-based information on traffic conditions thus, they do not represent the realistic traffic state.

With recent advances in technology, a growing number of vehicles are now equipped with wireless communication systems and global positioning system (GPS) sensors. Using such vehicles, called probe or connected vehicles, there is a promise of accurate and timely information without large infrastructure and construction expenses [24]. Therefore, instead of reliance on point sensors, signal systems would be able to use data transmitted wirelessly from in-vehicle sensors to the infrastructure (V2I connectivity), to the cloud (V2C connectivity) or even to everything (V2E connectivity) [25].

For safety applications, each vehicle transmits a basic safety message that trans-

mits its temporary identifier, location, speed, heading, lateral and longitudinal acceleration, brake system status, and vehicle size. By listening to these messages, or by processing measures that arise from these messages, such as queue estimations, a signal controller can gain a more comprehensive understanding of the movements of nearby vehicles than with spot sensors [25].

With connected vehicle innovation, traffic signal control would have access to many measures used for real-time estimation of traffic state, that were previously estimated or unknown, such as vehicle speeds, positions, arrival rates, rates of acceleration and deceleration, queue lengths, and stopped time [25].

The purpose of this thesis is to evaluate the performance of two real-time traffic control strategies, the Max-pressure and TUC strategy, when the real-time information needed to operate the control strategies is provided by connected network vehicles; to determine whether they can successfully compete with spot detectors.

In Section 4.2, it is briefly described how the collection of the necessary traffic information, for the operation of the TUC strategy and the Max-pressure algorithm, in the case of detectors has been done in this thesis, while Section 4.3 details the procedure followed in the case of the connected vehicles

## 4.2 Detector Scenario

### 4.2.1 Max-Pressure Algorithm

In Max-pressure algorithm, two detectors are plant in every link, one at the entrance and one at the exit of the link. All (detected) vehicles arriving at the link entrances during a prespecified time-step (e.g. 1 sec.) are grouped into clusters, which are assumed to move with constant speeds towards the stop line. Depending on the link length and the constant speed, we can split the link into time segments supposing that a cluster moves to the next segment during one time-step. The cluster which belongs to the last segment transforms to a queue cluster or exits the link (exit detector). The anticipated queue cluster is formed by the queue cluster, merged with clusters or parts of clusters that are expected to join the existing queue before it is cleared at the junction. The anticipated queue cluster is the first cluster that will be served when the corresponding approach receives right of way. Obviously, the anticipated queue cluster is continuously updated according to the difference of the number of expected vehicle arrivals and the number of (detected) link exiting vehicles. Each cluster is looked upon as an entity to be served without splitting it.

### 4.2.2 TUC Strategy

In TUC strategy, it is assumed that detectors exists around the middle of the approaches which provide the occupancy and flow information of links in a cycle time control interval. As far as its measurement requirements are concerned, an average estimate of the traffic load in every approach of the considered network over the last control interval is sufficient [19]. This information about occupancy is incorporated into an appropriate equation which estimates the accumulation of vehicles in the link. More details about the mathematical formulation are shown in [26].

### 4.3 Connected Vehicle Scenario

First of all a certain percentage of vehicles are assumed to be equipped with connected vehicle technology whereas GPS sensors and V2I or V2C communication technology in order to provide their location and speed in real-time at short sampling periods which equal the desired estimation sampling periods. The methodology used is suggested in [24].

As long as the measurements from connected vehicles are collected, they are appropriately treated at every time step. The first task of the algorithm is the determination of the queue tail location. Specifically, based on a velocity threshold (e.g. 8 km/h), any connected vehicle is assigned to the group of moving or the group of (virtually) stopped vehicles. Then, the connected vehicle located the farthest from the downstream end of the link with a speed lower than the threshold is obviously closest to the queue tail and may therefore be considered to provide a first rough estimation of the queue length, by assuming that the queue tail reaches up to that vehicle location; clearly, this may be an underestimation, since there may be farther, non-connected, vehicles queuing behind the last connected vehicle. This first estimation is calculated as follows:

$$L_q = \max_i(d_i) \quad (4.1)$$

where  $i \in I = \{n | v_n \leq v_{\min}\}$  for  $n = 1, \dots, N_c$ ,  $v_{\min}$  is the speed threshold that designates vehicles to either stopped or moving groups,  $N_c$  is the number of connected vehicles, and  $d_i$  and  $v_i$  are the distance of the  $i^{\text{th}}$ -vehicle measured from the downstream end of the link and its corresponding speed, respectively.

Therefore, (4.1) is the initial estimation for the queue tail location, counted from the stop line of the link. The robustness of this rough queue tail estimation in terms of accuracy, increases proportionally to the percentage of connected vehicles. Specifically, in cases of high penetration rates, the estimation of queue length using equation (4.1) is accurate in a great percentage since the probability for a connected vehicle to be at or very close to the actual queue tail is accordingly high. However, in cases of low penetration rates this estimation is clearly an underestimation, hence there may be further, non-connected, vehicles queuing behind the last connected vehicle. Given the fact that, lower penetration rates are more likely to prevail at the current and near future conditions, a further elaboration of the initial queue length estimation is necessary. In order to overcome this problem, a probability-based correction approach proposed in [24] was used. This approach suggests adding an error factor to the initial assessment of  $L_q$  which success to compensate the principal queue tail estimation and render the algorithm more robust to low penetration rates producing this way bias-free estimation.

The developed analytic approach [24], uses the penetration rate and the number of lanes on the link to conclude on the probability properties of the error due to dislocation of the queue tail compared to the exact estimation that would result in case of 100% penetration rate. In this work, it is assumed 1 to be the number of lanes of the link and  $\alpha$  the penetration rate of connected vehicles, which corresponds to the probability for a vehicle to be connected. In addition, it is considered that any vehicle in the queue covers a row, see Figure 4.1.

The probability of presence of one connected vehicle in the row  $i$ , is  $P_i = \alpha$ , hence the probability of the complementary event is  $1 - P_i$ , for  $i = 0, \dots, r$ . It is considered

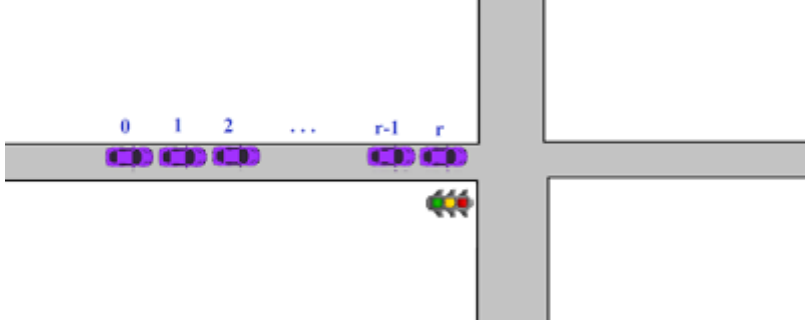


Figure 4.1: A snapshot of vehicles standing in rows behind the stop bar

that the space-headway of queuing vehicles is  $L_v$  which is empirically assumed to be 5m. Based on the derived probabilities, the following statements arise:

- If there is a connected vehicle in row 0, there is no error in identifying the real queue tail (with probability  $P_0$ ).
- If there is no connected vehicle in row 0, but there is one in row 1, there is an error equal to  $L_v$  (with probability  $(1 - P_0)P_1$ ).
- If there is no connected vehicle in row 0 and row 1, but there is one in row 2, there is an error equal to  $2L_v$  (with probability  $(1 - P_0)(1 - P_1)P_2$ ).
- The probability of error being  $iL_v$  is  $(1 - P_i)^i P_i$  for  $i = 0, \dots, r$ .

There are two possible error compensation options described in [24]. The first one proposes the production of a random value,  $y_k$  (where  $k = 1, 2, \dots$  is the discrete time index) based on the distribution function of queue tail estimation error, and adding it to  $L_q$  while the second one proposes to add the mean value,  $y_m$  (4.3), of the distribution function to  $L_q$ . It is proven in [24] that both approaches produce a bias-free estimation, but the second approach features lower (in fact, minimum)  $\gamma\mu$  for the final resulting estimation error. Given this, the second approach was chosen in order to compensate the initial queue tail location. We calculated  $y_m$  value as follows,

$$y_{m,r}(a) = \sum_{i=1}^r iL_v P_0 (1 - P_i)^i \quad (4.2)$$

$$\lim_{r \rightarrow \infty} y_{m,r}(a) = \frac{L_v(1 - a)}{a} = y_m(a) \quad (4.3)$$

where  $a$  is the penetration rate. After this, the initial queue tail estimation (4.1) is replaced by the compensated queue tail estimation

$$\hat{L}_q = L_q + \frac{y_m(a)}{\lambda} \quad (4.4)$$

where  $\lambda$  is the number of lanes of a section.

There is a consideration in apply the compensation approach in case of Equation (4.1) delivers  $L_q = 0$ . Actually, at very low demands and especially during the green traffic phase, there may be actually no queue. So compensating queue tail

estimation leads to over-estimations, which are greater in low penetration rates than in higher as Equation (4.3) declares. However the zero estimate may be inaccurate due to the lack of connected vehicles in the section. In order to overcome this consideration, it was used the decision tree depicted in Figure 4.2. This conditional compensation approach is proposed and tested over an unconditional compensation approach resulting in better results according to the queue tail Bias and RMSE values in [24] work. Depending on that, it was adopted in this work.

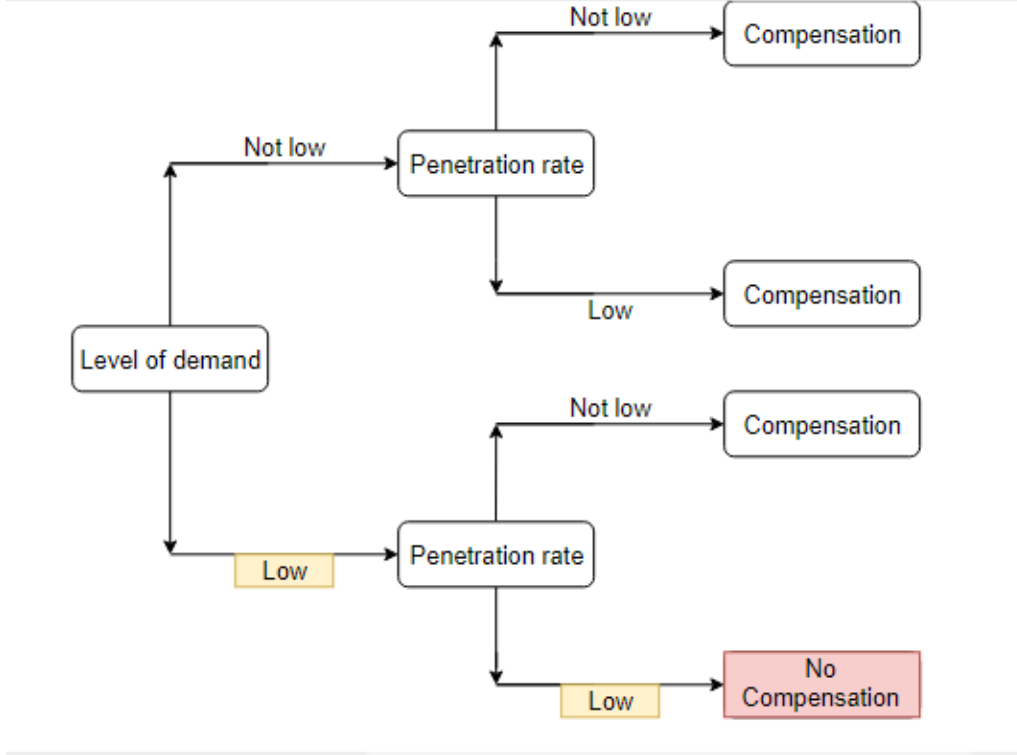


Figure 4.2: Decision tree of queue tail compensation in case of zero queue tail initial estimate

Decision tree 4.2 is based on the consideration that the probability of  $L_q = 0$  estimate to be accurate, is higher when both demand and penetration rate are low, since absence of a connected vehicle in a formed small queue is more probable so that compensation may lead to high and frequent over-estimates. So in this case it is worthy not to compensate the zero estimate.

After the queue tail location estimation, the next step is the estimation of queue length in vehicles, as in this work this measure consists the input information of Max-pressure and TUC strategy. Below is explained the logic followed for queue length estimation. For non-saturated intersections, when the traffic light turns red and a queue starts forming, all vehicles inside the queue have relatively low or zero speed, hence the number of vehicles in the downstream part of the queue length is calculated based on the average headway of queuing vehicles and the number of the lanes:

$$N_d(k) = \frac{\hat{L}_q(k)}{L_v} \lambda \quad (4.5)$$

where  $\hat{L}_q(k)$  is the estimation of the queue tail after compensation according to the

previous section and  $\lambda$  is the number of lanes of the link. However this equation can only be used when all vehicles inside the queue have almost zero speed.

In under-saturated intersections Equation (4.5) holds true only in cases there is no residual queue from the previous cycle-time, and the queue is forming during the red phase of the traffic light. However, during the green phase of the traffic light as well as in saturated traffic conditions, Equation (4.5) is not accurate because of the fact that some vehicle located downstream of the queue tail, may be moving with a far from zero velocity.

So in order to make a proper queue estimate, it is suggested in [24] a nonlinear function (4.6) that receives the prior estimation of number of vehicles,  $N_d(k)$ , and the average speed of connected vehicles inside the queue,  $V_d(k)$ , as input arguments and returns the  $\hat{N}_d(k)$ , via

$$\hat{N}_d(k) = f(N_d(k), V_d(k), \beta) \quad (4.6)$$

where  $\beta$  is a vector of unknown parameters. Based on Equation (4.5),  $N_d(k)$  is derived from  $\hat{L}_q$  and the assumed value for  $L_v$ , while in general  $L_v$  may vary from application to application. Therefore it is preferable to directly use  $\hat{L}_q$  as an input argument for the nonlinear function, in which case the value of  $L_v$  can be tuned accordingly. Thus, the following equation may be used instead of Equation (4.6)

$$\hat{N}_d(k) = f(\hat{L}_q(k), V_d(k), \beta) \quad (4.7)$$

Many mathematical approaches have been suggested to solve the above equation, ranging from physical (white-box) modeling to experimental (black-box) modeling [24]. In this work a physical model was used, based on traffic flow theory. For the physical modeling, it is assumed that there is a linear relationship between the speed  $V_j$  and the applied headway  $H_j$  of each individual vehicle  $j$ , i.e.  $V_j = -A + BH_j$ . Note that, from this equation and according to Equation (4.5), we have for  $V_j = 0$  that  $H_j = A/B = L_v$ , hence there is only one degree of freedom for parameters  $A$ ,  $B$  if  $L_v$  is known. Taking the average speed  $V_d$  for all queuing vehicles from the above equation, we get

$$V_d = -A + BH_d \quad (4.8)$$

where  $H_d$  is the average headway downstream of the queue tail. This equation corresponds to the right-hand side (congested part) of a triangular fundamental diagram, i.e. to a descending line; and  $-A$  is the corresponding negative slope, which is often called wave speed and is known empirically to be equal to -4 m/s. Thus, we have in place of equation (4.5)

$$N_d(k) = \frac{\hat{L}_q(k)}{H_d} \lambda \quad (4.9)$$

and, substituting  $\frac{A}{B} = L_v$  relation, we finally get

$$N_d(k) = \frac{\lambda A \hat{L}_q(k)}{L_v(V_d + A)} \quad (4.10)$$

This equation has the exact form of Equation (4.7), but has a physical significance and only two parameters to be tuned, namely  $A$  and  $L_v$ , which have both a physical

background and could be set to reasonable physical values,  $A = 4$  and  $L_v = 5$ , even without elaborative tuning.

However, in order to advance, it is assumed that there is an available set of  $K$  data points,  $(z_1, (x_1, y_1))$ ,  $(z_2, (x_2, y_2))$ ,  $\dots$ ,  $(z_K, (x_K, y_K))$  to be used for calibration, and a model function  $z = f(x, y, \beta)$ . It is desired to find the optimal values of the unknown parameters  $\beta$  in the least squares sense, that is, to minimize the sum of squares

$$S = \sum_{k=1}^K r_k^2 \quad (4.11)$$

where the errors  $r_k$  are given by

$$r_k = z_k - f(x_k, y_k, \beta) \quad (4.12)$$

For the physical modeling (4.10) the error function is nonlinear with respect to the unknown parameters. However, defining a new parameter  $P = \frac{L_v}{A}$  and considering the inverse of (4.10), i.e.  $[1/N_d(k)]$ , for computing the sum of squares of errors  $S$ , we end up with a linear-in-parameters function.

Hence in order to improve the results, the convex quadratic minimization problem (4.13) was solved analytically for the global minimum, offline, by a minimization algorithm designed in Matlab.

$$\hat{\beta} = \sum_{k=1}^K [z_k - f(x_k, y_k, \beta)]^2 \quad (4.13)$$

subject to Equation (4.7)

In Section 6.2 reference is made to the parameters used.

# Chapter 5

## Simulation Environment

### 5.1 Simulation Environment

To study and compare the efficiency of connected vehicles as source of queue information for two considered signal control approaches under realistic traffic conditions, the urban traffic network of Chania has been used see Figure 5.1. In particular, the simulation model, which had been developed for the needs of a past study in Aimsun, a well-known microscopic traffic modelling software, has been adopted herein.

Aimsun is a traffic modeling software that allows, complete road networks modelling. Aimsun software simulates static and dynamic traffic assignment with mesoscopic, microscopic and hybrid simulation. Moreover it permits the expandability of its function, allowing the user to intervene any time on simulation environment using Python or C++ language. In this work, it was used two main ways of interface with the main software, the Application Programming Interface and the Aimsun Microscopic Simulator Software Development Kit.

The Application Programming Interface or API is a collection of functions, in Python or C++, that allow the function of Intelligent Transportation Systems (ITS) in the simulation. These include non-standard adaptive traffic control, advanced traffic management, vehicle guidance and many more. The Aimsun Microscopic Simulator Software Development Kit or microSDK enables the user to override Aimsun's behavioral models (car-following, lane-changing, etc.) and apply its own behavioral models, programmed in C++. In this work, API was used in order to include adaptive traffic control algorithms, while microSDK to get necessary information like speed and position from vehicles of the simulation.

The considered network of Chania consists of 13 junctions with complex geometry and signal control, and 47 links; each link represents a road approach, which comprises one or more traffic streams that receive identical signaling; note that some physical roads may be reflected in more than one model links, whereby each link receives independent signaling. The specific characteristics of the links and their associated demands are given in Table 5.1. We have tested our algorithms in a heavy scenario according to demand, see Figure 5.2. In this scenario, using the real life traffic control, the network suffers from severe congestion problems, leading sometimes even to (partial) gridlocks as, especially during the peak hours of the day, traffic entering from the major network origins, located at junctions 1, 7, 8, 9 and 13, is directed towards the utmost central district of the city located in the vicinity of junctions 4, 5 and 6.

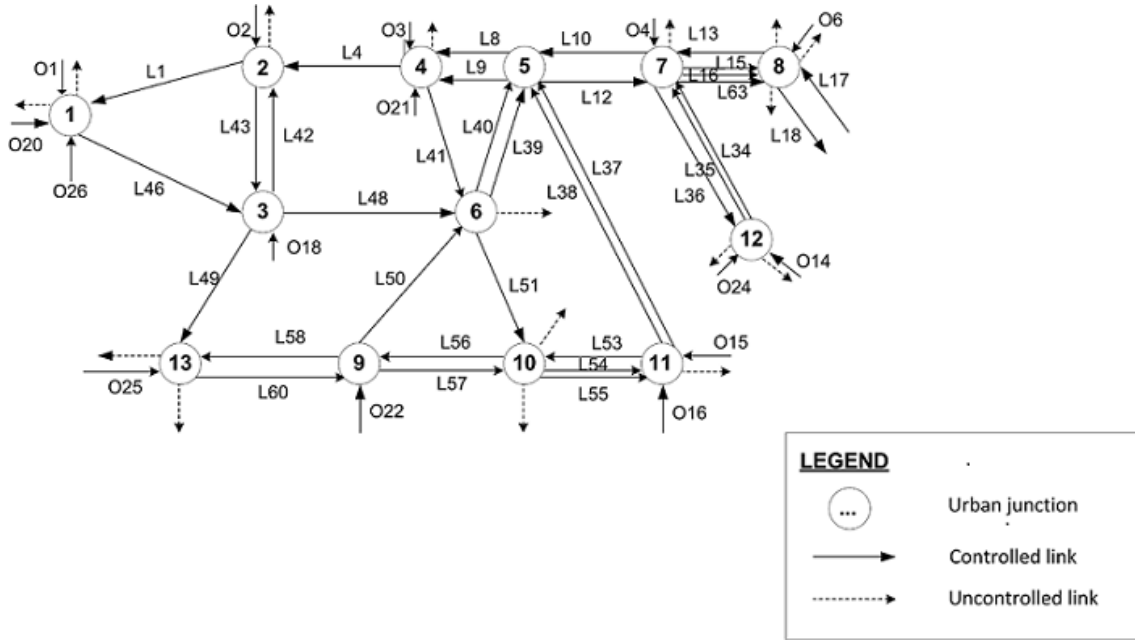


Figure 5.1: Chania traffic network

Each reported simulation lasts for one and a half hour, and data from detectors and connected vehicles are collected every one second. For control cases 4 and 5, different penetration rates of connected vehicles, ranging from 10% to 100% are considered. The vehicles are produced in the simulation environment with the average length of 4 m and 0.5 m standard deviation. The average distance between two stopped vehicles is 1 m with 0.3 m standard deviation.

The investigations performed herein involve comparisons for the following five control cases:

- Control case 1: Application of fixed 90 sec cycle time plans. These plans correspond to one of the fixed predefined network-wide signal plans used by the Traffic Control System (TCS) of the city.
- Control case 2: Application of the Max-pressure algorithm with detectors.
- Control case 3: Application of the TUC strategy with detectors.
- Control case 4: Application of the Max-pressure algorithm with connected vehicles.
- Control case 5: Application of the TUC strategy with connected vehicles.

The comparison criterions of the above cases are Delay (the average delay per car per kilometer) and Density ( the average network density).

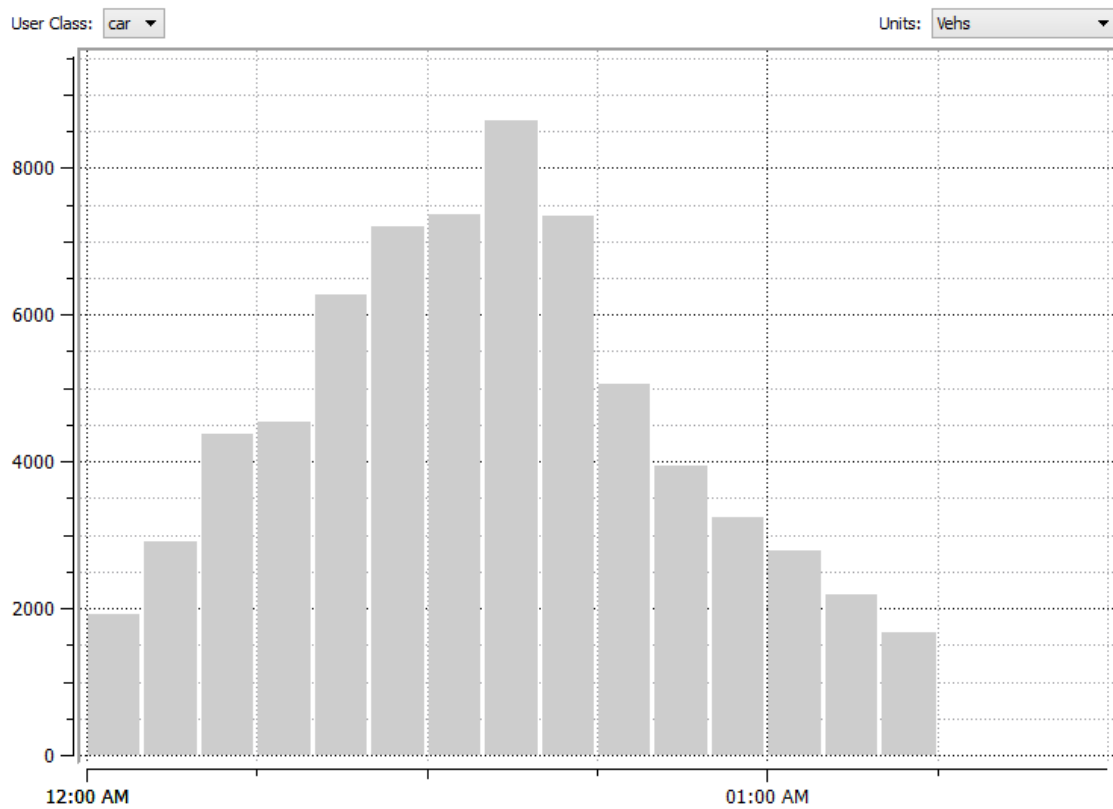


Figure 5.2: Traffic demand of Chania network, for all cases of simulations

Network characteristics			
Junction id	Sections	Length(m)	Number of lanes
1	L1	70.4	2
	O20	150.0	2
	O26	100.0	1
	O1	66.0	1
2	L4	70.1	2
	O2	49.9	1
	L42	48.3	2
3	L46	34.0	2
	L43	70.5	2
	O18	62.4	1
4	L8, L9	40.0	4
	O21	19.0	2
	O3	50.0197	1
5	L10	80.7	3
	L39, L40	71.5	2
	L37, L38	59.1	2
6	L48	62.0	2
	L41	119.9	2
	L50	60.0	1
7	L13	64.0	3
	L12	78.6	2
	O4	80.0	2
	L34, L35	55.5	1
8	L17	65.6	2
	O6	90.0	1
	L15, L16	55.5	2
9	O22	200.0	2
	L60	93.3	1
	L56	145.2	1
10	L51	66.6	2
	L53	61.1	1
	L57	148.9	1
11	O16	170.0	2
	L54, L55	58.1	1
	O15	120.0	1
12	L36	119.0	1
	O14	160.0	1
	O24	111.7	1
13	L49	63.1	2
	O25	305.0	1
	L58	33.0	1

Table 5.1: Characteristics of Chania urban network

# Chapter 6

## Queue Estimation Results

### 6.1 Characteristics and Assumptions

Our queue estimation method assumes the following conditions:

- There is no communication error, sensor failure, etc., hence the locations and speeds of all connected vehicles are known.
- The connected vehicles are randomly distributed in the link inflow; the exact prevailing penetration rate is unknown; but the average penetration rate is known and used for queue tail error compensation.
- Vehicles are equally distributed across all the lanes of a link.
- Vehicles are not allowed to park in the utilized link lanes.

In order to evaluate the quality of the produced results, the statistical measures used are the Bias and the Root Mean Square Error (RMSE) of the estimation. Suppose that the produced estimate and the ground truth for a quantity are  $\hat{y}$  and  $y$ , respectively. Then, the statistical measures mentioned, are calculated as follows:

$$\text{Bias} = \sum_{k=1}^n \frac{(\hat{y}_k - y_k)}{n} \quad (6.1)$$

$$\text{RMSE} = \sqrt{\sum_{k=1}^n \frac{(\hat{y}_k - y_k)^2}{n}} \quad (6.2)$$

For reasons of easier conclusion it was chosen to present statistical data for some crucial junctions of the network; 4, 5 and 6 around which the collision phenomenon is more pronounced and junction 12 which is the only junction composed entirely of one lane sections.

## 6.2 Parameter Calibration

For estimating the number of vehicles downstream of the queue tail, the physical mathematical modelling approach (4.10) was used, based on the estimation of queue tail location, the average speed of connected vehicles inside the queue and the unknown parameters  $A$  and  $L_v$  (see Section 4.3).

In this work, it was first used the modelling approach with  $A$  and  $L_v$  getting their physical values,  $A = 4$  m/s and  $L_v = 5$  m, as both parameters have a physical background so they can be used in their physical empirically produced values leading to accurate results [24]. Parameter  $A$  represents the slope, i.e. in a more general sense, the speed at which congestion increases. In addition, parameter  $L_v$  represents the space-headway of queuing vehicles.

However, in order to improve the upcoming results, the modelling function (4.10) was fitted once, by the analytic solution of the convex quadratic minimization problem (4.13) (see Section 4.3), for all the links of the network, in a simulation with 100% penetration rate. The same parameter values were used for links with the same number of lanes (i.e the average value of the best values obtained for links with the same number of lanes), as an attempt for wider use of the parameters. The resulting parameters are then used for all different penetration rates. The clustering of parameters by the number of lanes on each section seems to be an accurate effort of a wider use of parameters based on the Table 6.1 and Figure 6.1.

Table 6.1 shows the queue estimation error for all sections of Chania traffic network, as well as the queue estimation mean error and the root mean square error of queue estimation, of the whole network for the use of physical parameters, optimal and broadly optimal parameters. Mean error (ME) and RMSE values of network queue estimation, are calculated as the average of mean error and RMSE values of network links. Considering Table 6.1, the mean error of queue estimation in the case of using broadly optimal parameters (0.10 veh) does not differ significantly with the use of optimal parameters (0.13 veh), while it tends to be considerably lower than the use of physical parameters (0.44 veh). In addition, the root mean square error of network queue estimation is lower using optimal parameters (0.62 veh), as the minimization problem (4.13) (based on the sum of queue estimation's squared errors) indicates, while it is insignificantly higher in the case of using broadly optimal parameters (0.78 veh).

It should be noted that links L8-L9, L10 and L13 present higher mean error values from the average mean error value, this is because the original assumption for the equal distribution of vehicles on the lanes of links is not always valid for some links because of the existence of different approaches and for some others because the vehicles tend to move to the left or right lanes to ensure a turn in a downstream junction. We can solve this problem by taking the separate approaches as separate links, what we did in the implementation of the TUC strategy hence TUC needs this kind of formulation, or by reducing some unused lanes for our calculations. It was decided not to change our formulation because the links where the problem occurs, are the links of the main phases of central junctions 4 and 5 where we would prefer some overestimation and high green times for the implemented strategies.

Queue estimation error (veh)			
Link (id)	Physical values	Optimal values	Broadly optimal values
L1	0.02	0.01	0.01
O20	0.42	0.26	0.09
O26	0.01	0.00	0.01
O1	0.08	0.01	0.02
L4	0.08	0.07	0.07
O2	0.04	0.01	0.01
L42	0.28	0.17	0.23
L46	0.14	0.06	0.10
L43	0.45	0.35	-0.23
O18	0.00	0.00	0.00
L8, L9	2.18	0.92	1.57
O21	0.29	0.28	0.29
O3	0.02	0.01	-0.06
L10	3.00	0.45	1.06
L39, L40	1.82	0.38	0.92
L37, L38	0.60	0.20	-0.23
L48	0.62	0.11	-0.04
L41	1.11	0.20	-1.9
L50	0.11	0.02	-0.03
L13	2.92	0.86	1.25
L12	-0.12	-0.23	-0.44
O4	1.37	0.22	0.50
L34, L35	0.21	0.02	0.03
L17	0.30	0.20	0.05
O6	-0.38	0.01	0.00
L15, L16	0.34	0.04	0.19
O22	0.61	0.21	0.27
L60	-0.62	-0.01	0.14
L56	0.02	0.01	0.01
L51	1.00	0.09	-0.02
L53	0.15	0.00	-0.04
L57	0.29	0.04	-0.25
O16	0.65	0.15	0.29
L54, L55	-0.36	0.10	0.04
O15	0.05	0.01	0.01
L36	0.03	0.01	0.01
O14	0.00	0.00	0.00
O24	0.08	0.00	0.01
L49	0.34	0.16	0.24
O25	0.04	0.00	0.01
L58	0.03	0.01	0.01
ME of network queue estimation (veh)	0.44	0.13	0.10
RMSE of network queue estimation (veh)	1.03	0.62	0.78

Table 6.1: Queue estimation error of Chania traffic network, in vehicles.

Figure 6.1 shows the difference in queue estimation and actual value in vehicles in the three different possible parameter set options (left subplot) and in the case of selecting optimal or broadly optimal parameters (right subplot).

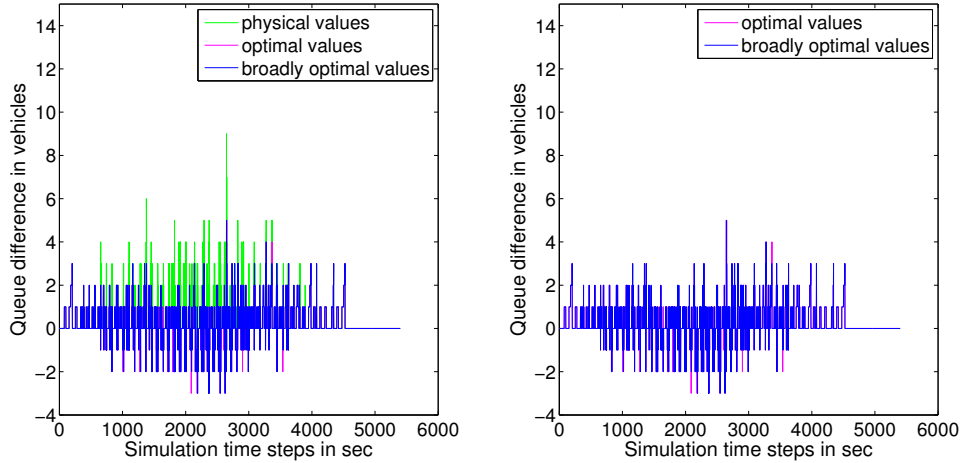


Figure 6.1: Difference of queue estimation and real queue value for 100% penetration rate in different parameter set values

By observing the diagrams of Figure 6.1 we can again see the use of widely optimal values lead to queue estimation that is no different from queue estimation when using the optimum parameter values. In addition, it appears again that widely optimal values are superior to the quality of the estimation they produce, in relation to the proposed physical values.

Table 6.2 presents the tuned values for the parameters of the physical model approach (4.10), which were used in network simulations. Finally, it should be noted that all used parameter sets of all links have been tested to lead to the optimal solution area of minimization problem (4.13). Figure 6.2 shows the result of (4.13) for different sets of parameters  $A$  and  $L_v$  for link L36. The vertical axis represents  $A$  while the horizontal axis represents  $L_v$ . As we can see, the broadly optimal values for link L36,  $A = 3.4$  and  $L_v = 5.3$ , lead to the dark red area, which is the area of the optimal values of (4.13). The same happens in all links of the network. That means that the parameters  $A$  and  $L_v$  present low sensitivity around their best value.

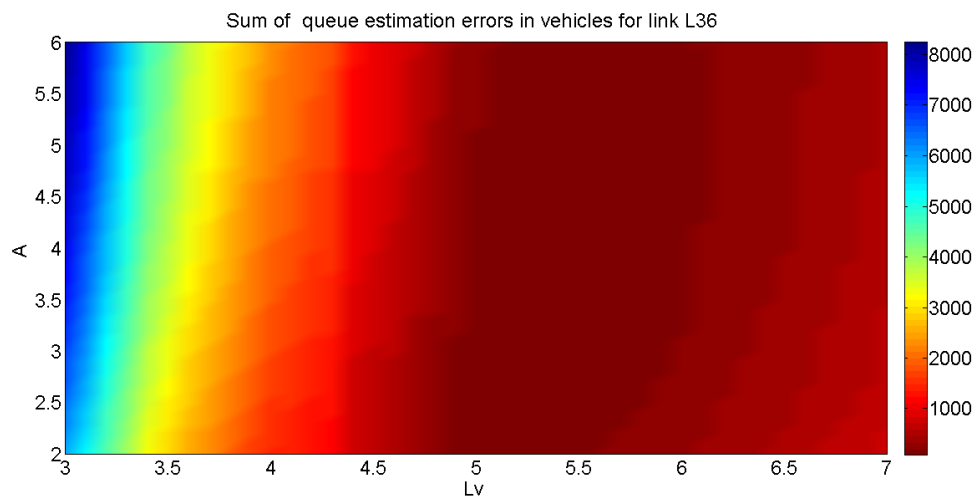


Figure 6.2: Colormap of sum of squared queue estimation errors for link L36 according to parameters  $A$  and  $L_v$ .

Broadly optimal values		
Link (id)	A (m/s)	Lv (m)
L1	3.3	6.1
O20	3.3	6.1
O26	3.4	5.3
O1	3.4	5.3
L4	3.3	6.1
O2	3.4	5.3
L42	3.3	6.1
L46	3.3	6.1
L43	3.3	6.1
018	3.4	5.3
L8, L9	3.3	6.1
O21	3.3	6.1
O3	3.4	5.3
L10	3.3	6.1
L39, L40	3.3	6.1
L37, L38	3.3	6.1
L48	3.3	6.1
L41	3.3	6.1
L50	3.4	5.3
L13	3.3	6.1
L12	3.3	6.1
O4	3.3	6.1
L34, L35	3.4	5.3
L17	3.3	6.1
O6	2.5	4.1
L15, L16	3.3	6.1
O22	3.3	6.1
L60	2.5	4.1
L56	3.4	5.3
L51	3.3	6.1
L53	3.4	5.3
L57	3.4	5.3
O16	3.3	6.1
L54, L55	2.5	4.1
015	3.4	5.3
L36	3.4	5.3
O14	3.4	5.3
O24	3.4	5.3
L49	3.3	6.1
O25	3.4	5.3
L58	3.4	5.3

Table 6.2: Broadly optimal values used in Chania traffic network simulations.

## 6.3 Statistical Evaluation

### 6.3.1 Estimation of the Queue Tail Location

As stated in Section 4.3, a first estimate of queue tail location is attained based on Equation (4.1), which accuracy depends on the penetration rate. Low penetration rates indicate a low probability of a connected vehicle existence close to the real queue tail location, therefore this initial estimation may be subject to significant error. To reduce the error, a probability-based approach was used to conditionally compensate queue tail initial estimation.

In this work, for fixed signal control scenario, the speed threshold used in Equation (4.1) is 3.0 m/s, the thresholds used for conditional compensation are 10% for the penetration rate and the time period of high demand in seconds is,  $t \in [1200, 3600]$  for simulations of one and a half hour duration.

The following tables show the statistic values of Bias and Root Mean Square Error of queue tail estimation for the network and for some significant junctions 4, 5, 6 and 12, calculated as Equations (6.1), (6.2) indicate. Moreover the following figures present estimates and real queue tail difference (6.3) for different penetration rates, for a certain link of those junctions, following the mathematical relationship where  $y_k$  is the actual queue tail value and  $\hat{y}_k$  is the queue tail estimate.

$$Dif = y_k - \hat{y}_k \quad (6.3)$$

The results are obtained from samples of 10 fixed-time control simulations and different penetration rate in each sample, in order to evaluate the accuracy of the estimation approach under different rate of demand information. The rows of tables represent the penetration rate of connected vehicles while the columns represent the sections of a junction. Obviously there was no need to present the queue tail estimation for 100% as it is equal with the actual queue tail value.

Network statistics (m)		
Penetration rate (%)	Average Bias (m)	Average RMSE (m)
50	1.6	5.0
30	4.9	8.7
10	2.5	13.8

Table 6.3: Network statistics (in meters).

Considering RMSE Tables, 6.8, 6.9, 6.10, 6.11, Bias Tables 6.4, 6.5, 6.6, 6.7 and the Table with statistics of the network 6.3, we see that Bias, except of 10% penetration rate case, and RMSE values increase as penetration rate decreases, indicating that the accuracy of queue tail estimation is continually improving with increasing penetration rates of connected vehicles. In the case of 10% connected vehicles, some bias values present an improvement because of conditional compensation of queue estimate, see Section 4.3. In particular, in low penetration rates such us 10% we would expect higher absolute estimation bias. However, avoiding some wrong estimates at the begin and at the end of the simulation, by not adding the mean error when the estimated queue is zero, leads to a decreased absolute bias value as happens in links O21, O3, L48, L50, L36, O14 and L50. Furthermore, considering

plus and minus signs in Bias Tables 6.4, 6.5, 6.6 and 6.7, it seems that there is not a specific overestimate or underestimate tendency.

Bias (m)			
Penetration rate (%)	Links		
	L8	O21	O3
50	0.3	1.5	2.4
30	0.2	4.6	6.3
10	-2.1	3.4	-0.1

Table 6.4: Bias of queue tail estimation for junction 4 (in meters).

Bias (m)			
Penetration rate (%)	Links		
	L10	L39	L37
50	-0.8	-0.6	0.7
30	-0.5	0.9	2.9
10	-4.1	-3.4	-0.5

Table 6.5: Bias of queue tail estimation for junction 5 (in meters).

Bias (m)			
Penetration rate (%)	Links		
	L48	L41	L50
50	0.5	0.2	1.4
30	2.1	0.9	6.2
10	-0.3	-2.4	1.6

Table 6.6: Bias of queue tail estimation for junction 6 (in meters).

Bias (m)			
Penetration rate (%)	Links		
	L36	O14	O24
50	3.5	4.7	2.6
30	9.5	11.2	6.6
10	8.7	10.0	4.2

Table 6.7: Bias of queue tail estimation for junction 12 (in meters).

RMSE (m)			
Penetration rate (%)	Links		
	L8	O21	O3
50	4.4	3.0	5.5
30	6.1	5.5	9.7
10	8.9	6.4	16.1

Table 6.8: RMSE of queue tail estimation for junction 4 (in meters).

RMSE (m)			
Penetration rate (%)	Links		
	L10	L39	L37
50	5.8	6.9	4.6
30	8.7	8.8	6.8
10	14.8	15.6	12.8

Table 6.9: RMSE of queue tail estimation for junction 5 (in meters).

RMSE (m)			
Penetration rate (%)	Links		
	L48	L41	L50
50	5.8	4.8	6.9
30	8.9	8.5	10.8
10	13.8	19.2	15.3

Table 6.10: RMSE of queue tail estimation for junction 6 (in meters).

RMSE (m)			
Penetration rate (%)	Links		
	L36	O14	O24
50	5.5	4.9	5.7
30	10.9	11.3	12.3
10	16.2	15.6	15.5

Table 6.11: RMSE of queue tail estimation for junction 12 (in meters).

Figures 6.3, 6.4, 6.5 and 6.6 show the difference of queue tail actual value and queue tail estimation in different penetration rates confirming that lower penetration rates provide lower accuracy estimates. In particular, it appears that both underestimations and overestimations are increasing in frequency and value as the penetration rate decreases. The underestimations are due to the lack of connected vehicle information, due to low penetration rate. Overestimations are due to the compensation error process. Serious overestimations occur in case of zero value queue tail estimation especially for low penetration rates, as several times this estimation is accurate, so compensation is causing overestimations.

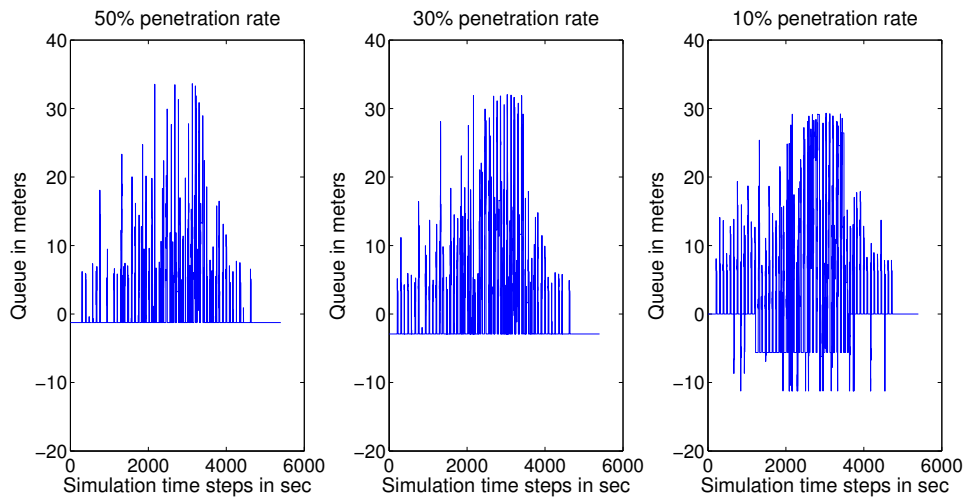


Figure 6.3: Difference of actual queue tail value and queue tail estimation for section L8, for different penetration rates

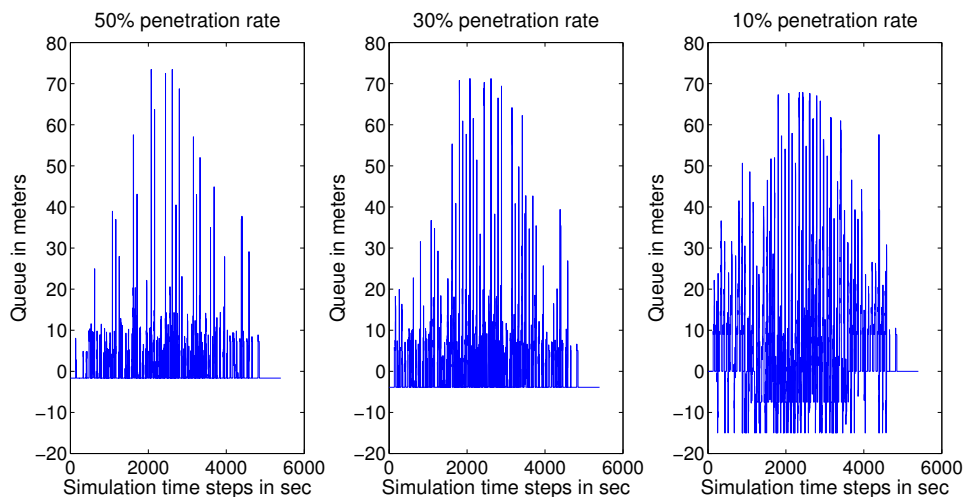


Figure 6.4: Difference of actual queue tail value and queue tail estimation for section L10, for different penetration rates

However, underestimations have higher values than overestimations, which means that there is a greater estimation error due to the low number of connected vehicles in the network than due to the error compensation process. It follows from this that the compensation error contributes more to reduce the estimation error than to increase it, since without this process the underestimations would be even more.

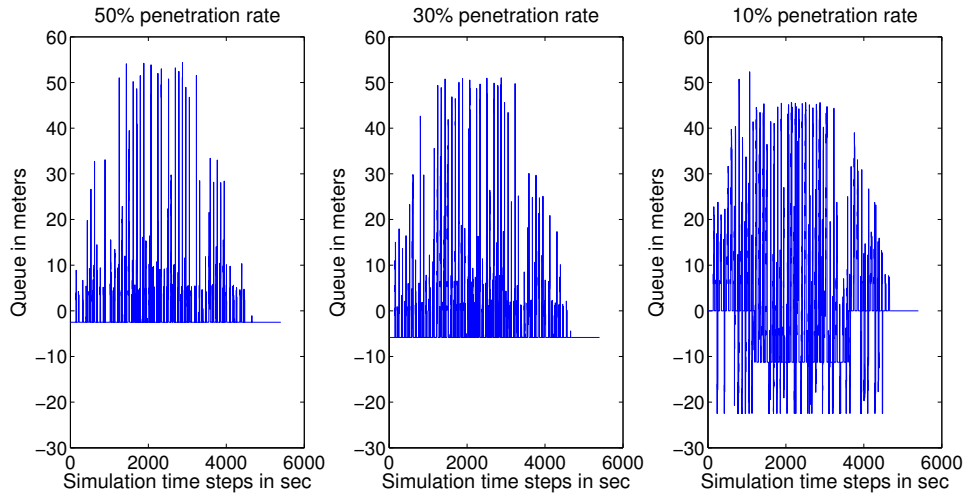


Figure 6.5: Difference of actual queue tail value and queue tail estimation for section L48, for different penetration rates

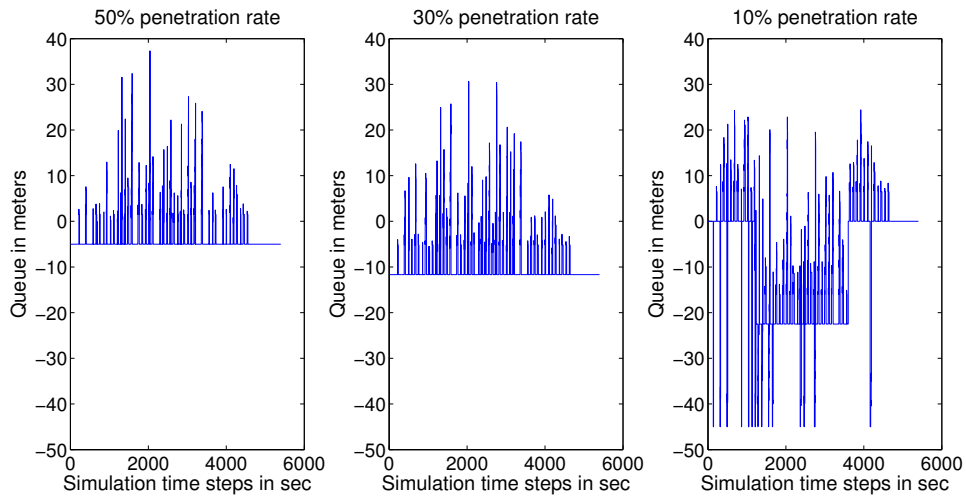


Figure 6.6: Difference of actual queue tail value and queue tail estimation for section L36, for different penetration rates

It is also observed that in the 10% diagrams in the initial and final times appear small underestimations instead of overestimations, opposed to the larger penetration rates. This is due to the conditional compensation error process, where for small penetration rates it was chosen not to apply error compensation during periods of low demand (4.3).

Finally, Figure 6.7 shows the distribution of the absolute error of queue tail estimation in order to test empirically the validity of the analytic approach. An empirical approach to find such distribution functions was employed and functions were fitted from data of the average simulation of each sample set (10 simulations) of different penetration rate. It is clear that the probability of having lower absolute error values of 1 meter is very small for 50% and 30% penetration rates, while it is quite large (near 0.45 probable ) when the penetration rate of connected vehicles is 10%. This is justified by the conditional compensation error approach.

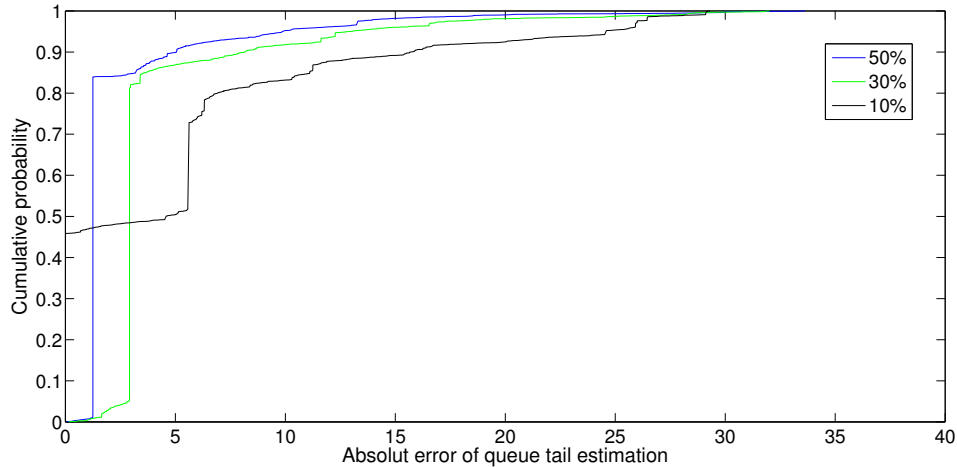


Figure 6.7: Empirical Probability Distribution

In fact, we achieve more zero value estimation because at times of low demand for 10% penetration rate, we do not compensate the initial estimate at all, whereby at times of high demand we compensate the estimation at half the grade than for the higher rates. However, it seems that the probability of error to be less than  $X$  for  $X > 3$  m decreases as the penetration rate decreases as the cause of the error is now the low information due to the small penetration rate.

### 6.3.2 Estimation of Link Vehicle Accumulation Downstream of Queue Tail

The following tables show the statistic values of Bias and Root Mean Square Error of queue estimation, calculated as Equations (6.1), (6.2) indicate. The following tables refer to the whole network, some junctions with typical links (6 and 12) and specific junctions with links that present some peculiarities (4 and 5), in order to get an overview of the results and to comment on certain specific points. Moreover the following figures show the queue estimation and the actual queue value in vehicles for a certain link of those specific junctions. The results are obtained from samples of 10 fixed-time control simulations and different penetration rate in each sample, in order to evaluate the accuracy of the estimation approach under different rate of demand information. The broadly optimized parameters values have been used to calculate the estimation function. The rows of tables represent the penetration rate of connected vehicles while the columns represent the sections of a junction.

Table 6.12 shows the Bias and the RMSE of the network. We can see that Bias and RMSE values increase as the penetration rate decreases, indicating that the estimation accuracy decreases as the percentage of connected vehicles in the network gets lower. However, bias value for 10% penetration rate has some improvement over 30% due to the conditional compensation approach followed; below is analyzed more precisely what is going on. In addition, it is clear that the bias of the estimation is close to zero for high penetration rates while for lower penetration rates is close to 1 vehicle, hence the estimation approach described in Section (4.3) is effective for high penetration rates and quite accurate for lower penetration rates of connected vehicles.

Network statistics (veh)		
Penetration rate (%)	Average Bias (veh)	Average RMSE (veh)
100	0.1	0.8
50	0.2	1.3
30	1.2	2.2
10	0.8	3.4

Table 6.12: Network statistics (in vehicles).

Bias (veh)			
Penetration rate (%)	Links		
	L8	O21	O3
100	1.6	0.3	-0.1
50	1.0	0.0	0.5
30	0.7	1.9	1.0
10	1.0	1.6	-0.1

Table 6.13: Bias of queue estimation for junction 4 (in vehicles).

Observing Tables 6.13, 6.14, 6.15 and 6.16 it is clear that in general the bias of the estimation is close to zero and especially to node 12 for 100% penetration rate our estimation seems to be totally unbiased. Furthermore different conclusions are made according to lane number of each section.

Bias (veh)			
Penetration rate (%)	Links		
	L10	L39	L37
100	1.0	0.9	-0.2
50	0.7	0.5	-0.5
30	0.4	1.7	0.9
10	0.1	0.6	0.0

Table 6.14: Bias of queue estimation for junction 5 (in vehicles).

Bias (veh)			
Penetration rate (%)	Links		
	L48	L41	L50
100	-0.0	-1.9	-0.0
50	-0.3	-2.0	-0.2
30	1.0	-1.3	1.1
10	0.4	-2.0	0.3

Table 6.15: Bias of queue estimation for junction 6 (in vehicles).

For one lane links, such as O3, L50, L36, O12 and O24, it is observed that the absolute bias values increase, hence estimation is getting worse, as the penetration rate decreases, except for the 10% cases mentioned below. In addition, positive and negative signs of estimation bias reveal that there is not a certain tendency to overestimate or underestimate the number of vehicles inside the queue, by reducing or increasing the penetration rate because of the assumption of connected vehicle random distribution (see Section 6.1).

For links with more lanes we see that the absolute value of bias is lower for lower percentages than for 100 %. Specifically, on some 2-lane streets such as O21 and L39, the bias value in case of 50% penetration rate, improves to a small extent than the 100% bias and increases sharply in 30% penetration rate case. Also on L8 and L10 streets consisting of 4 and 3 lanes respectively, we see that there is an improvement in bias even in the case of penetration 30%. This is because of the incompleteness of the original assumption that has been made for the equal distribution of vehicles in the lanes of a road (see Section 6.1). Although this assumption is accurate in real networks, in Aimsun simulations for Chania Network, on links with several lanes, this condition is not fully applicable. As a result some of the lanes are not covered in the same way as the others, while the estimation model assumes that there is equal distribution of vehicles in the lanes. That is the reason that bias of those links for 100% connected vehicle rate indicates a large overestimation which is reduced to the lower penetration rates, as low penetration rates counterbalance the uncovered lanes, indicating this way a more accurate traffic state than high penetration rates. Obviously, the more lanes a road has, the more intense this happens, so on L8 and L10 links, even in case of 30% connected vehicle rate, present an improvement in bias.

As far as it concerns 10% penetration rate cases, by studying the results obtained from the simulations of Chania urban network, it was clear that for a penetration rate of connected vehicles less than 10% the queue estimation was quite inaccurate

Bias (veh)			
Penetration rate (%)	Links		
	L36	O14	O24
100	0.0	0.0	0.0
50	0.8	0.9	0.6
30	1.6	1.9	1.1
10	1.6	1.8	0.8

Table 6.16: Bias of queue estimation for junction 12 (in vehicles).

and specifically over-biased. This was due to the fact that for a low penetration rate the mean error added to the initial vehicle estimation was too large resulting in overestimation of the queue. To improve the estimation, it was decided for the case of zero queue to add half the mean error to the initial estimation at the time of the high demand of the network that is assumed to be between 1200 - 3600 sec. for the simulations of 1.30 h carried out, while no adding it, the other time moments. This is why in most links the queue estimation for 10% penetration rate exhibits a lower bias than for higher penetration rates and the same is observed for the average bias of the network (see Table 6.12).

RMSE (veh)			
Penetration rate (%)	Links		
	L8	O21	O3
100	3.4	0.6	0.3
50	3.2	0.7	1.0
30	3.1	2.0	1.7
10	3.8	2.5	3.0

Table 6.17: RMSE of queue estimation for junction 4 (in vehicles).

RMSE (veh)			
Penetration rate (%)	Links		
	L10	L39	L37
100	2.4	1.9	1.1
50	2.8	2.5	1.6
30	3.2	3.2	2.3
10	5.4	4.3	4.0

Table 6.18: RMSE of queue estimation for junction 5 (in vehicles).

Regarding the accuracy of estimation model, RMSE values indicate that the accuracy of the provided estimation is worsened by increasing the penetration rate (see Tables 6.17, 6.18, 6.19, 6.20) which was expected as with a lower penetration rate there is not a precise sense of network demand throughout the simulation, since the only source of information is connected vehicles.

However, it is observed that section L8, see Table 6.17, show a differentiation in this generalization. In particular, it appears that the RMSE decreases as the penetration rate decreases while rising sharply to 10%. This is because of the incom-

RMSE (veh)			
Penetration rate (%)	Links		
	L48	L41	L50
100	0.9	3.2	0.3
50	1.6	3.6	1.2
30	2.5	4.2	1.9
10	3.8	6.7	2.7

Table 6.19: RMSE of queue estimation for junction 6 (in vehicles).

RMSE (veh)			
Penetration rate (%)	Links		
	L36	O14	O24
100	0.1	0.0	0.1
50	1.0	1.0	1.1
30	1.8	1.9	2.1
10	2.9	2.8	2.7

Table 6.20: RMSE of queue estimation for junction 12 (in vehicles).

pleteness of the original assumption that has been made for the equal distribution of vehicles in the lanes of a road, as it was mentioned before.

Figures 6.8, 6.9, 6.10, 6.11 provide a comparison between actual and estimated number of vehicles downstream of the queue tail for different penetration rates. The figures of all the other links follows at the Appendix A. Figures 6.12, 6.13 show the queue estimation of vehicles and the actual queue during a low demand period and a high demand period in order to clarify the relationship between the estimation for different rates of connected vehicles and network demand.

Chart analysis agree with the comments made up taking into account the statistical results, confirming that :

- There seems to be no particular tendency for overestimation or underestimation relevant with the penetration rate increase or decrease.
- The accuracy of the estimation decreases as the percentage of connected vehicles is reduced for all links irrespective of their number of lanes, that is because the information of traffic state is reduced.
- The assumption of equal distribution between the lanes is a very crucial one.
- The estimation has serious problems in low demand periods especially when there is a low penetration rate of connected vehicles. That is why for 10% penetration rate the different way to add the mean error at the periods of low demand has resulted in estimation improvements compared to higher penetration rates (see Figure 6.12).
- In high demand period especially when there is a high penetration rate of connected vehicles, estimation succeeds to reach the actual number of vehicles in some time-steps (see Figure 6.13).

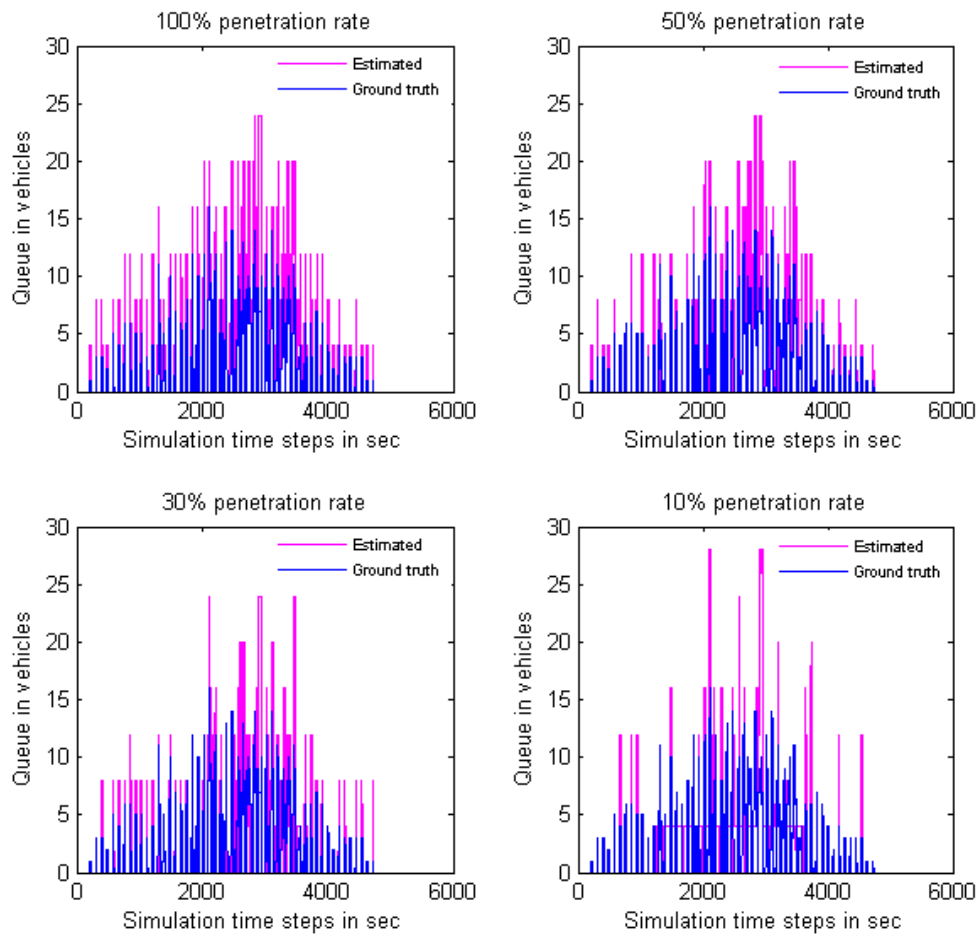


Figure 6.8: Difference of queue estimation and real queue value for section L8, for different penetration rates

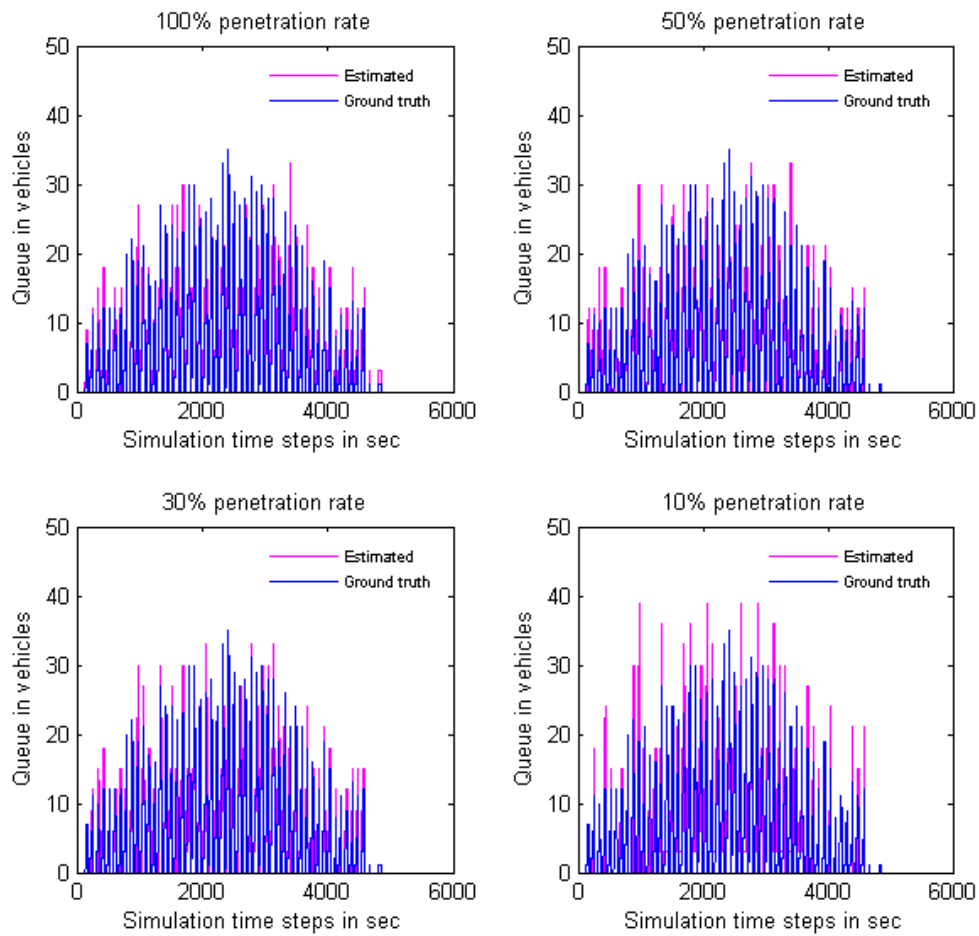


Figure 6.9: Difference of queue estimation and real queue value for section L10, for different penetration rates

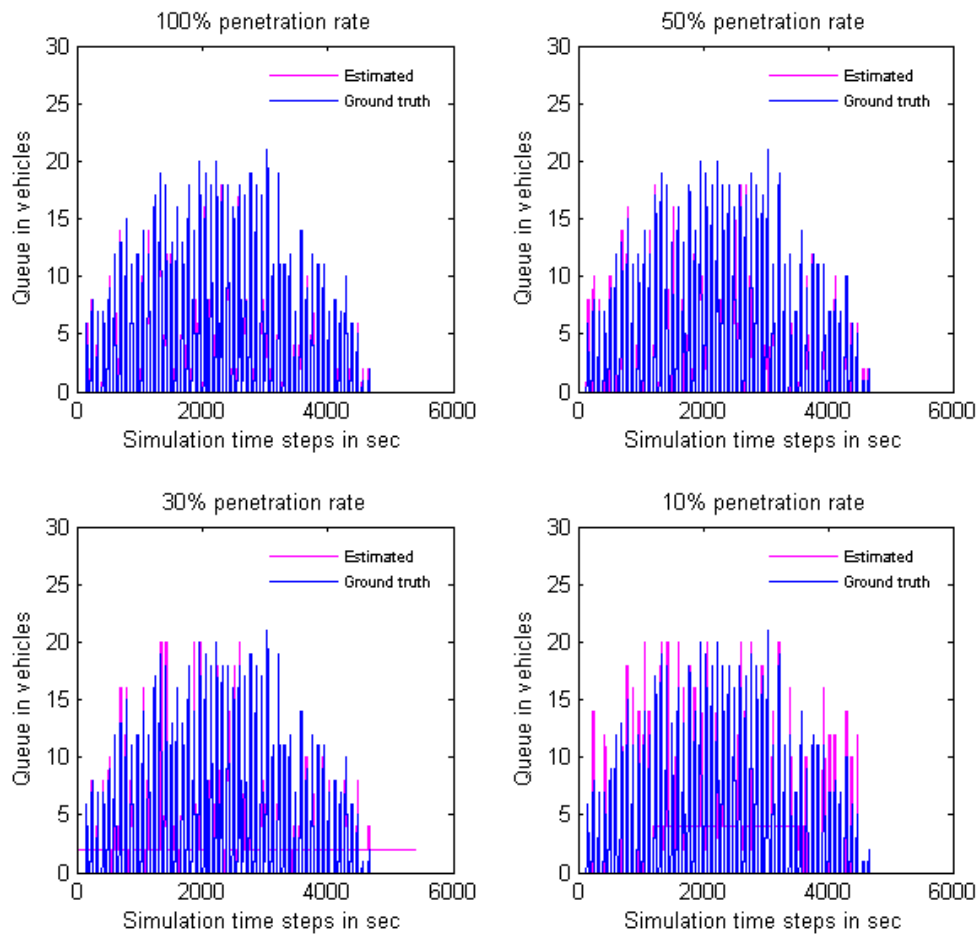


Figure 6.10: Difference of queue estimation and real queue value for section L48, for different penetration rates

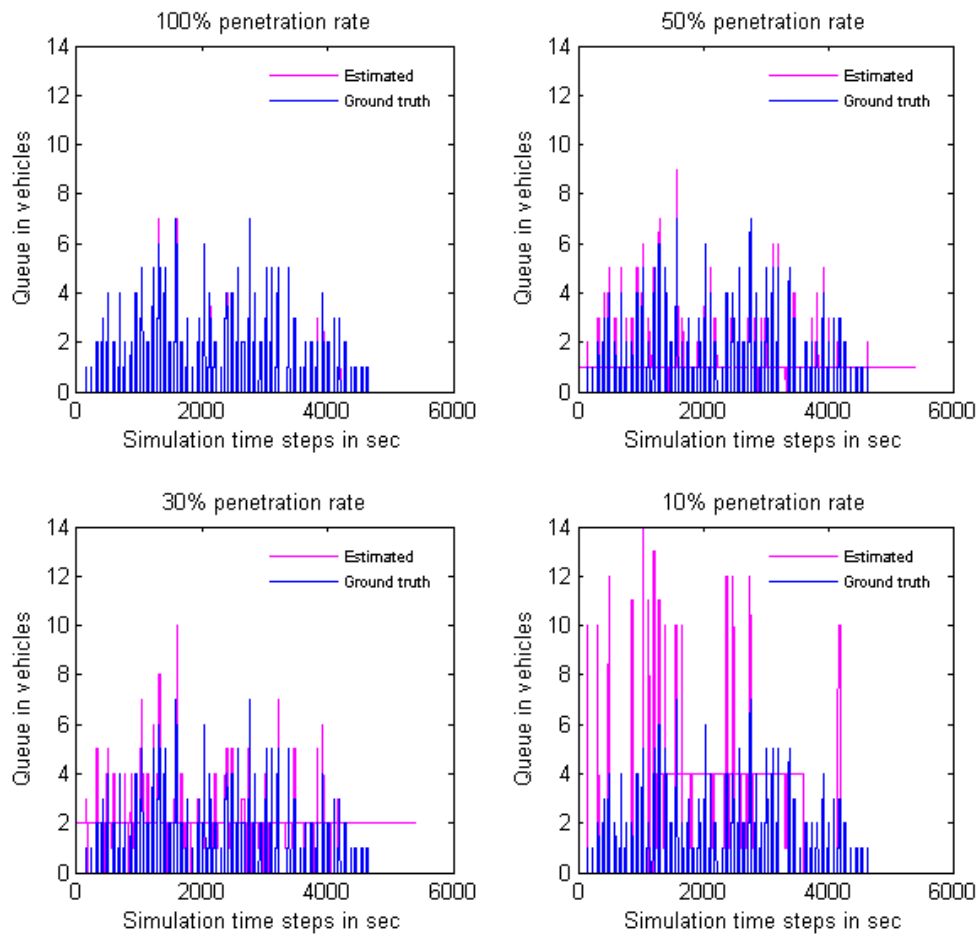


Figure 6.11: Difference of queue estimation and real queue value for section L36, for different penetration rates

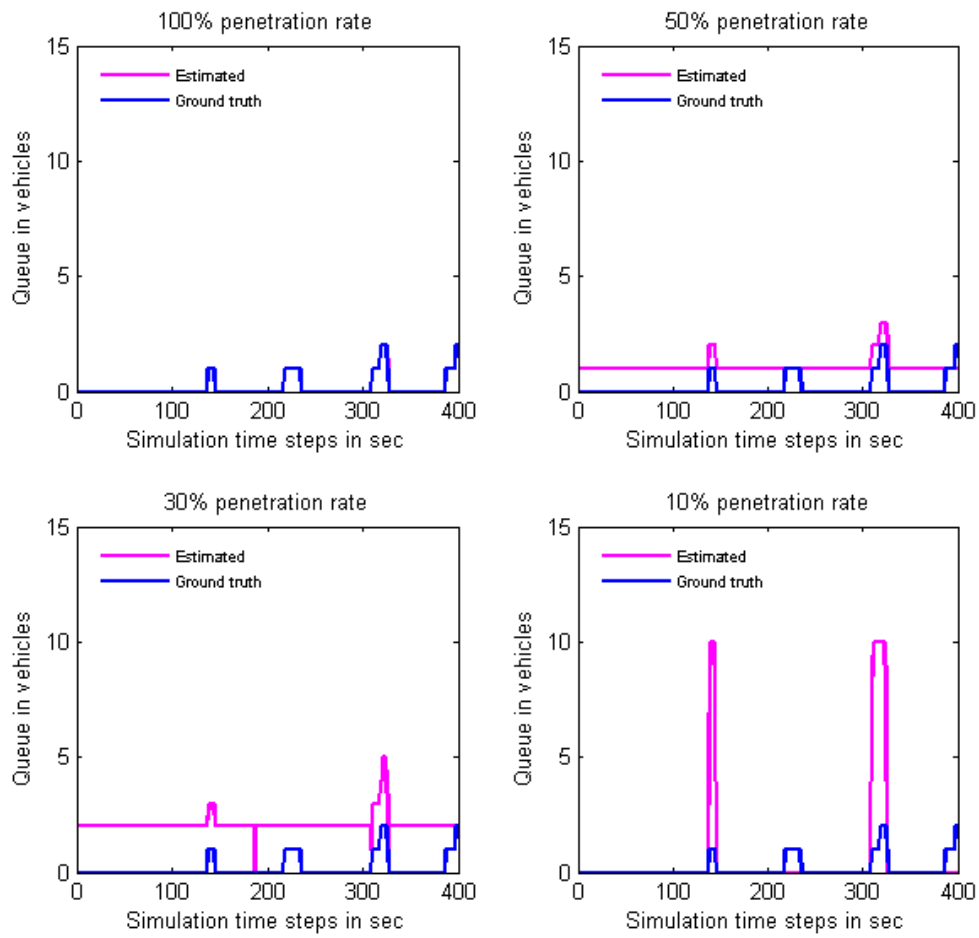


Figure 6.12: Difference of queue estimation and real queue value for section L36, for different penetration rates, in a low demand period

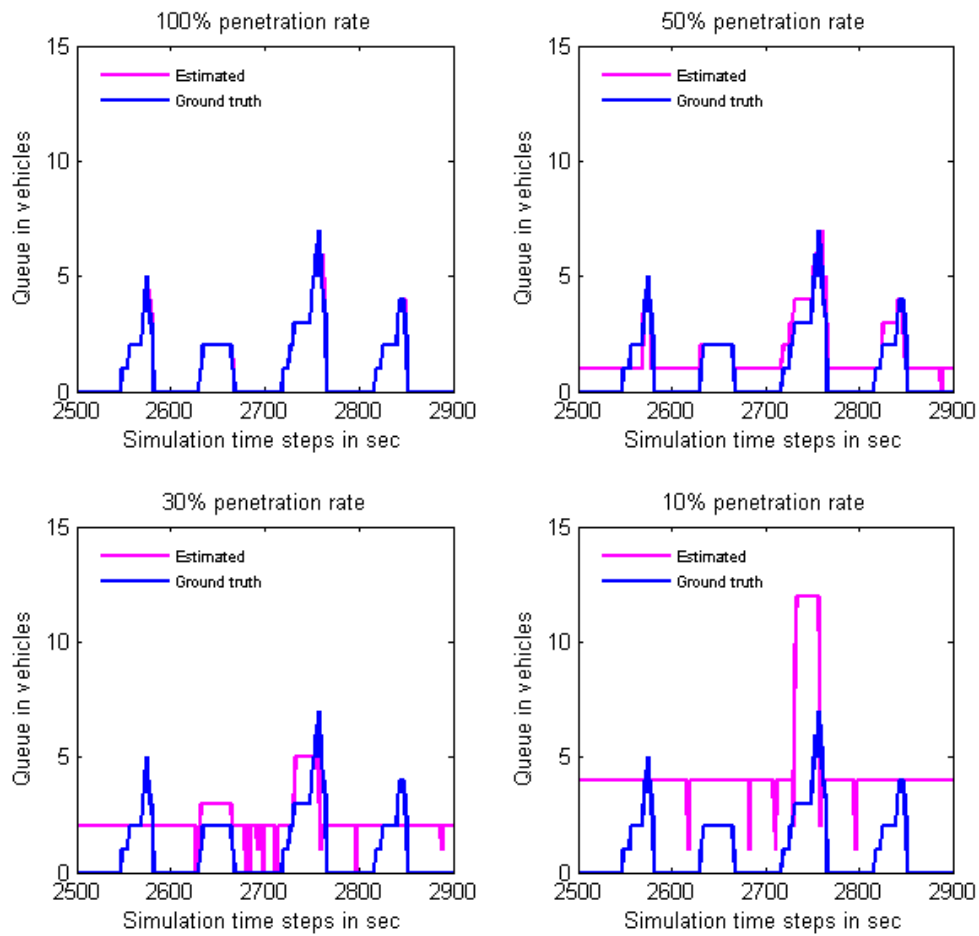


Figure 6.13: Difference of queue estimation and real queue value for section L36, for different penetration rates, in a high demand period

# Chapter 7

## Control Strategies Results

### 7.1 Introduction

The evaluation of mathematical approach (4.10) in Section 6.3.2 shows that connected vehicles could provide realistic information about the traffic state, which accuracy increases as the available connected vehicle rate increases in the urban network. Thereafter, mathematical estimation approach (4.10) was embedded in two different real-time traffic control strategies, the centralized TUC strategy (see Section 3.3) and the decentralized Max-pressure algorithm (see Section 3.4) so that to test their reaction on connected vehicle information and figure out how traffic control could function in an urban network given the availability of connected vehicle provided information.

The control strategies have been tested using simulation environment of Chania network, see Section 5.1. In order to make some general conclusions, it was used a sample of 10 simulation replications for each control case, while traffic control efficiency was evaluated using the control indexes of average delay and density (see Section 2.2). Sections 7.2, 7.3 light up the performance of the two strategies individually to compare the use of spot detectors and connected vehicles. Finally, Section 7.4 compares the two strategies (in the case of detectors and connected vehicles) with the fixed control, to determine which strategy case best responds. For reasons of comprehension, it should be noted that FT, MP and TUC abbreviations in following result tables refer to Fixed control, MP control with detectors and TUC control with detectors. Abbreviations such as MP p.r % or TUC p.r %, refer to control cases with the corresponding penetration rate of connected vehicles.

### 7.2 TUC Strategy

Considering tables 7.1 and 7.2, both the average delay and density seem to stand in the same level of value in all different penetration rates. At TUC strategy, the real-time information about vehicles accumulation inside the queue is the average of estimates selected in a cycle control interval. However, the average queue estimate in vehicles tends to be similar despite the different existing rates of connected vehicles, as the bias of queue estimation does not vary significantly with different penetration rates, see Section 6.3.2. Consequently, since the average estimated real-time queue is almost similar in different penetration rates, the performance of the strategy remains about the same in different connected vehicle rates.

Moreover standard deviation of both indexes shows that for all penetration rates results are low deviated, in particular density results, which means that both are accurate control index of the sample. However for some penetration rate there is a higher value of delay standard deviation which is justified by the initial assumption that connected vehicles are randomly distributed in the link so the penetration rate indicates an average and not the exact prevailing value.

In order to more accurately check the quality of the results and consequently the conclusions we made, a statistical t-test was carried out. A t-test is commonly used to determine whether the mean of a population significantly differs from a specific value (called the hypothesized mean) or from the mean of another population. In our case, the t-test was applied between all penetration rate cases per two, showing there was no statistically significant difference in the average performance of different samples, so we accept the zero hypothesis. Therefore conclusions are typically accurate. The results of t-Test follows at the Appendix B.

Delay evaluation data			
	Average Delay (sec/km)	St.Deviation (sec/km)	% Improvement
TUC	122.0	4.2	
TUC 100 %	125.9	3.3	-3.2
TUC 50 %	124.3	6.9	-1.9
TUC 30 %	122.6	6.1	-0.5
TUC 10 %	126.8	7.6	-3.9

Table 7.1: TUC delay evaluation data

Density evaluation data			
	Average Density (veh/km)	St.Deviation (veh/km)	% Improvement
TUC	8.1	0.3	
TUC 100 %	8.4	0.2	-3.6
TUC 50 %	8.3	0.3	-2.5
TUC 30 %	8.1	0.2	-0.6
TUC 10 %	8.3	0.3	-2.7

Table 7.2: TUC density evaluation data

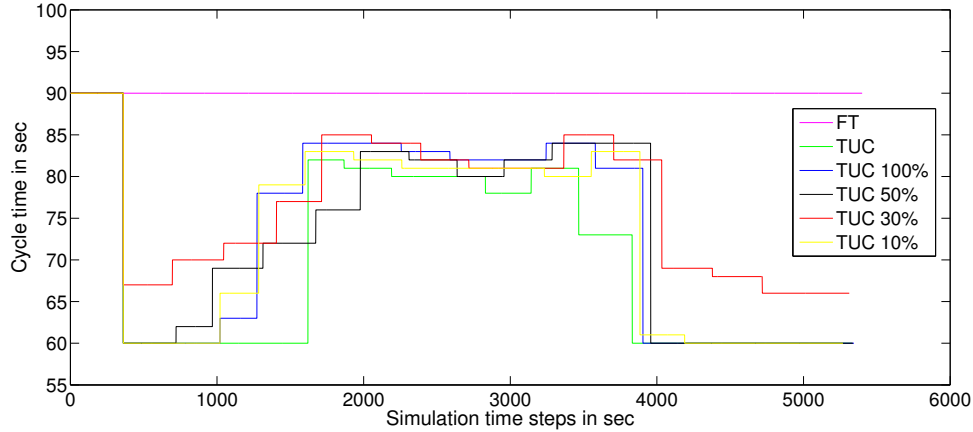


Figure 7.1: Cycle time of Fixed control and TUC control cases

Figure 7.1 shows how cycle time is formed during the simulation time for Fixed control, TUC detector control case and TUC with different connected vehicle rate cases. Recall that, under TUC, there is one common cycle time for all junctions at any time which is based on the most dense junctions in the network. The presented cycle times are derived from the simulation of which the delay time is closer to the average delay time of the 10 simulations performed, in any traffic control case.

Chart shows that all TUC cases form smaller cycles than the fixed control case. Therefore, it is justified that they also exhibit lower delay values, as lower cycles typically decrease delay time. As far as it concerns TUC cases, it is generally observed that same decisions are made about increasing or decreasing the cycle, varying in the specific cycle duration, exact size and response to change. However the variations are small and this confirms the small variations in TUC performance for different percentages of connected vehicles. With a more careful observation of the diagram, we can see that detector case is more delaying to increase the cycle, which increases sharply, and also throws it faster than other cases.

In addition, in 30% penetration rate case, the cycle does not fall to its minimum value as in the rest of penetration rate cases. This is because the smaller the penetration rate, the compensation approach (see Section 4.3) increases the queue estimate, so it is estimated that there is some demand even in periods that it does not exist and consequently the cycle grows unnecessarily. However, this is not the case for 10% penetration rate because we do not apply the compensation approach in times of low demand. For that reason 10% penetration rate seems to behave closer to 100% penetration rate in the control cycle configuration, in low demand periods, than the other rates.

It should be noted that TUC application starts under the typical for the network 90 s cycle time, which is updated by TUC's cycle control module after 5 min. This means that during the first 5 minutes of the simulation horizon, the cycle time is rather high for the respective network load, which is still low, thus imposing further delays.

### 7.3 Max-Pressure Algorithm

The results of the third column of tables 7.3, 7.4 show that the Max-pressure algorithm in the case of the use of connected vehicles with a percentage greater than or equal to 50% best performs the criteria of delay and density, from the case of the algorithm using spot detectors. However, for smaller percentages of 30% the algorithm performs worse than using spot detectors. This is normal, since the algorithm uses the estimation of queue in vehicles provided by Equation (4.10) in each step. Specifically, as the percentage of connected vehicles increases, the accuracy of the estimate increases, as the RMSE results of the queue estimation in vehicles confirm in Section 6.3.2, therefore the quality of the algorithm control is also improved.

As for Max-pressure response to different percentages of connected vehicles, the results show that it achieves better traffic control performance as the proportion of connected vehicles grows according to the delay and density indicators.

The results of the standard deviation of the two indices indicate that, as the penetration rate decreases, both the two criterion values deviate in the samples of 10 simulation replications. This is justified by the assumption that the connected vehicles are randomly distributed in the link inflow; at low penetration rates, since there is already inaccurate information, the additional relative variations in the penetration rate intensify the difference in algorithm decisions.

However, as in the case of TUC results, a statistical t-test was carried out confirming that there is a significant statistical difference in the average performance results of tested penetration rates, indicating that the difference in the average values of the criteria for tested penetration rates are indeed significant differences. Consequently, the conclusions we reached are based on precise considerations. The results of t-Test follows at the Appendix B.

Delay evaluation data			
	Average Delay (sec/km)	St.Deviation (sec/km)	% Delay Improvement
MP	118.1	12.7	
MP 100 %	106.9	6.0	9.4
MP 50 %	115.2	6.0	2.4
MP 30 %	129.1	10.3	-9.3
MP 10 %	180.9	21.1	-53.2

Table 7.3: Max-pressure delay evaluation data

Density evaluation data			
	Average Density (veh/km)	St.Deviation (veh/km)	% Density Improvement
MP	8.4	0.7	
MP 100 %	7.7	0.3	8.1
MP 50 %	8.2	0.3	2.3
MP 30 %	9.0	0.5	-8.1
MP 10 %	11.7	1.1	-40.5

Table 7.4: Max-Pressure density evaluation data

Figures 7.2, 7.3, 7.4 show cycle time created by Fixed control, MP algorithm with detectors and Max-pressure algorithm with different penetration rates in 1.5 hours

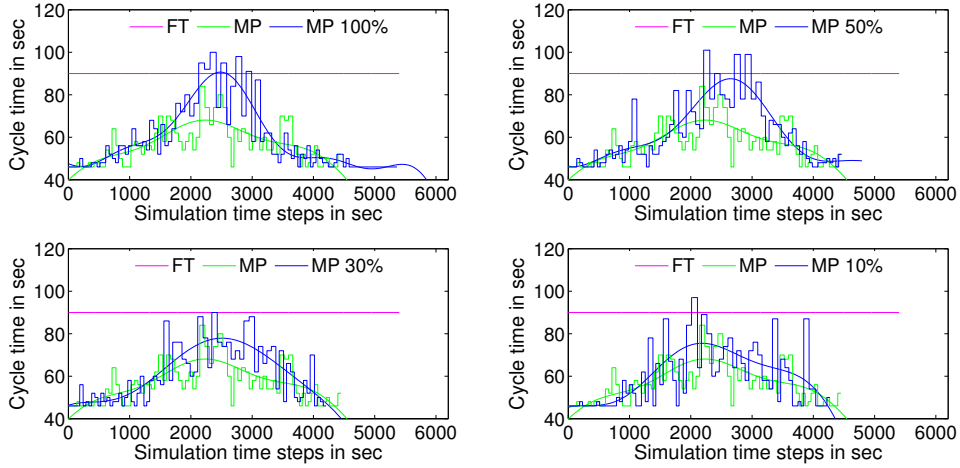


Figure 7.2: Cycle time of Fixed control and Max-pressure control cases for junction 5

simulation. Cycle data for each different control case belongs to the simulation closer to the average delay index, so it is not directly comparable to each other. Therefore, the following conclusions relate to the general tendency of cycle time configuration for each control case. The junctions 5, 6 and 9 was selected as there is a high demand on these junctions and therefore considered important. In addition, in order to make the chart information clearer, Equation 7.1 was fitted to cycle data of Max-pressure control cases.

$$a1 \cdot \sin(b1 \cdot x + c1) + a2 \cdot \sin(b2 \cdot x + c2) + a3 \cdot \sin(b3 \cdot x + c3) \quad (7.1)$$

Observing the graphs, we can see that Max-pressure shapes the cycles with the expected tendency at the highest rates of connected vehicles where the information about the network traffic state is high. More precisely, the algorithm forms low cycles at the beginning of the simulation where demand is still low, then increases the cycles in the high demand period and towards the end of the simulation again throws the cycles at the lowest price, indicating that by the decisions it took, manages to serve the demand and thus clear the queues.

However, at the lower penetration rates, especially at 10%, the cycles do not seem to be shaped this way. At the end of the simulation, at nodes 5 and 9 we see that high cycles are formed because there are still high queues in the network; so the algorithm did not perform well enough. That is explained by the second by second control decisions which are taken with the use of inaccurate estimations.

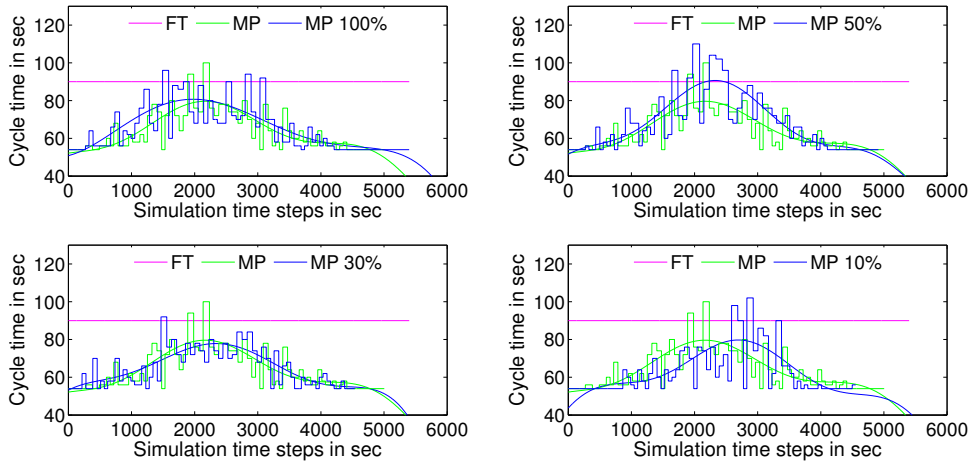


Figure 7.3: Cycle time of Fixed control and Max-pressure control cases for junction 6

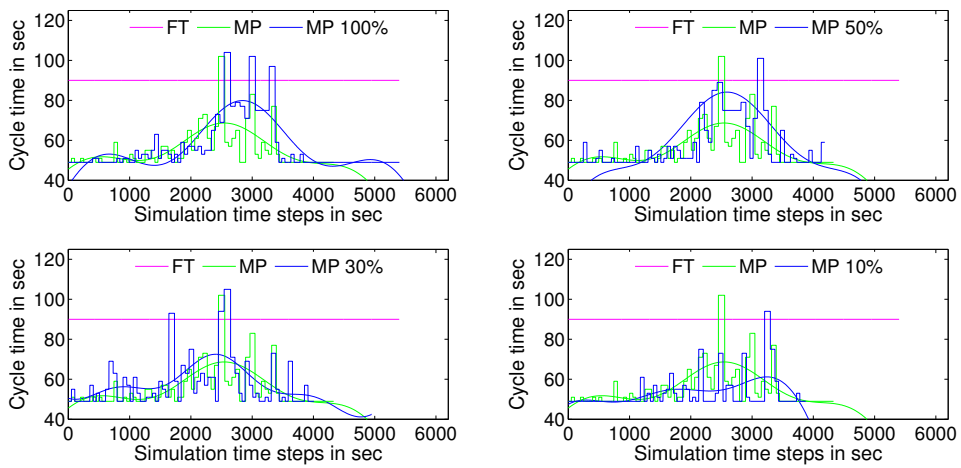


Figure 7.4: Cycle time of Fixed control and Max-pressure control cases for junction 9

## 7.4 Strategies Comparison

Table 7.5 summarize Max-pressure and TUC results in terms of the calculated criteria of delay and density for the network as a whole. According to these results, both examined real-time control methods perform significantly better than fixed-time control in case of detector scenario or in connected vehicle scenario of any penetration rate, except of Max-pressure case with 10% connected vehicle rate. Max-pressure case with 100% connected vehicle rate, outperforms all the others, achieving reductions in delay and density at the levels of about 40.4% and 31.3%, respectively. Next best performance is the Max-pressure algorithm with 50% connected vehicle rate, achieving reductions in delay and density at the levels of about 35.8% and 27.0%. However, the worst performance occurs in the case of Max-pressure with 10% connected vehicle rate, leading to an increase in delay and density at the levels of about 0.7% and 5.0% respectively. Results show that Max-pressure algorithm achieve a better performance in penetration rates higher or near to 50% while TUC is superior to Max-pressure in lower penetration rates achieving better average delay time and average density. We have to remind that the TUC strategy does not use all the modules that improve its performance. At the low demand periods if there was inflow or outflow information, TUC could use its Hybrid form or local actuation control respectively and achieve higher improvements.

Evaluation Data				
	Average Delay (sec/km)	% Improvement of average de- lay compered to fixed control	Average Density (veh/km)	% Improvement of average den- sity compered to fixed control
FT	179.6		11.2	
TUC	122.0	32.1	8.1	27.7
TUC 100 %	125.9	29.9	8.4	25.1
TUC 50 %	124.3	30.8	8.3	25.9
TUC 30 %	122.6	31.7	8.1	27.3
TUC 10 %	126.8	31.8	8.3	25.7
MP	118.1	34.2	8.4	25.3
MP 100 %	106.9	40.4	7.7	31.3
MP 50 %	115.2	35.8	8.2	27.0
MP 30 %	129.1	28.1	9.0	19.2
MP 10 %	180.9	-0.7	11.7	-5.0

Table 7.5: Strategies evaluation data

# Chapter 8

## Epilogue

### 8.1 Conclusions

Finally, some conclusions were drawn from this work related to the two issues examined in this thesis; the reliability of mathematical modeling approach (4.10) described at Section 4.3 and evaluated at Section 6.3, and the performance of TUC and Max-pressure strategies, after the integration of the approach, which was evaluated in Chapter 7.

#### 8.1.1 Conclusions for Chapter 6

In Chapter 6 it was shown the statistical analysis results of tested mathematical approach (4.10), which achieves real-time queue estimation, based on connected vehicle measurements. Results have shown that the mathematical approach provide accurate estimates for different tested penetration rates, hence the overall estimation methodology described in Section 4.3 is satisfactorily effective. The key points are, that the estimation accuracy decreases as the penetration rate of connected vehicles decreases and the approach does not present overestimation or underestimation tendency. Therefore, it was proved that connected vehicles could function as accurate moving sensors of traffic state in an urban traffic network, providing information which reliability increases as the penetration rate increases.

#### 8.1.2 Conclusions for Chapter 7

In Chapter 7, the statistical evaluation of real-time control strategies, TUC and Max-pressure, was performed in case of traffic state information from detectors or from connected vehicles (using the mathematical model (4.10)), using the delay and density indicators.

According to these results, both examined real-time control methods perform significantly better than fixed-time control in case of any penetration rate of connected vehicles or in detector scenario, except from Max-pressure algorithm in case of 10% penetration rate. As far as it concerns TUC strategy, results presented in Chapter 7.2 have shown that in all different connected vehicle cases, strategy remain roughly stable on its performance. This is due to the use of the average information collected during a cycle, and thus the elimination of instantaneous errors that may occur at low rates of connected vehicles. Also, the performance of TUC in

spot detector case is not significantly different from that of connected vehicles. So we conclude that TUC strategy could work equally effectively when obtaining spot detector and connected vehicle information.

As far as it concerns Max-pressure algorithm in connected vehicle cases, we conclude that its performance improves as the penetration rate increases. This is because the algorithm uses time-step measurements (1 sec) and is strongly affected by faults in queue estimations especially in cases of low penetration rates of connected vehicles, where failures are more intense. Also from the results of Section 7.3 it appeared that the algorithm using connected vehicles exceeds the spot detector performance when on average at least half of the vehicles in the network are connected.

We therefore conclude that connected vehicles can operate reliably as moving sensors, providing TUC control strategy with accurate information of local traffic state in any case of penetration rate. The same applies to the Max-pressure algorithm only in existence of high connected vehicle penetration rates ( $\geq 30\%$ ).

## 8.2 Future Work

We could improve TUC strategy performance by using connected vehicles to make some flow estimations and use them for the hybrid-TUC strategy. We could also improve the stability of Max-pressure algorithm according to the penetration rate, by increasing the time of the decision making and using average queue estimations, but this is expected to reduce its performance for high penetration rates due to the delays in Max-pressure reactions. It is a trade-off that someone should examine because it is not clear how such a change could interact in an urban traffic network. Another way to improve Max-Pressure performance, especially in low penetration rates, is to provide smoothed queue estimations as input of the algorithm.

# Bibliography

- [1] Paul P.Jovanis and F.D.Hobbs. *Traffic control— Encyclopædia Britannica, Encyclopædia Britannica, inc.* 2018. URL: <https://www.britannica.com/technology/traffic-control>.
- [2] Wikipedia contributors. *Traffic light — Wikipedia, The Free Encyclopedia.* 2018. URL: [https://en.wikipedia.org/w/index.php?title=Traffic\\_light&oldid=861787923](https://en.wikipedia.org/w/index.php?title=Traffic_light&oldid=861787923).
- [3] Luo Qi. “Research on intelligent transportation system technologies and applications”. In: *Power Electronics and Intelligent Transportation System, 2008. PEITS’08. Workshop on.* IEEE. 2008, pp. 529–531.
- [4] Ashley Russell Kotwal, Soon Jae Lee, and Yoo Jae Kim. “Traffic Signal Systems: A Review of Current Technology in the United States”. In: *Science and Technology* 3.1 (2013), pp. 33–41.
- [5] Francesco Calabrese et al. “Real-time urban monitoring using cell phones: A case study in Rome”. In: *IEEE Transactions on Intelligent Transportation Systems* 12.1 (2011), pp. 141–151.
- [6] Mark Bartolomeo. “Internet of things: Science fiction or business fact”. In: *A Harvard Business Review Analytic Services Report, Tech. Rep* (2014).
- [7] Markos Papageorgiou et al. “Review of road traffic control strategies”. In: *Proceedings of the IEEE* 91.12 (2003), pp. 2043–2067.
- [8] Dipti Srinivasan, Min Chee Choy, and Ruey Long Cheu. “Neural networks for real-time traffic signal control”. In: *IEEE Transactions on Intelligent Transportation Systems* 7.3 (2006), pp. 261–272.
- [9] Madan G Singh and Andre Titli. *Systems: decomposition, optimisation, and control.* Pergamon, 1978.
- [10] LD Baskar, Bart De Schutter, and Hans Hellendoorn. “Decentralized traffic control and management with intelligent vehicles”. In: *Proceedings of the 9th TRAIL Congress, Delft, The Netherlands.* 2006.
- [11] Dennis I Robertson and R David Bretherton. “Optimizing networks of traffic signals in real time—the SCOOT method”. In: *IEEE Transactions on vehicular technology* 40.1 (1991), pp. 11–15.
- [12] Arthur G Sims and Kenneth W Dobinson. “The Sydney coordinated adaptive traffic (SCAT) system philosophy and benefits”. In: *IEEE Transactions on vehicular technology* 29.2 (1980), pp. 130–137.
- [13] Anastasios Kouvelas et al. “Maximum Pressure Controller for Stabilizing Queues in Signalized Arterial Networks”. In: 2421 (Dec. 2014), pp. 133–141.

- [14] Christina Diakaki, Markos Papageorgiou, and Kostas Aboudolas. “A multi-variable regulator approach to traffic-responsive network-wide signal control”. In: *Control Engineering Practice* 10.2 (2002), pp. 183–195.
- [15] Nathan H Gartner. *OPAC: A demand-responsive strategy for traffic signal control*. 906. 1983.
- [16] Jean-Jacques Henry, Jean Loup Farges, and J Tuffal. “The PRODYN real time traffic algorithm”. In: *Control in Transportation Systems*. Elsevier, 1984, pp. 305–310.
- [17] Pitu Mirchandani and Larry Head. “A real-time traffic signal control system: architecture, algorithms, and analysis”. In: *Transportation Research Part C: Emerging Technologies* 9.6 (2001), pp. 415–432.
- [18] F Boillot et al. “Optimal signal control of urban traffic networks.” In: *Road Traffic Monitoring, 1992 (IEE Conf. Pub. 355)*. IET. 1992, p. 75.
- [19] Diamantis Manolis et al. “Centralised vs decentralised signal control of large-scale urban road networks in real time: A simulation study”. In: *IET Intelligent Transport Systems* (2018).
- [20] Anastasios Kouvelas et al. “Adaptive performance optimization for large-scale traffic control systems”. In: *IEEE Transactions on Intelligent Transportation Systems* 12.4 (2011), pp. 1434–1445.
- [21] Diamantis Manolis et al. “Simulation investigations of the coordinated traffic-responsive signal control strategy TUC with actuation at the local junction level”. In: *European Transport Research Review* 10.2 (2018), p. 25.
- [22] Christina Diakaki et al. “Extensions and new applications of the traffic-responsive urban control strategy: Coordinated signal control for urban networks”. In: *Transportation Research Record: Journal of the Transportation Research Board* 1856 (2003), pp. 202–211.
- [23] Xiao-Feng Xie et al. “Real-time traffic control for sustainable urban living”. In: *Intelligent transportation systems (itsc), 2014 iee 17th international conference on*. IEEE. 2014, pp. 1863–1868.
- [24] Majid Rostami Shahrbabaki et al. “A data fusion approach for real-time traffic state estimation in urban signalized links”. In: *Transportation Research Part C: Emerging Technologies* 92 (2018), pp. 525–548.
- [25] Noah Goodall, Brian Smith, and Byungkyu Park. “Traffic signal control with connected vehicles”. In: *Transportation Research Record: Journal of the Transportation Research Board* 2381 (2013), pp. 65–72.
- [26] Christina Diakaki. “Integrated control of traffic flow in corridor networks”. In: *Ph. D. Thesis, Department of Production Engineering and Management, Technical University of Crete* (1999).



# Appendix A

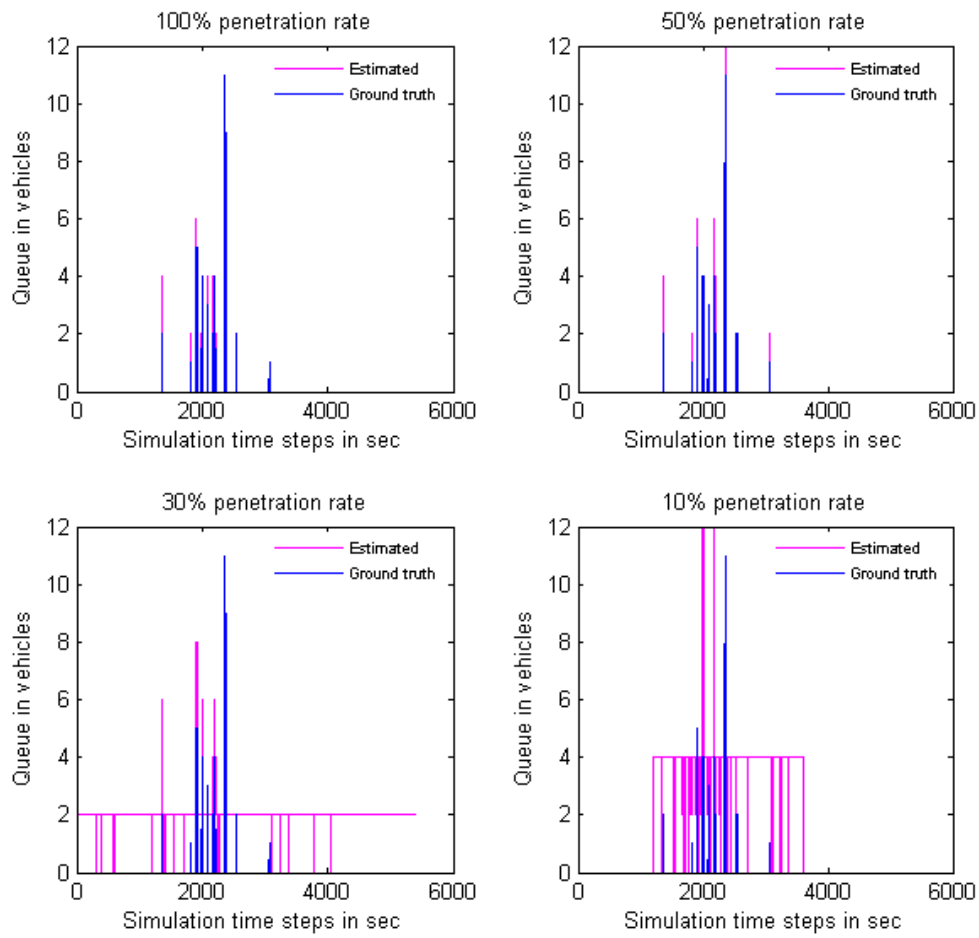


Figure A.1: Difference of queue estimation and real queue value for section L1, for different penetration rates

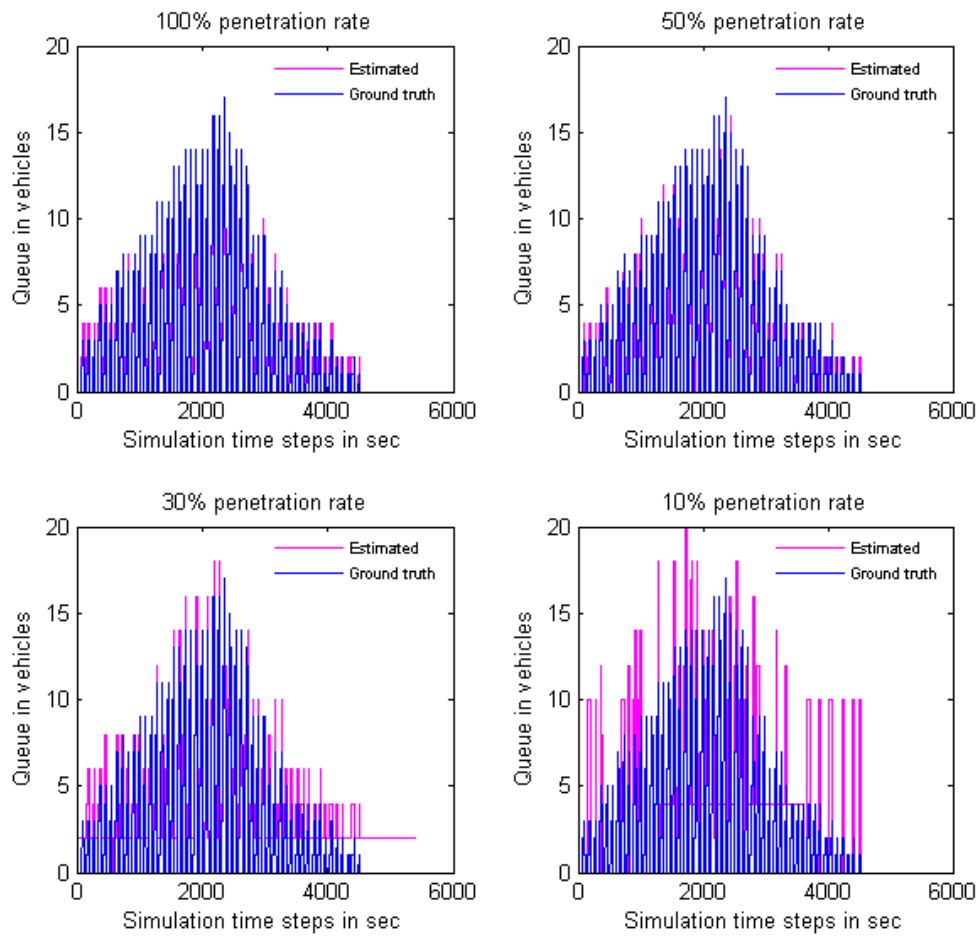


Figure A.2: Difference of queue estimation and real queue value for section O20, for different penetration rates

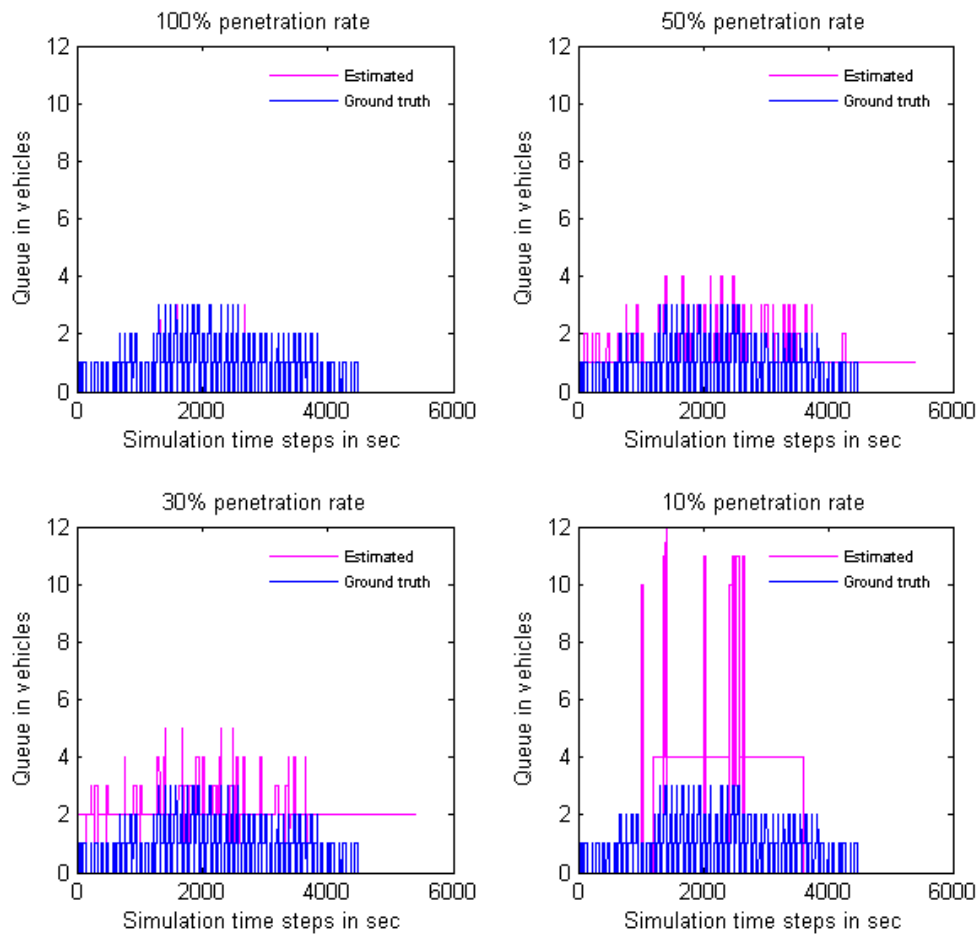


Figure A.3: Difference of queue estimation and real queue value for section O26, for different penetration rates

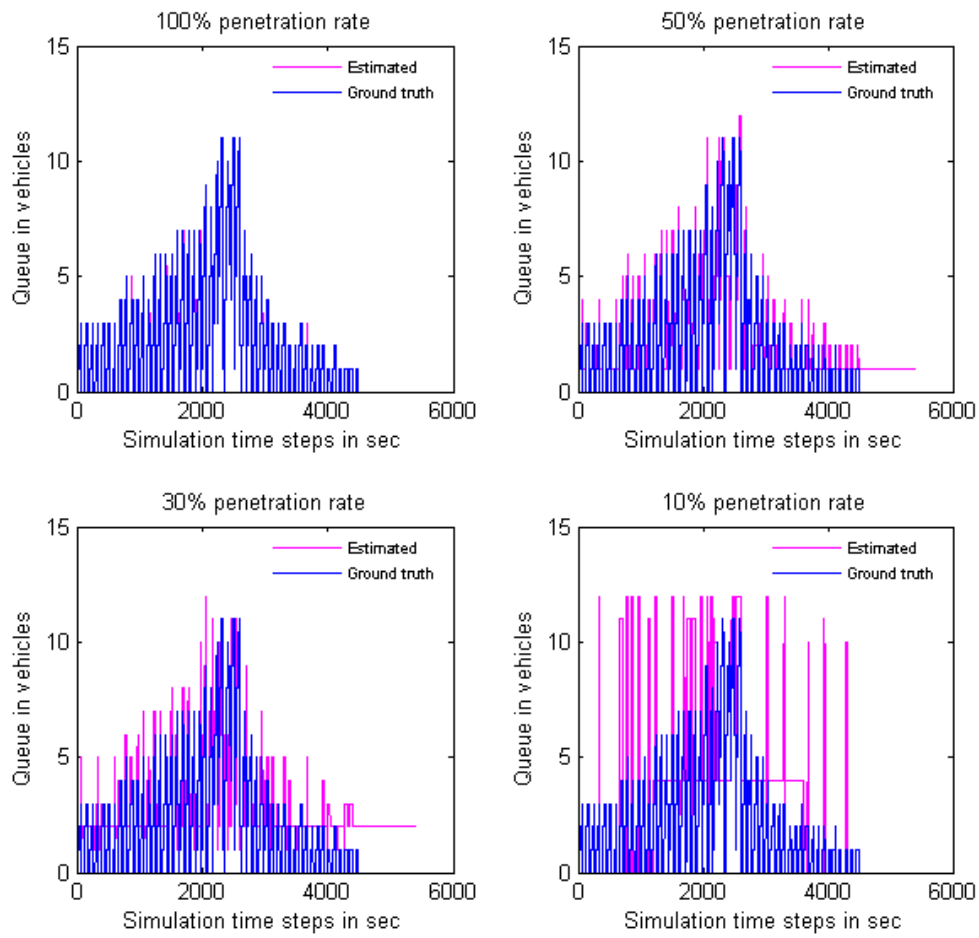


Figure A.4: Difference of queue estimation and real queue value for section O1, for different penetration rates

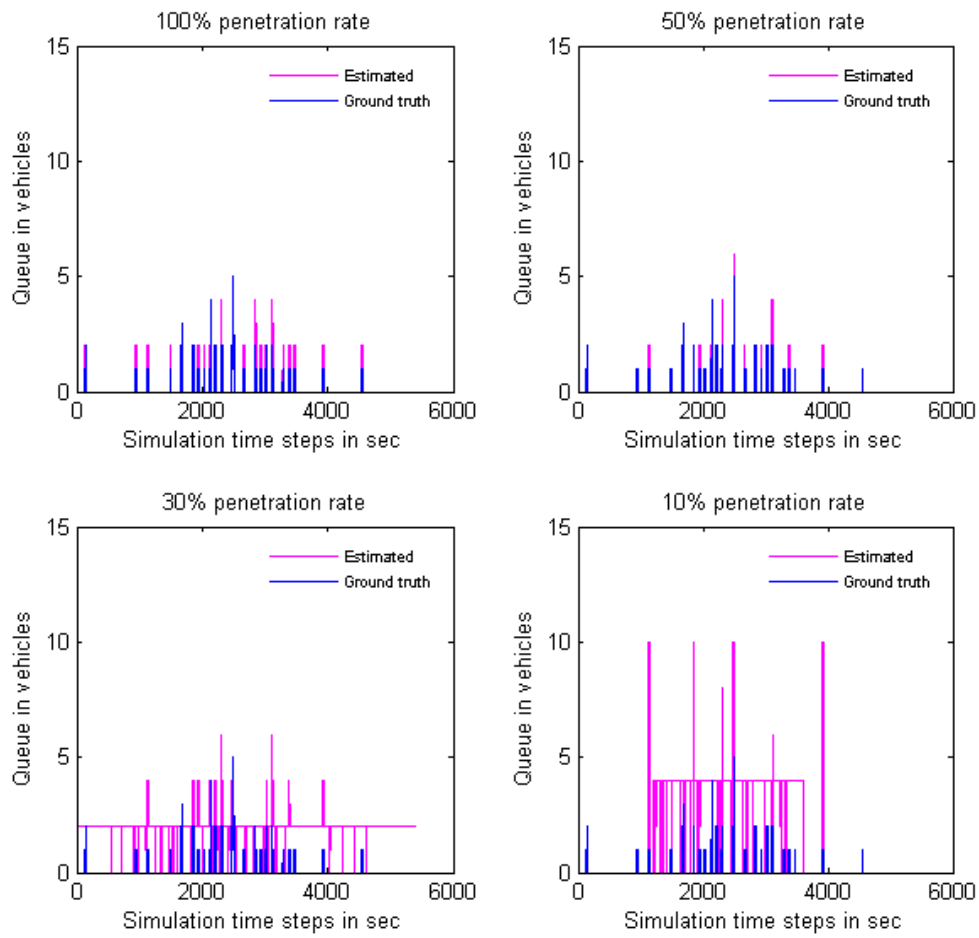


Figure A.5: Difference of queue estimation and real queue value for section L4, for different penetration rates

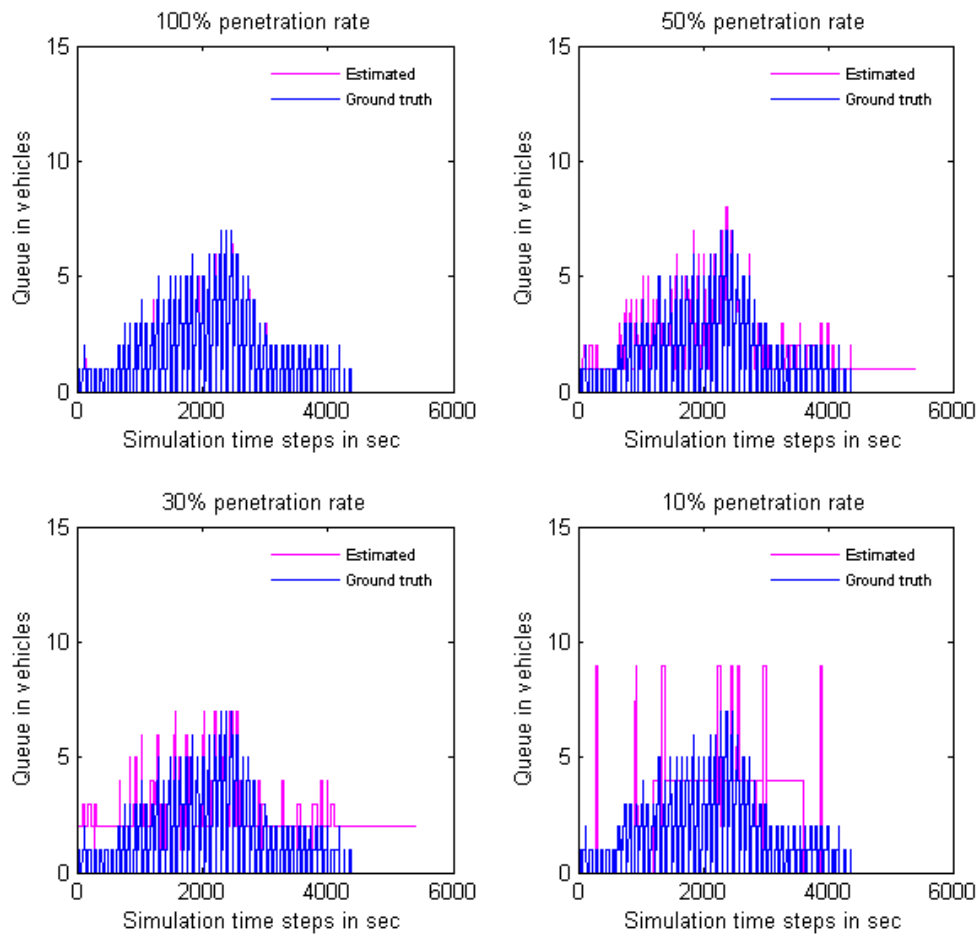


Figure A.6: Difference of queue estimation and real queue value for section O2, for different penetration rates

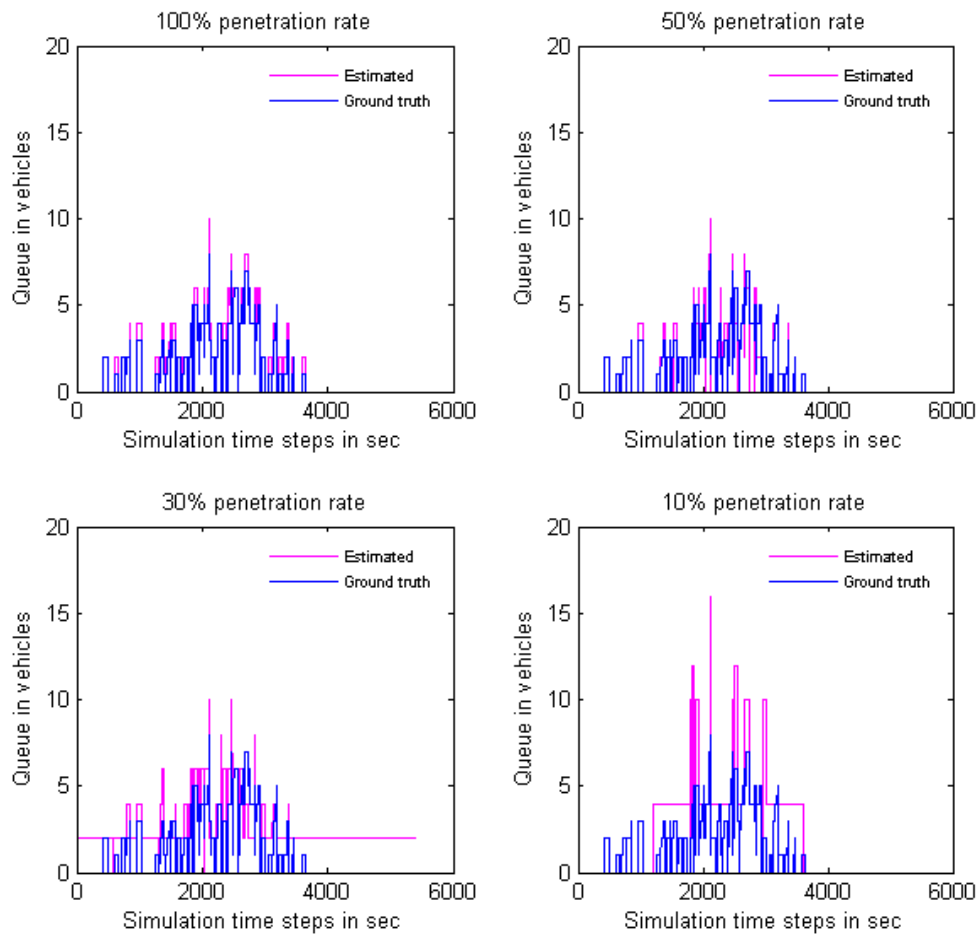


Figure A.7: Difference of queue estimation and real queue value for section L42, for different penetration rates

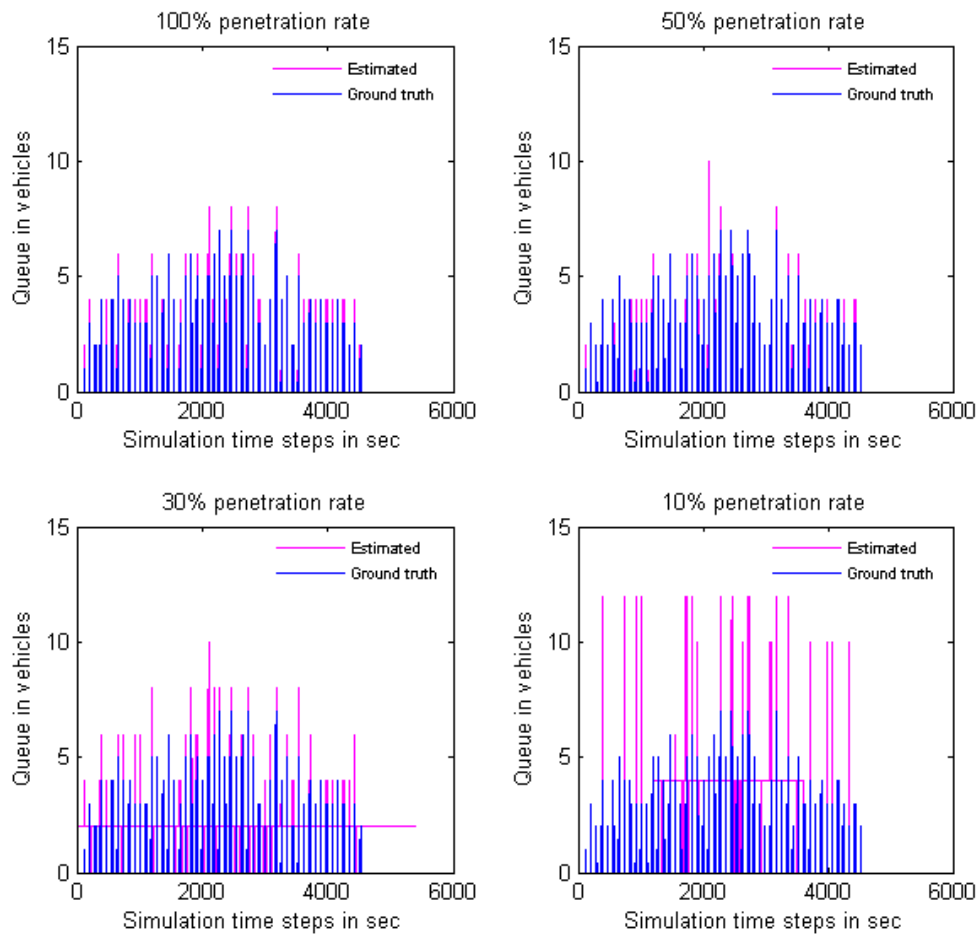


Figure A.8: Difference of queue estimation and real queue value for section L46, for different penetration rates

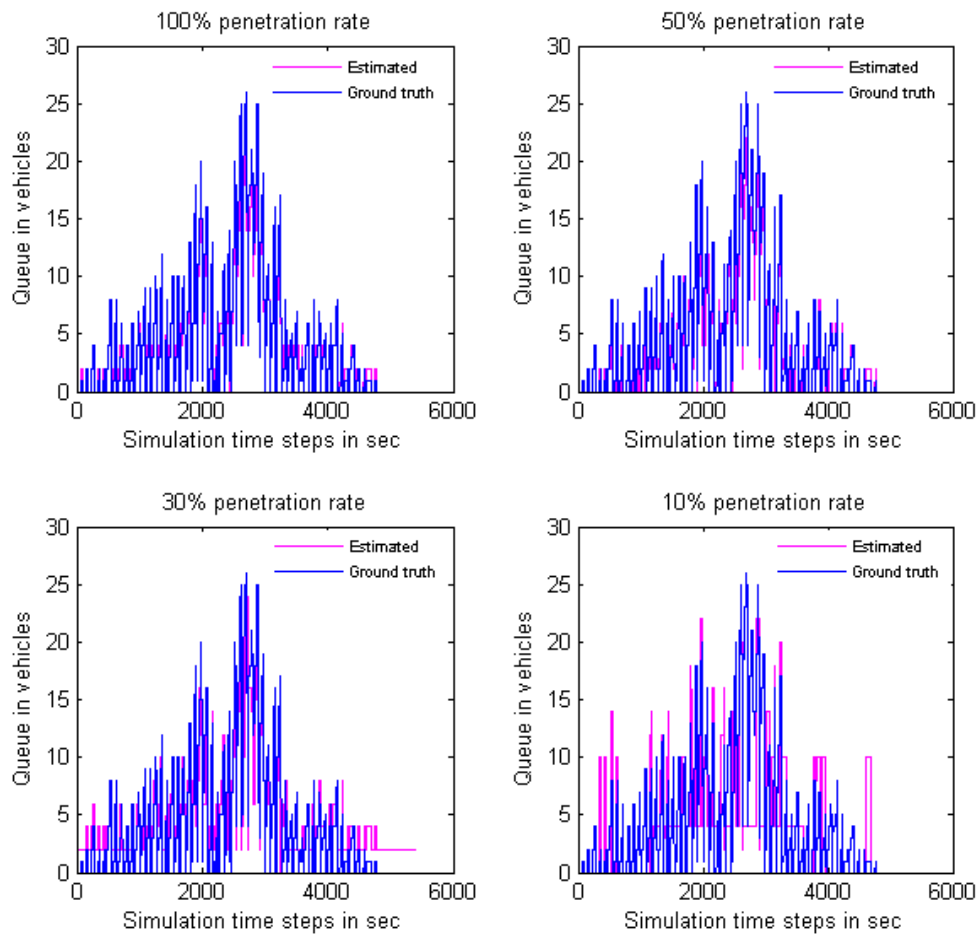


Figure A.9: Difference of queue estimation and real queue value for section L43, for different penetration rates

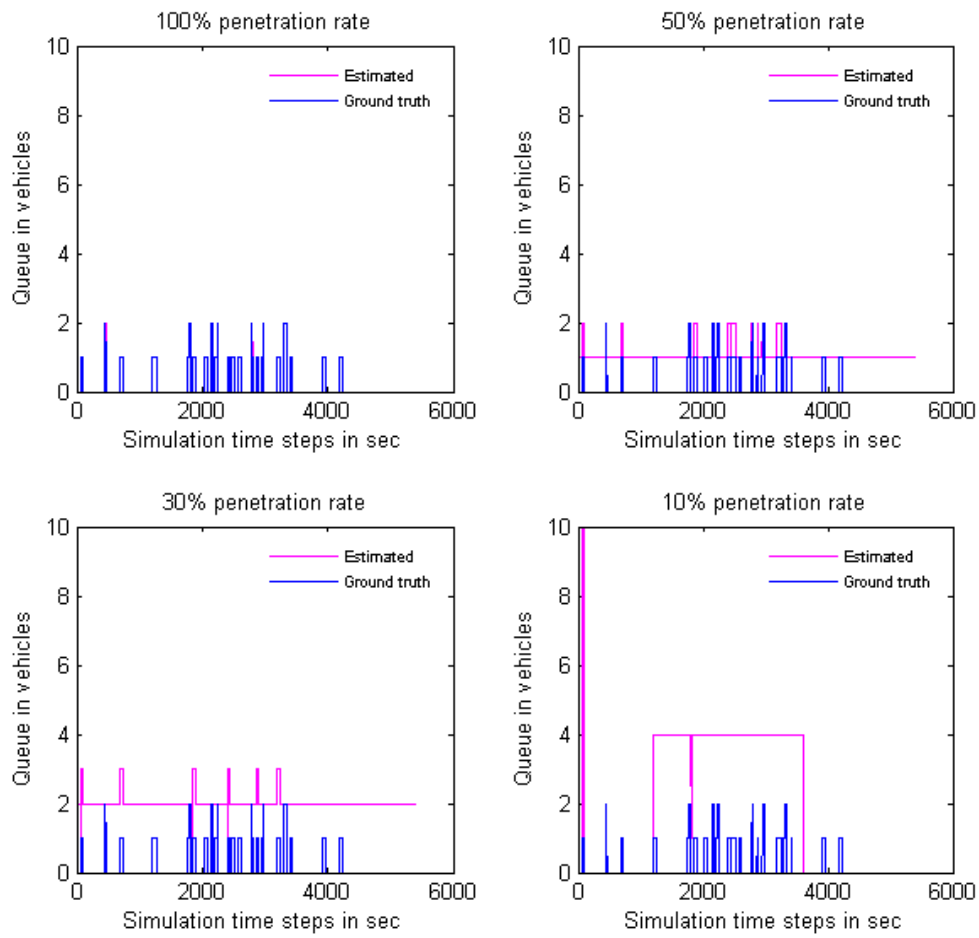


Figure A.10: Difference of queue estimation and real queue value for section O18, for different penetration rates

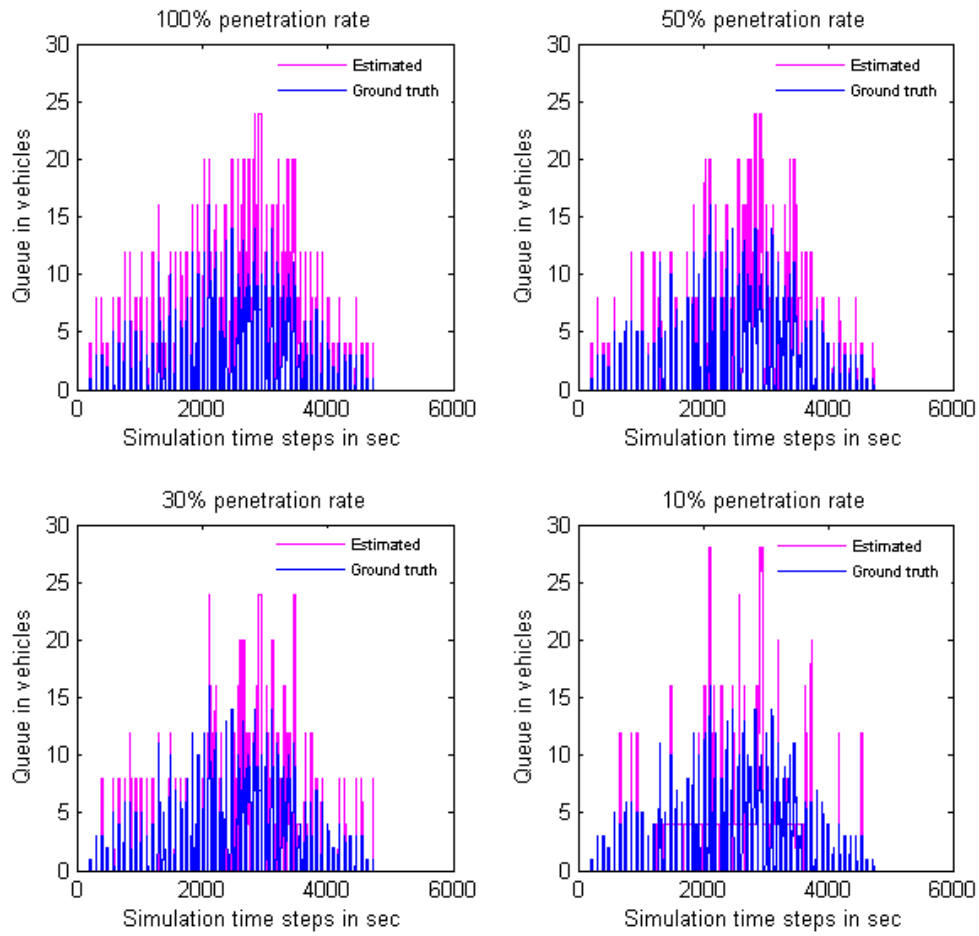


Figure A.11: Difference of queue estimation and real queue value for section L8, for different penetration rates

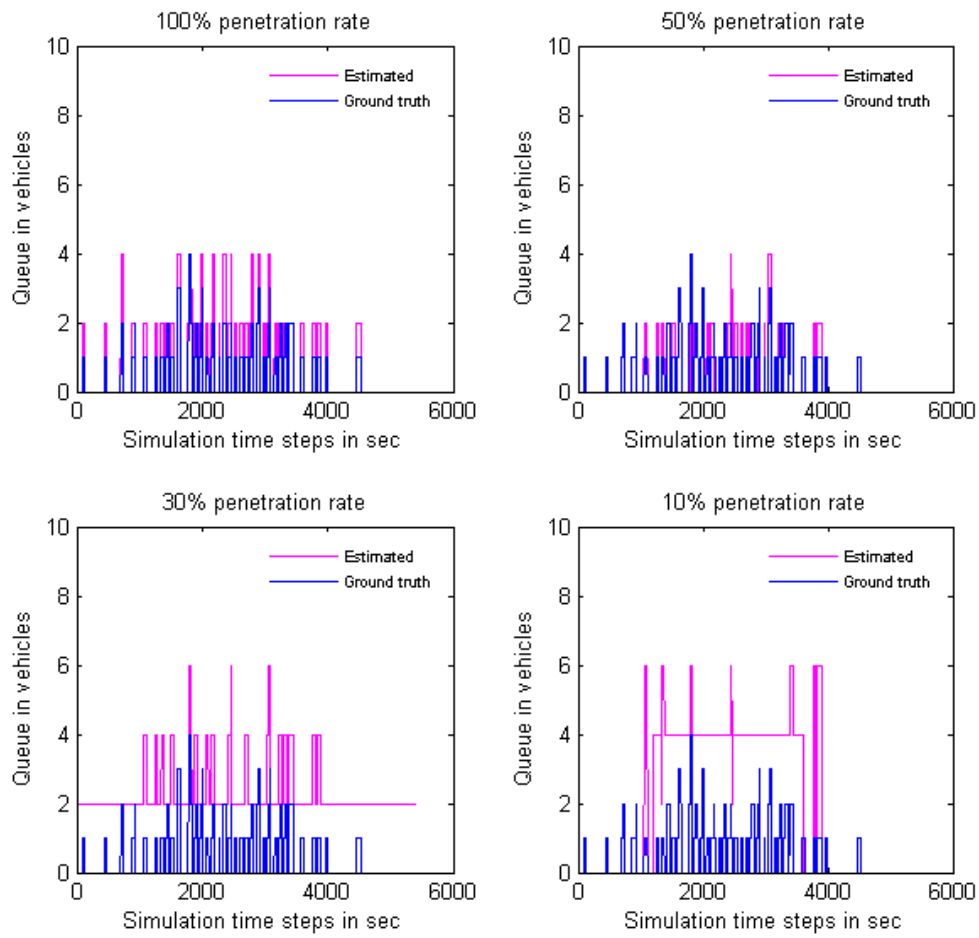


Figure A.12: Difference of queue estimation and real queue value for section O21, for different penetration rates

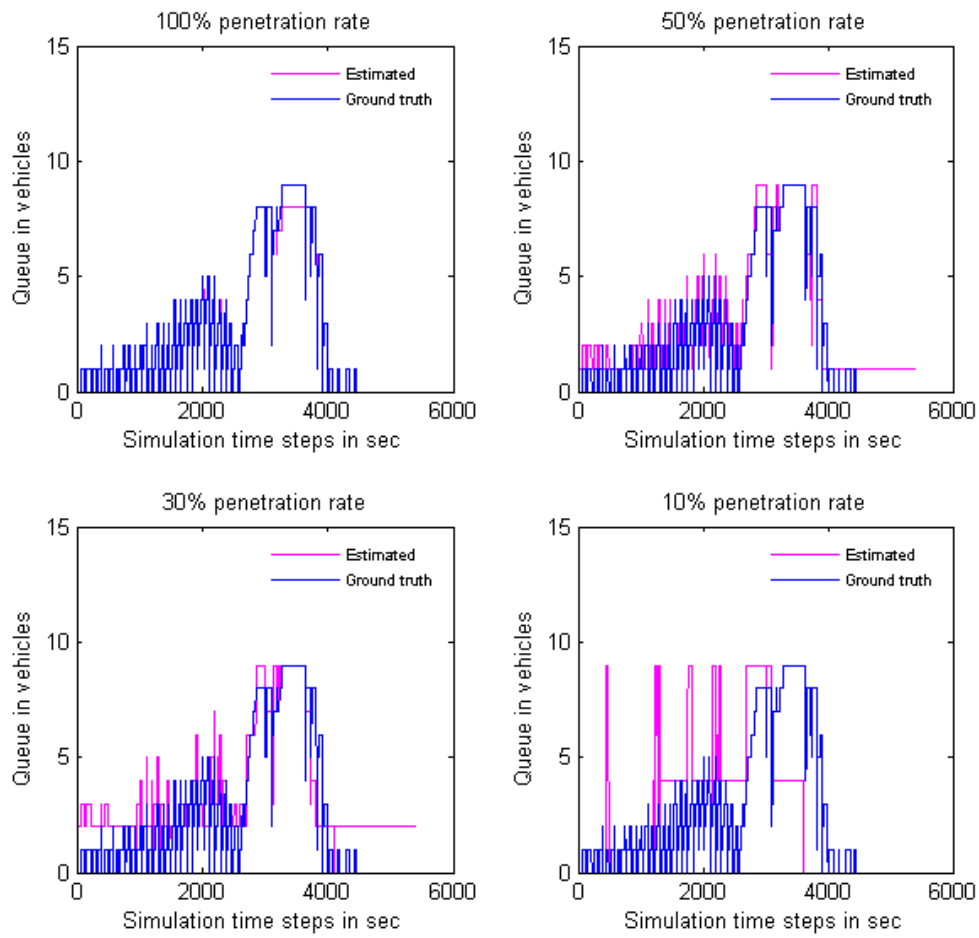


Figure A.13: Difference of queue estimation and real queue value for section O3, for different penetration rates

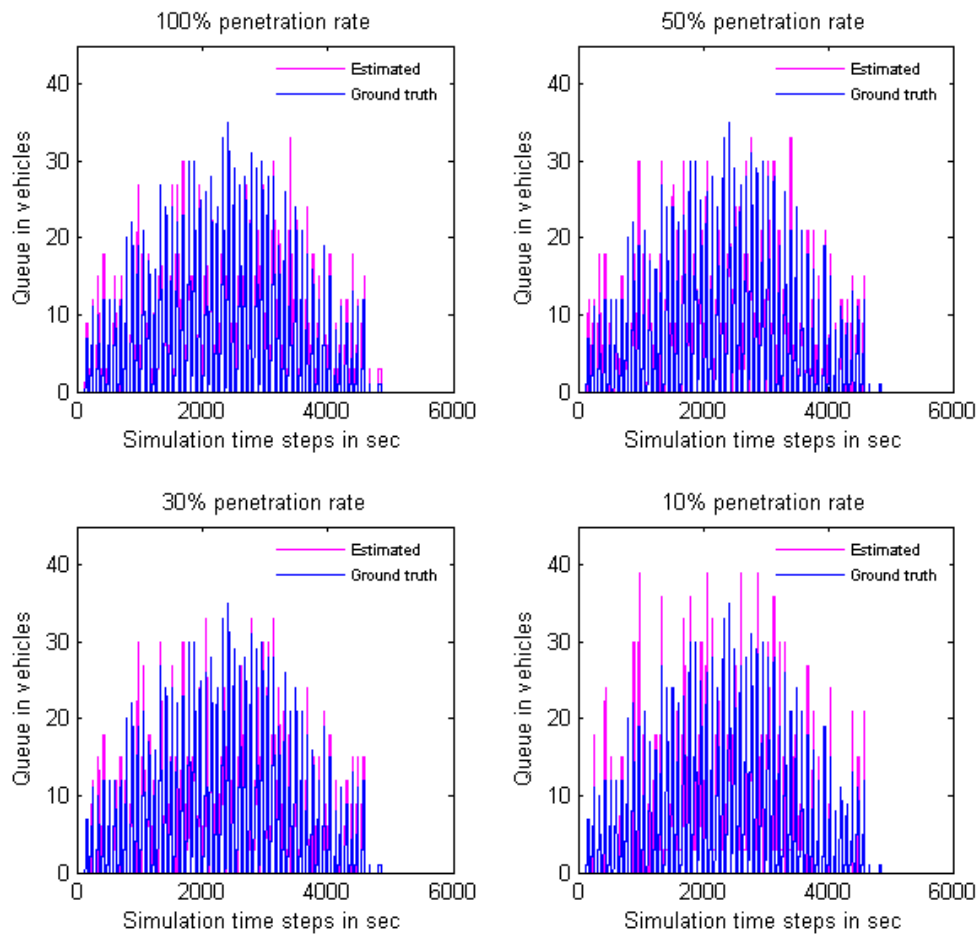


Figure A.14: Difference of queue estimation and real queue value for section L10, for different penetration rates

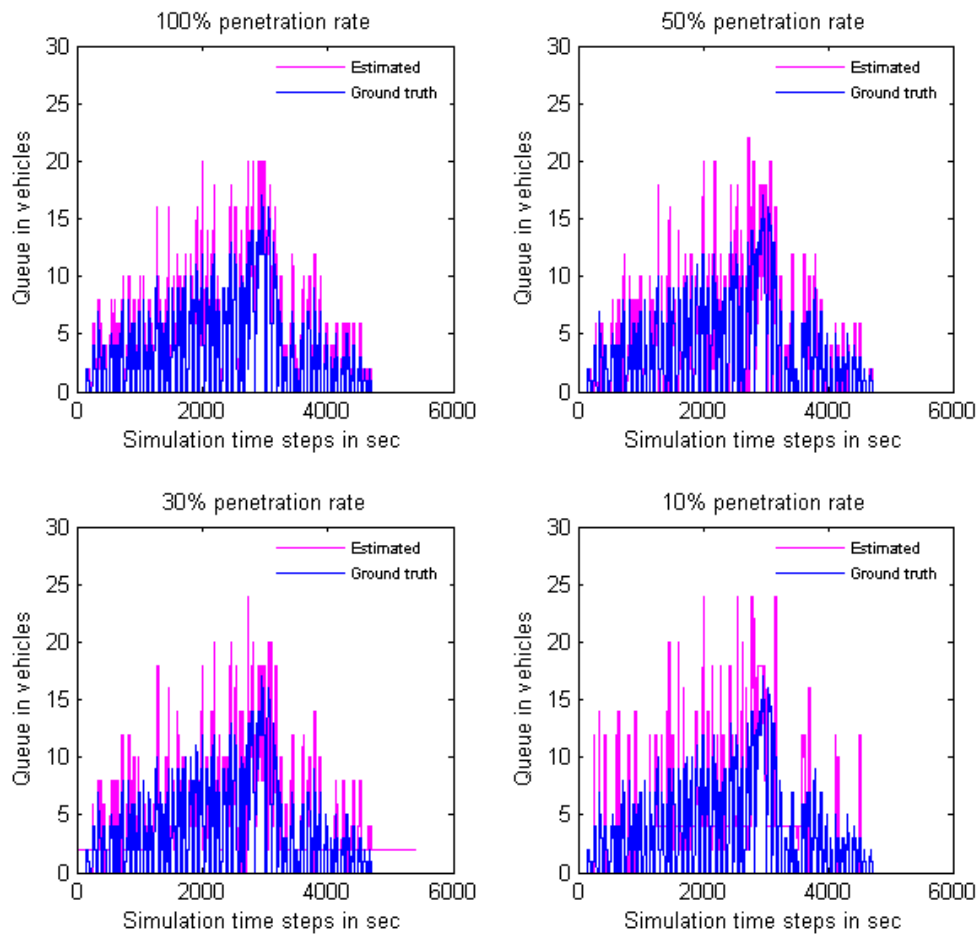


Figure A.15: Difference of queue estimation and real queue value for section L39, for different penetration rates

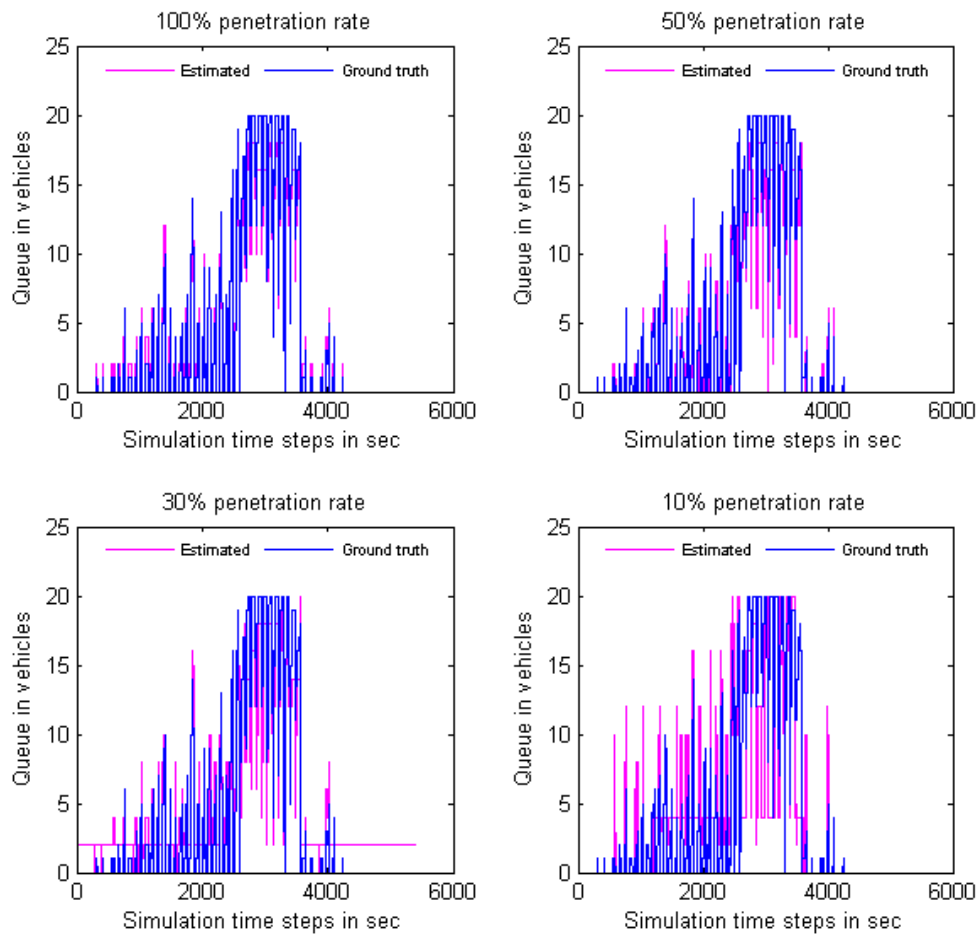


Figure A.16: Difference of queue estimation and real queue value for section L37, for different penetration rates

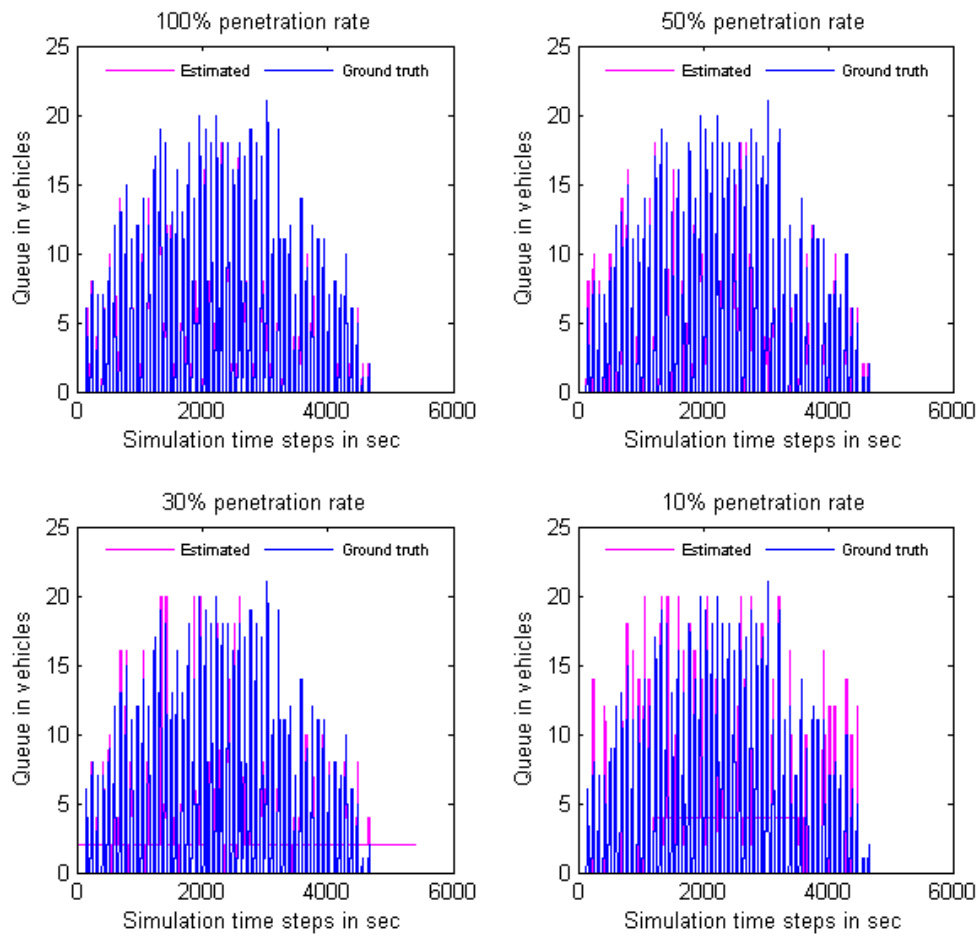


Figure A.17: Difference of queue estimation and real queue value for section L48, for different penetration rates

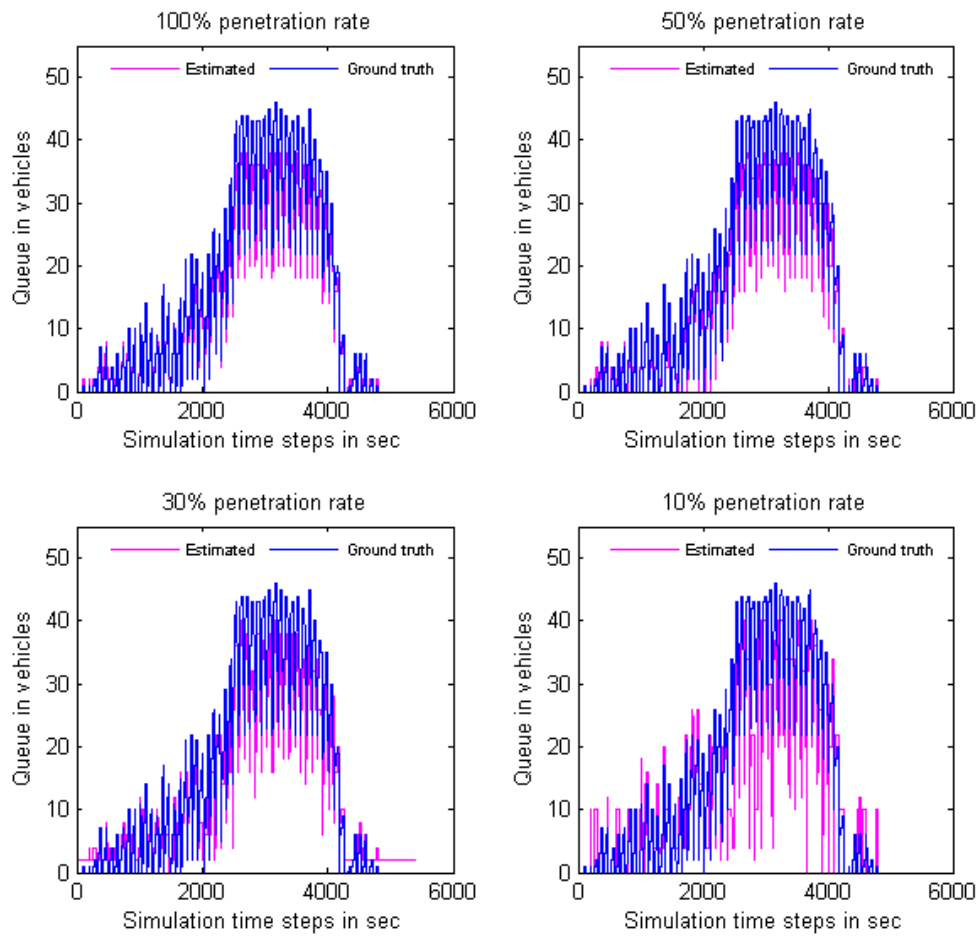


Figure A.18: Difference of queue estimation and real queue value for section L41, for different penetration rates

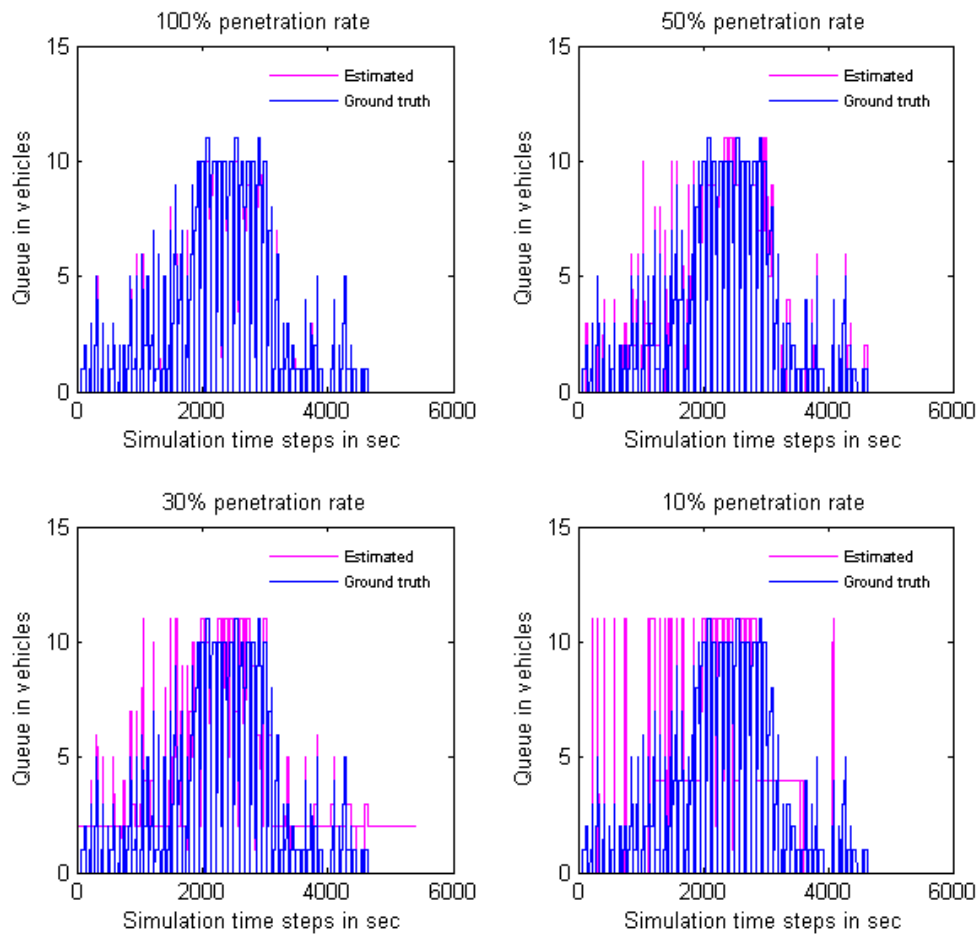


Figure A.19: Difference of queue estimation and real queue value for section L50, for different penetration rates

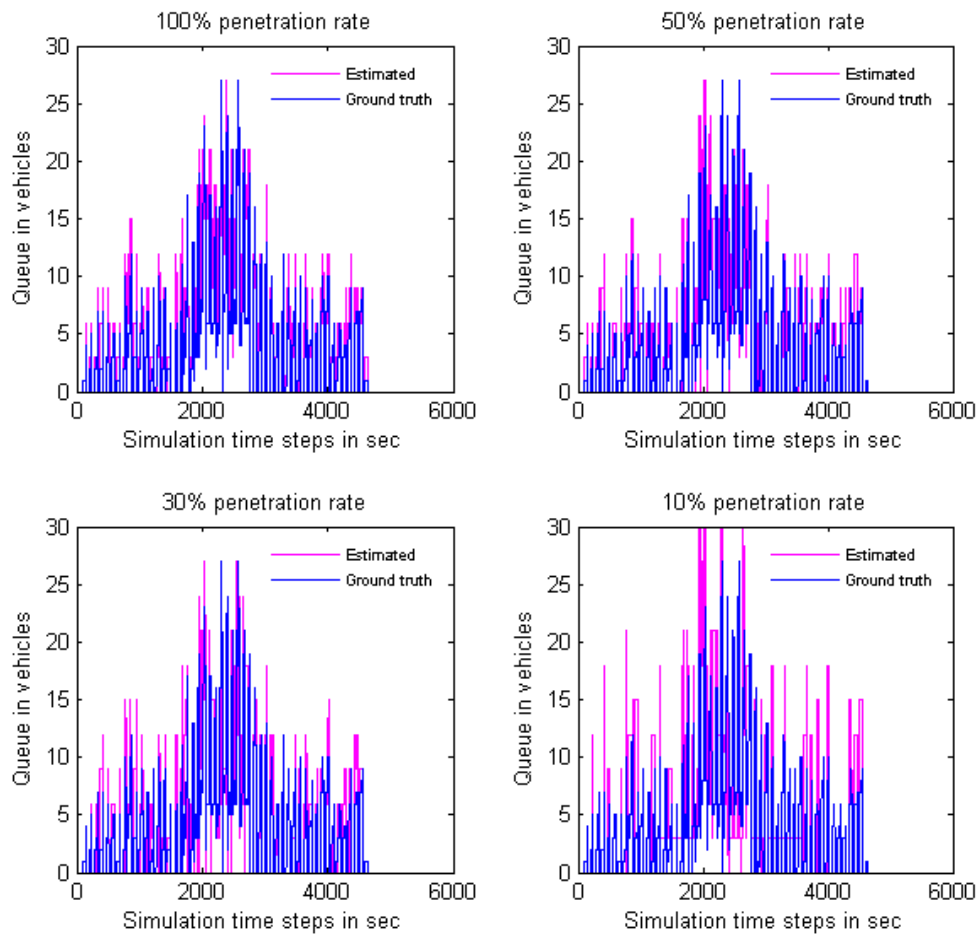


Figure A.20: Difference of queue estimation and real queue value for section L13, for different penetration rates

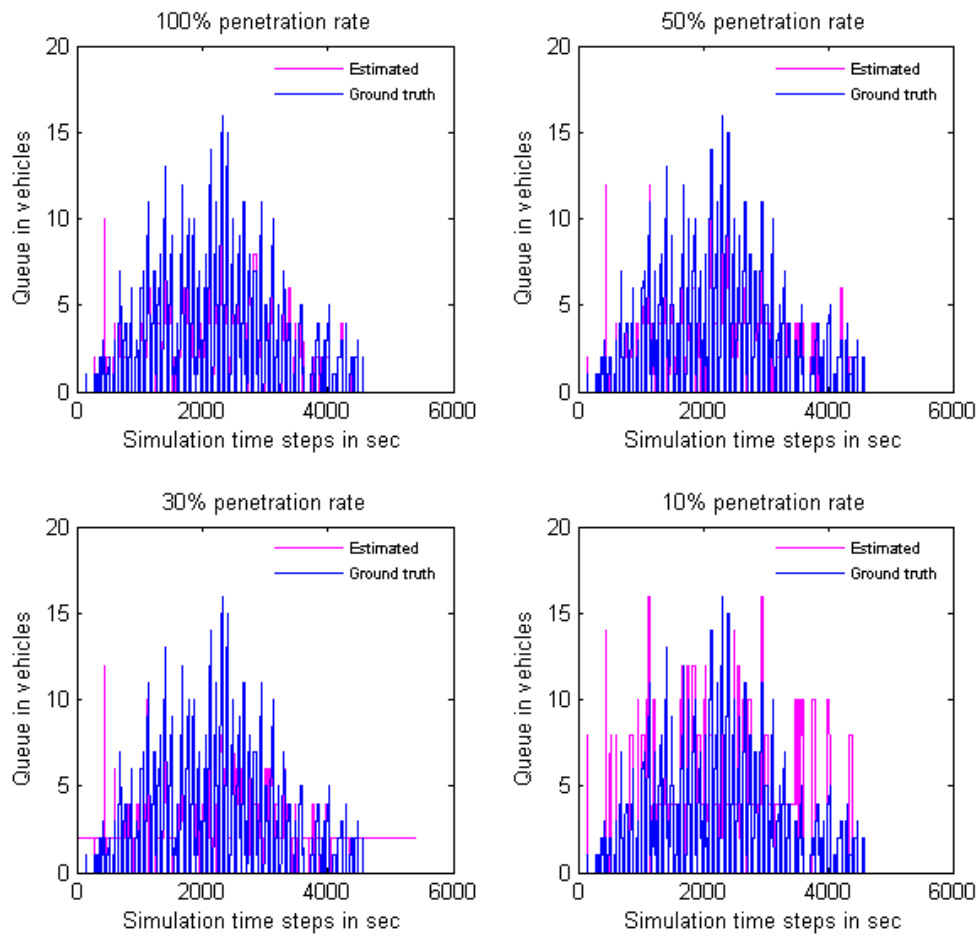


Figure A.21: Difference of queue estimation and real queue value for section L12, for different penetration rates

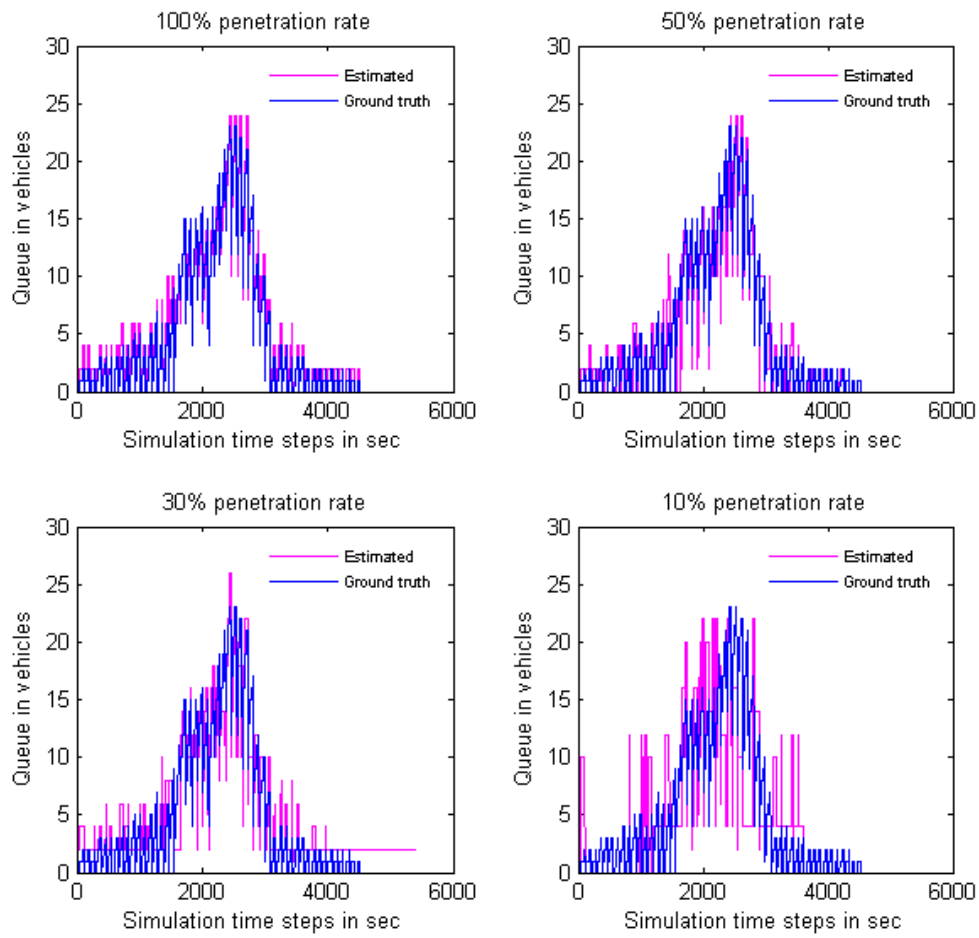


Figure A.22: Difference of queue estimation and real queue value for section O4, for different penetration rates

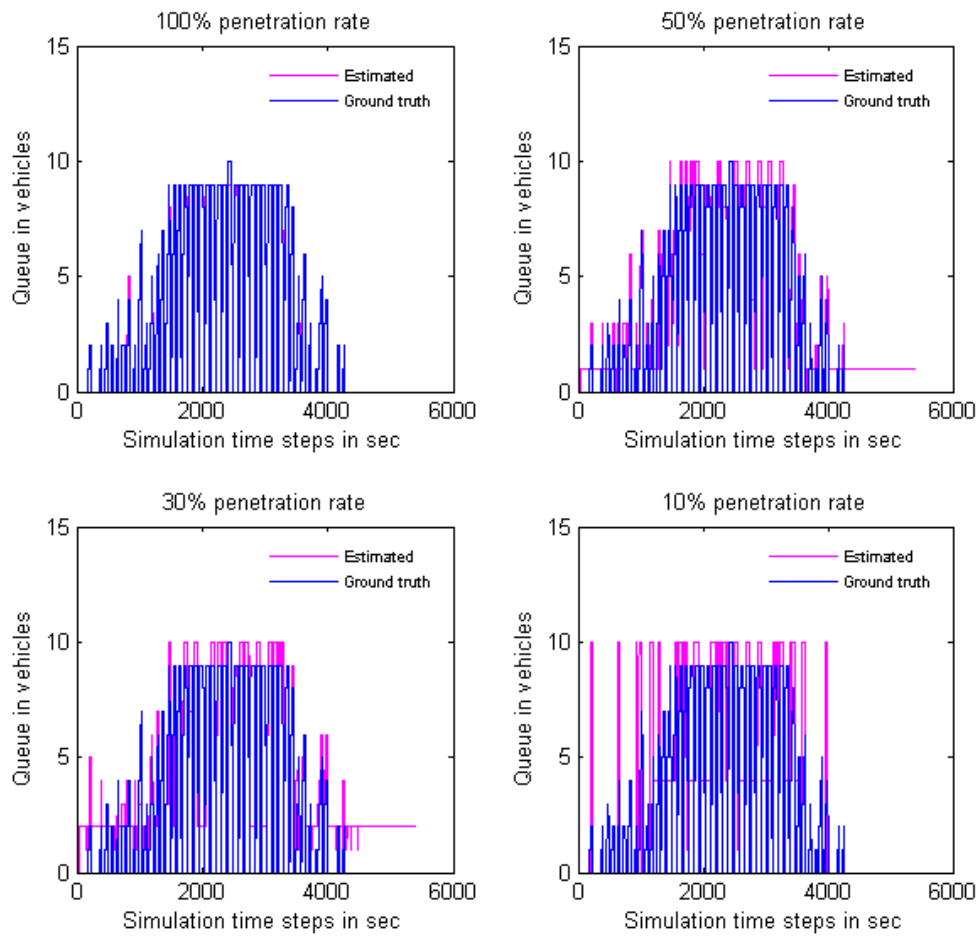


Figure A.23: Difference of queue estimation and real queue value for section L34, for different penetration rates

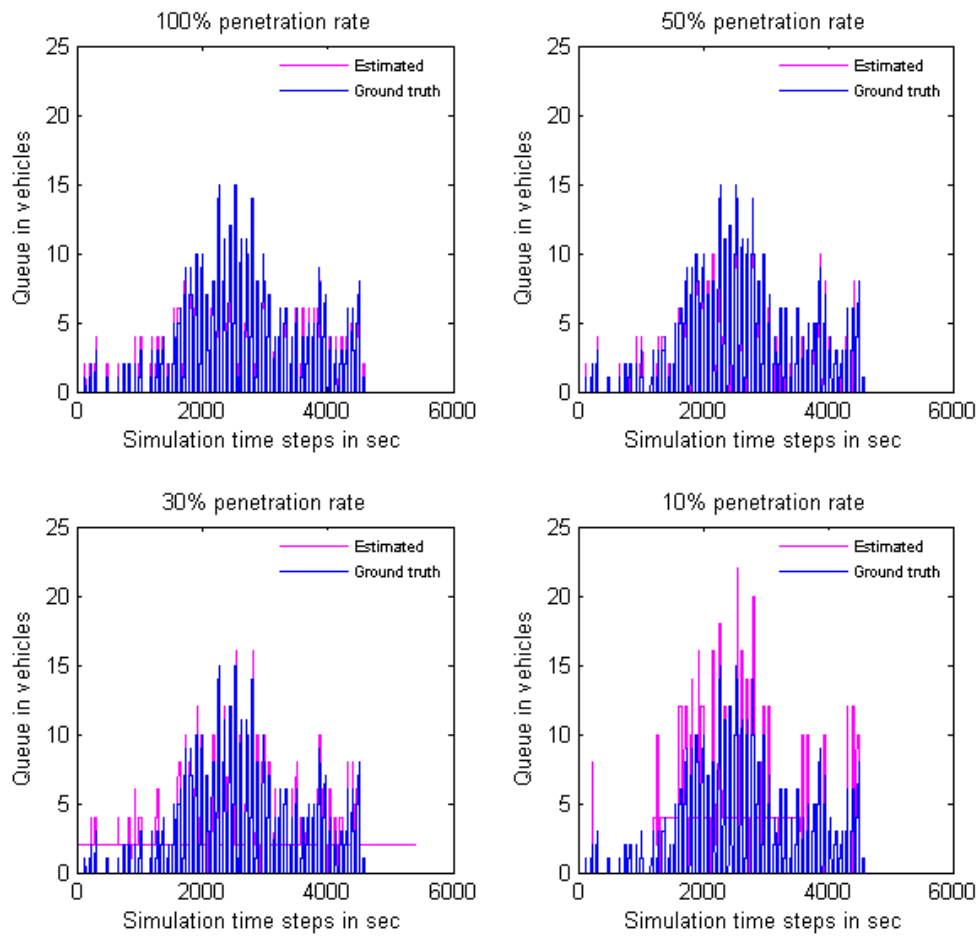


Figure A.24: Difference of queue estimation and real queue value for section L17, for different penetration rates

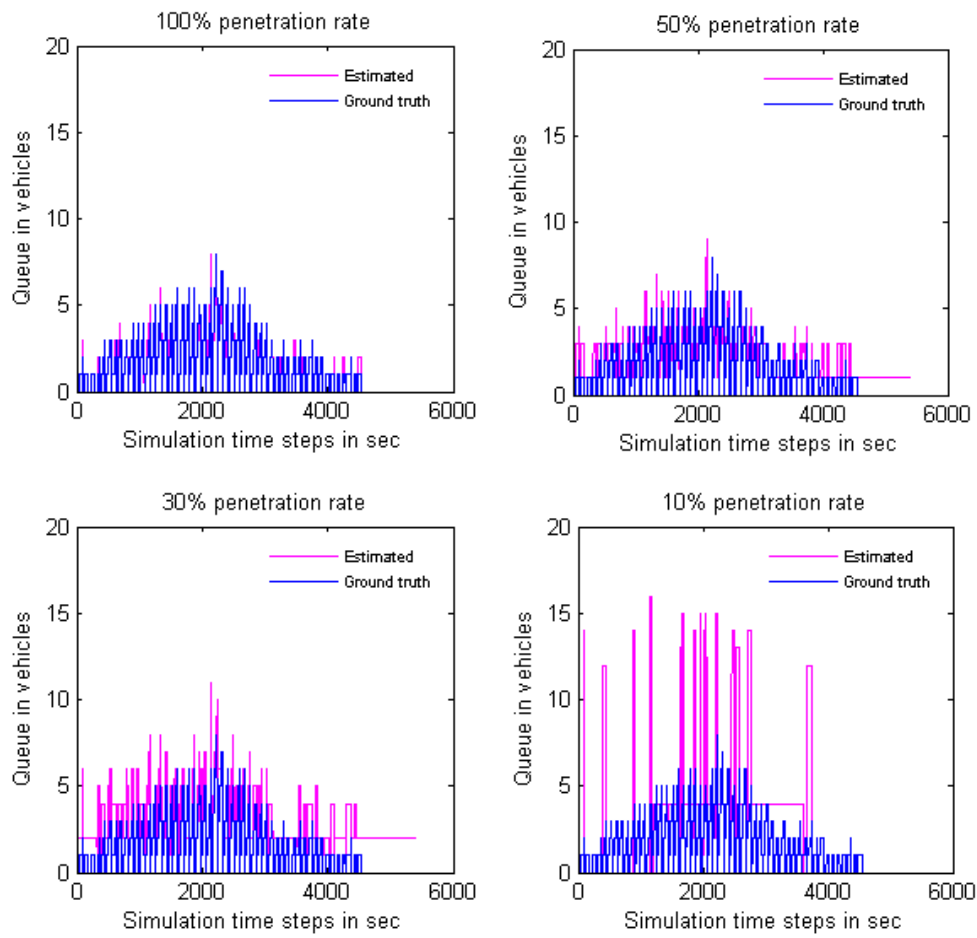


Figure A.25: Difference of queue estimation and real queue value for section O6, for different penetration rates

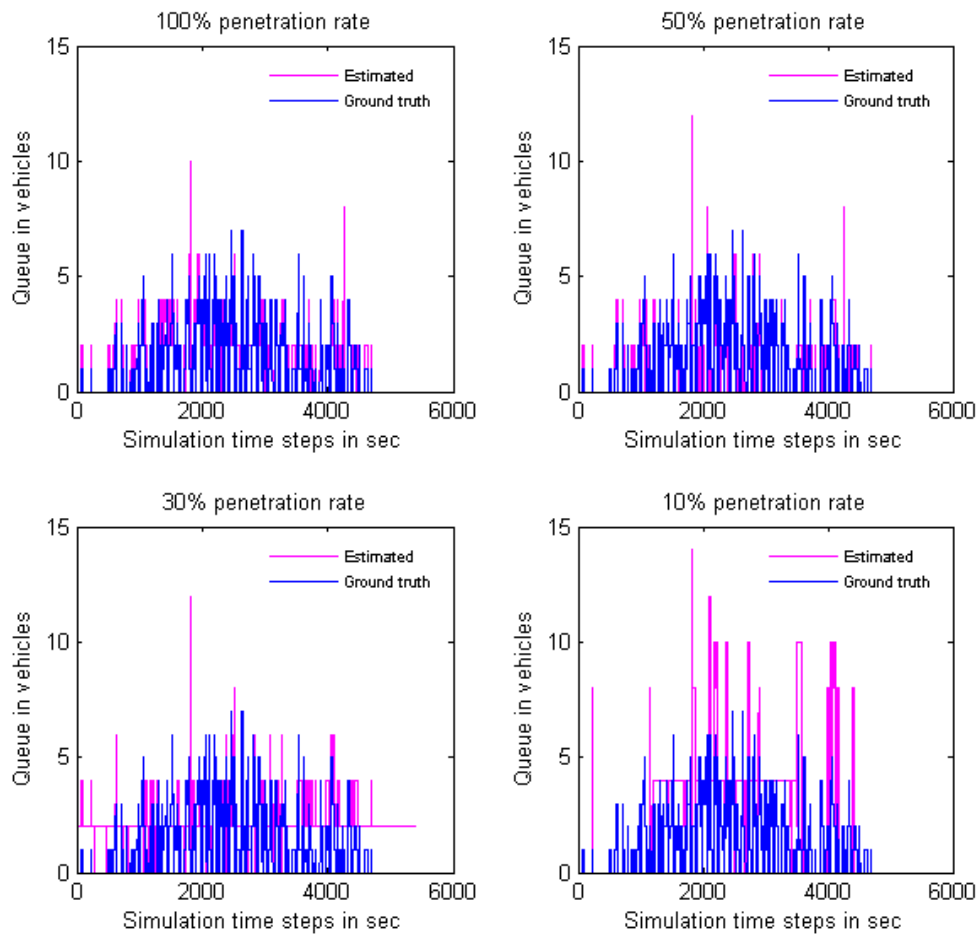


Figure A.26: Difference of queue estimation and real queue value for section L15, for different penetration rates

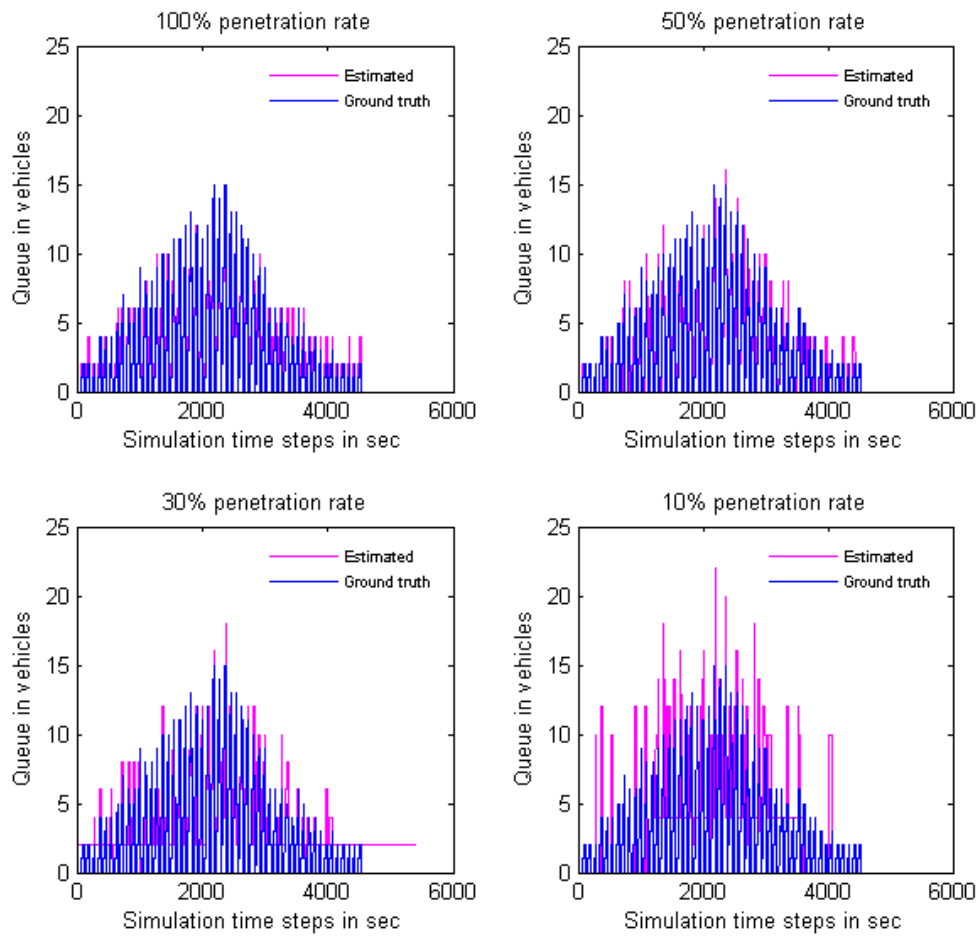


Figure A.27: Difference of queue estimation and real queue value for section O22, for different penetration rates

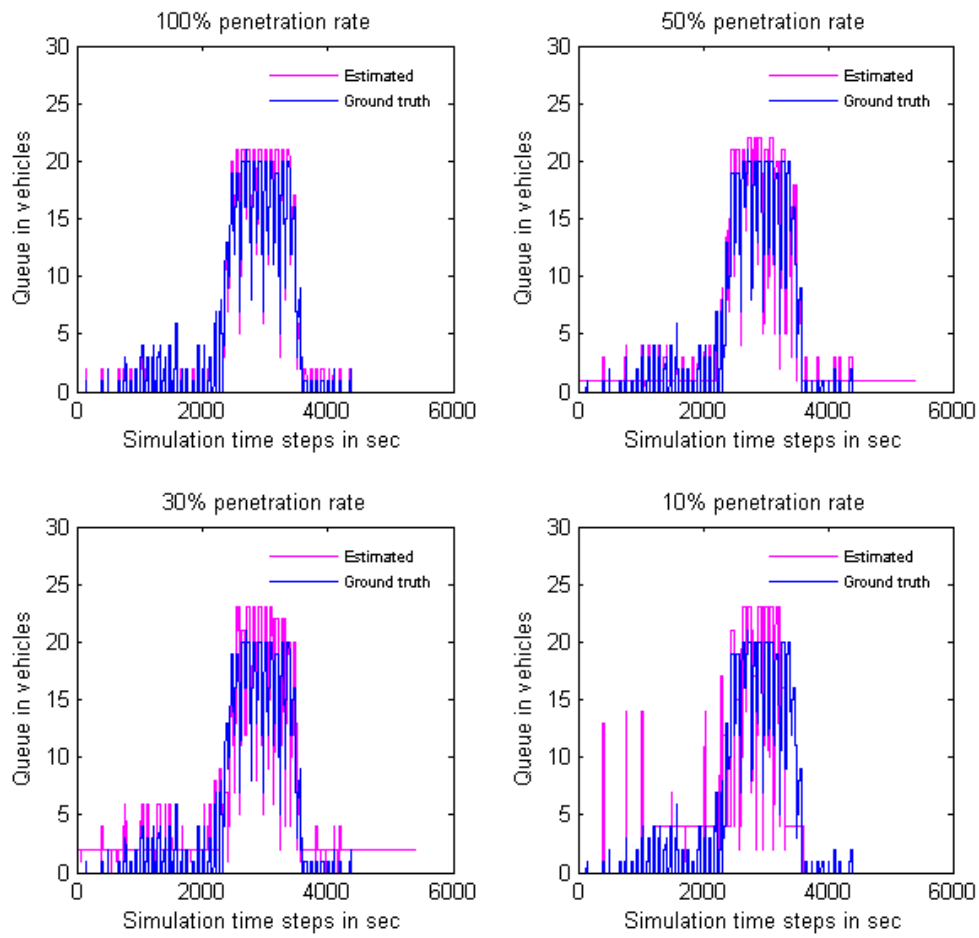


Figure A.28: Difference of queue estimation and real queue value for section L60, for different penetration rates

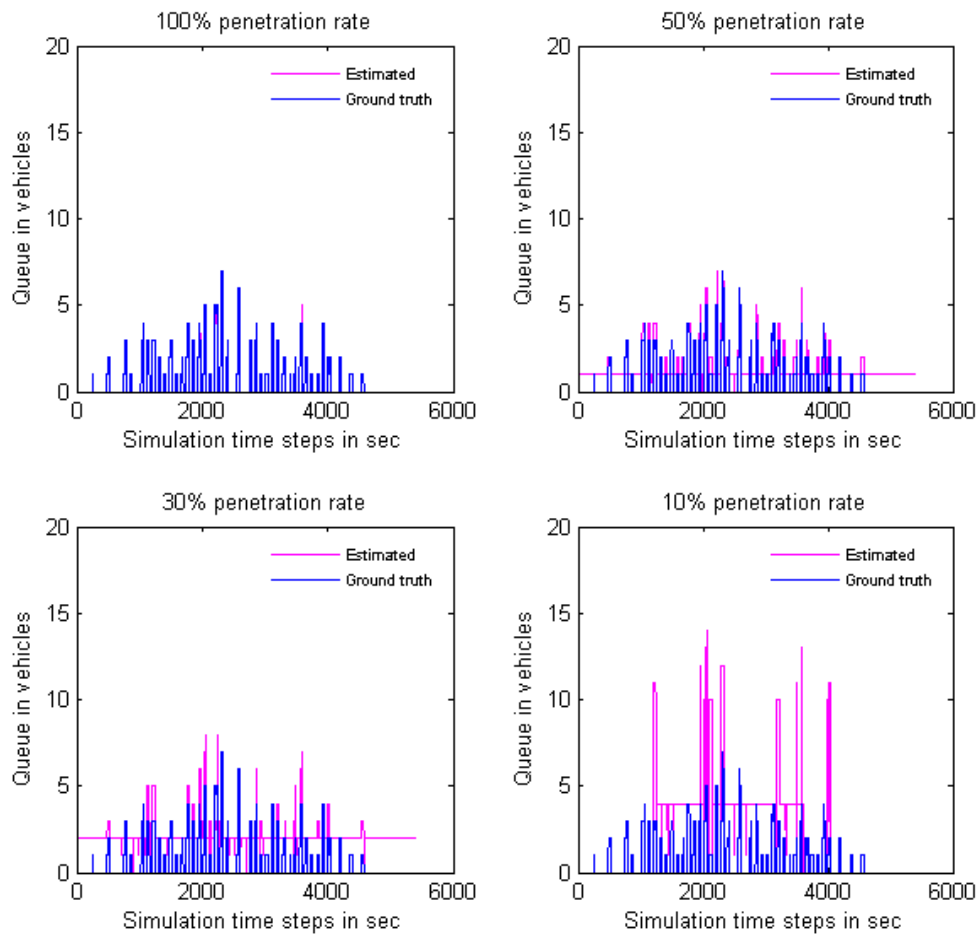


Figure A.29: Difference of queue estimation and real queue value for section L56, for different penetration rates

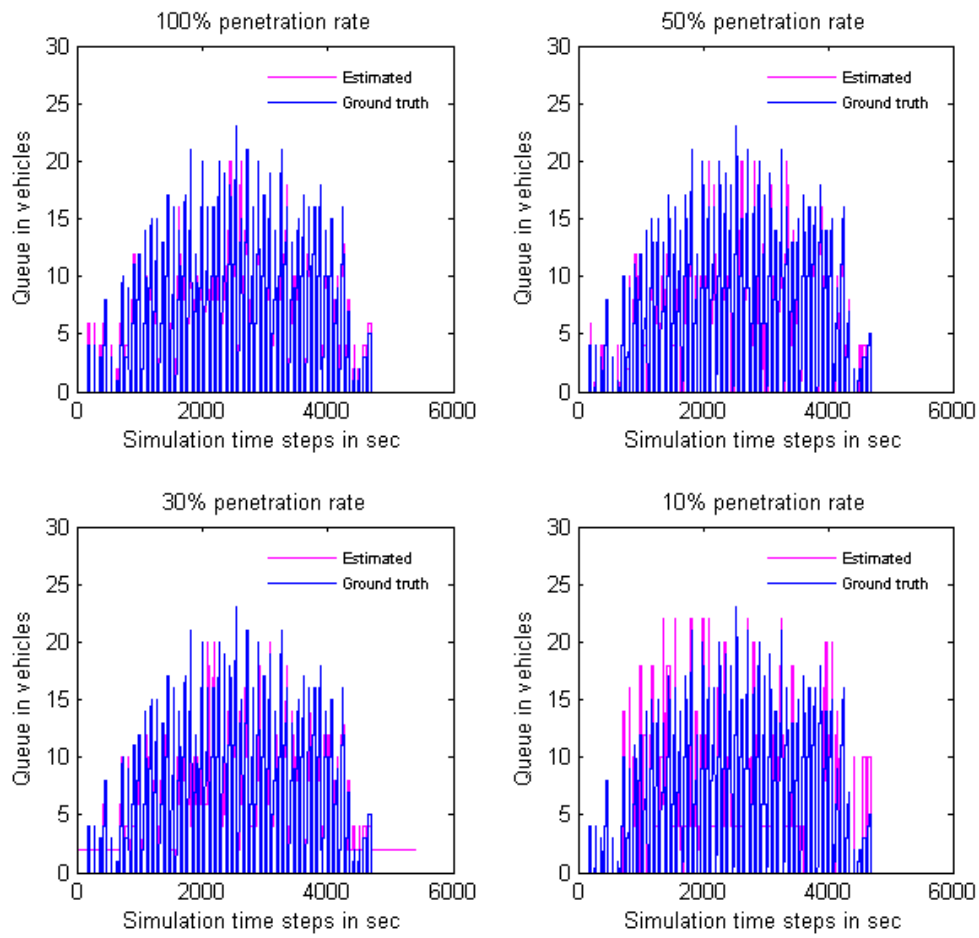


Figure A.30: Difference of queue estimation and real queue value for section L51, for different penetration rates

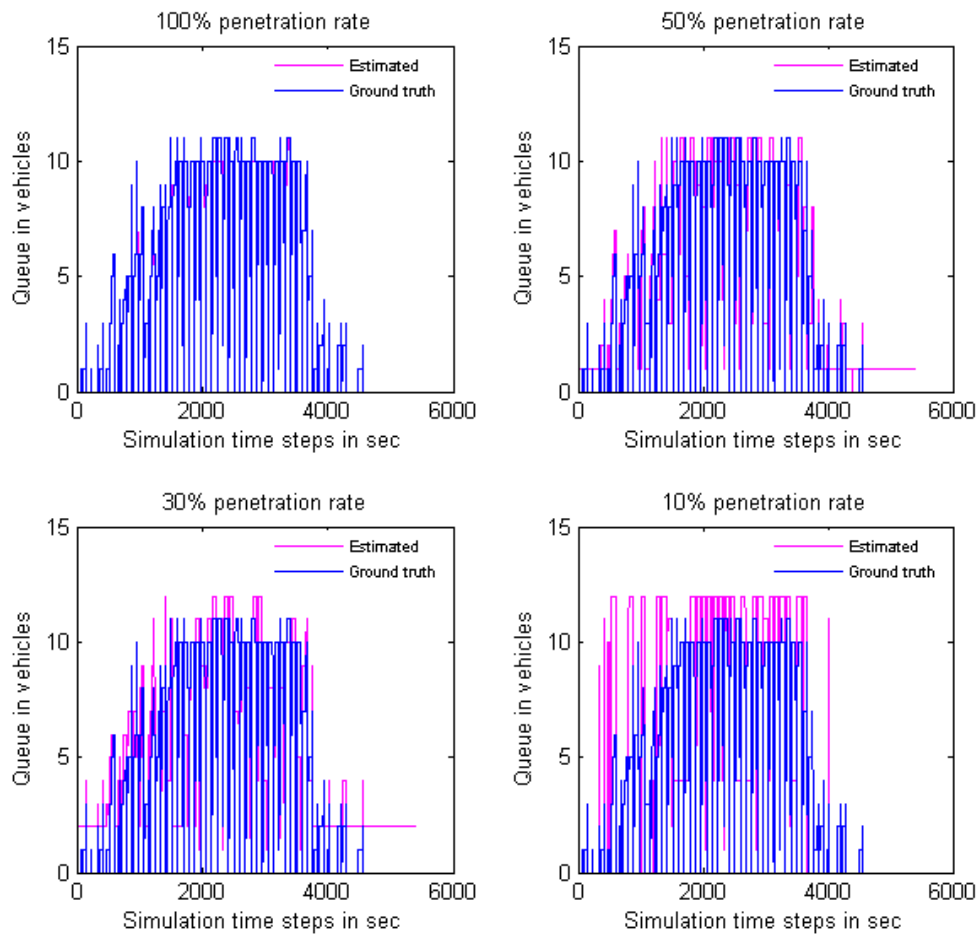


Figure A.31: Difference of queue estimation and real queue value for section L53, for different penetration rates

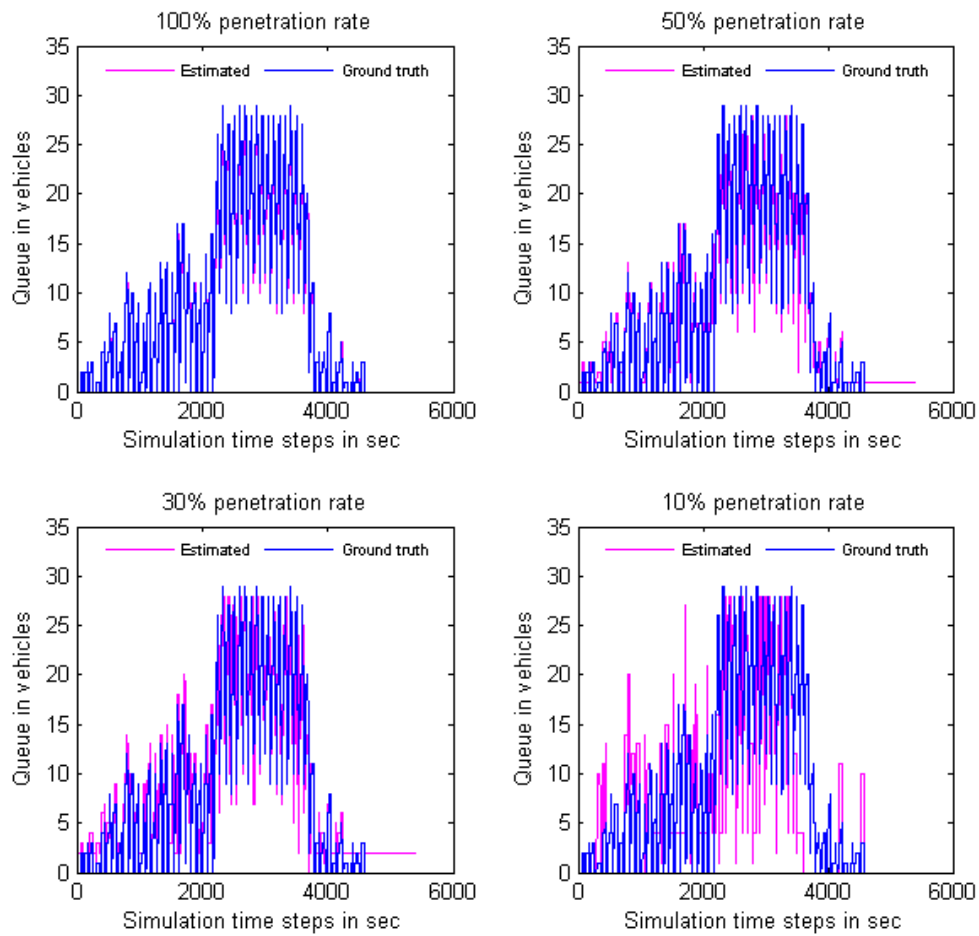


Figure A.32: Difference of queue estimation and real queue value for section L57, for different penetration rates

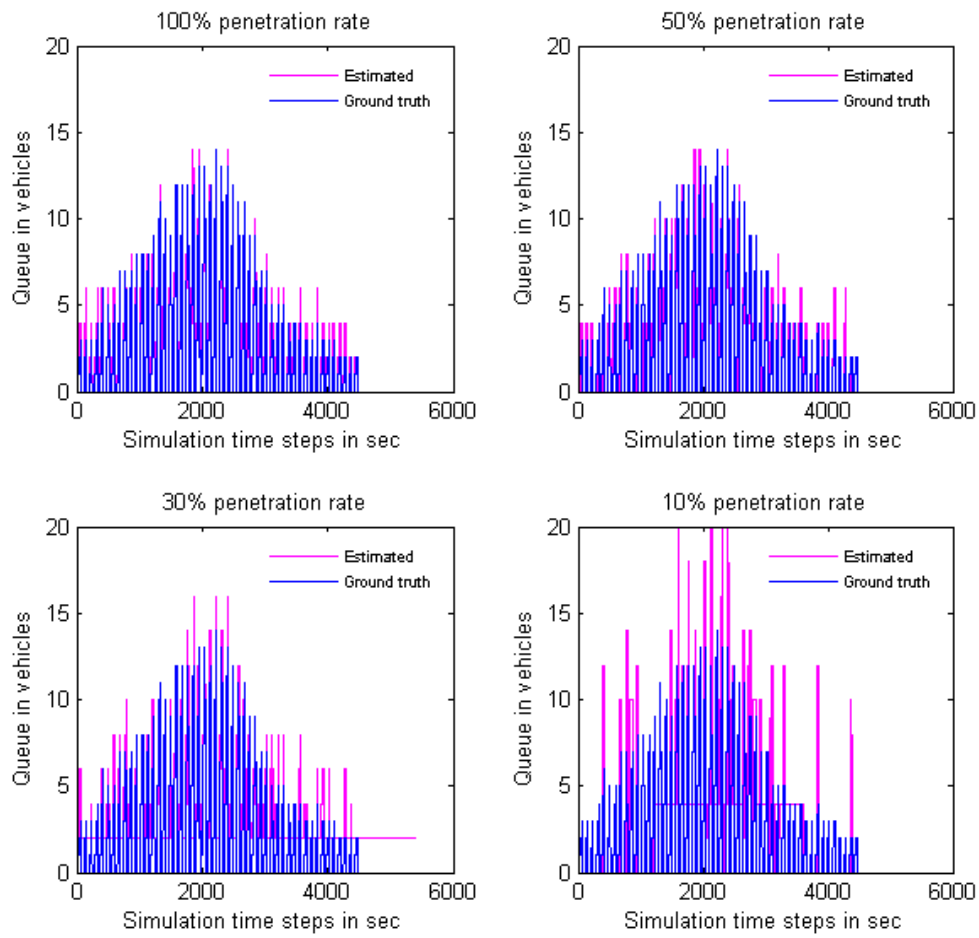


Figure A.33: Difference of queue estimation and real queue value for section O16, for different penetration rates

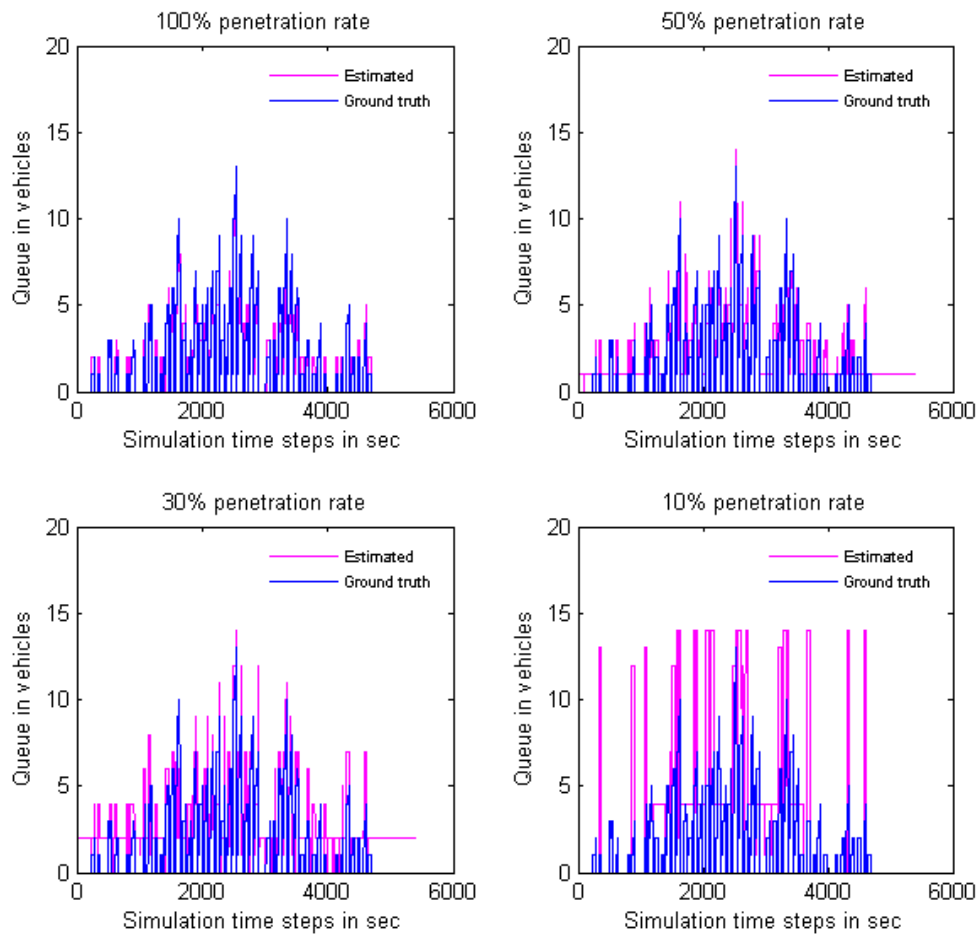


Figure A.34: Difference of queue estimation and real queue value for section L54, for different penetration rates

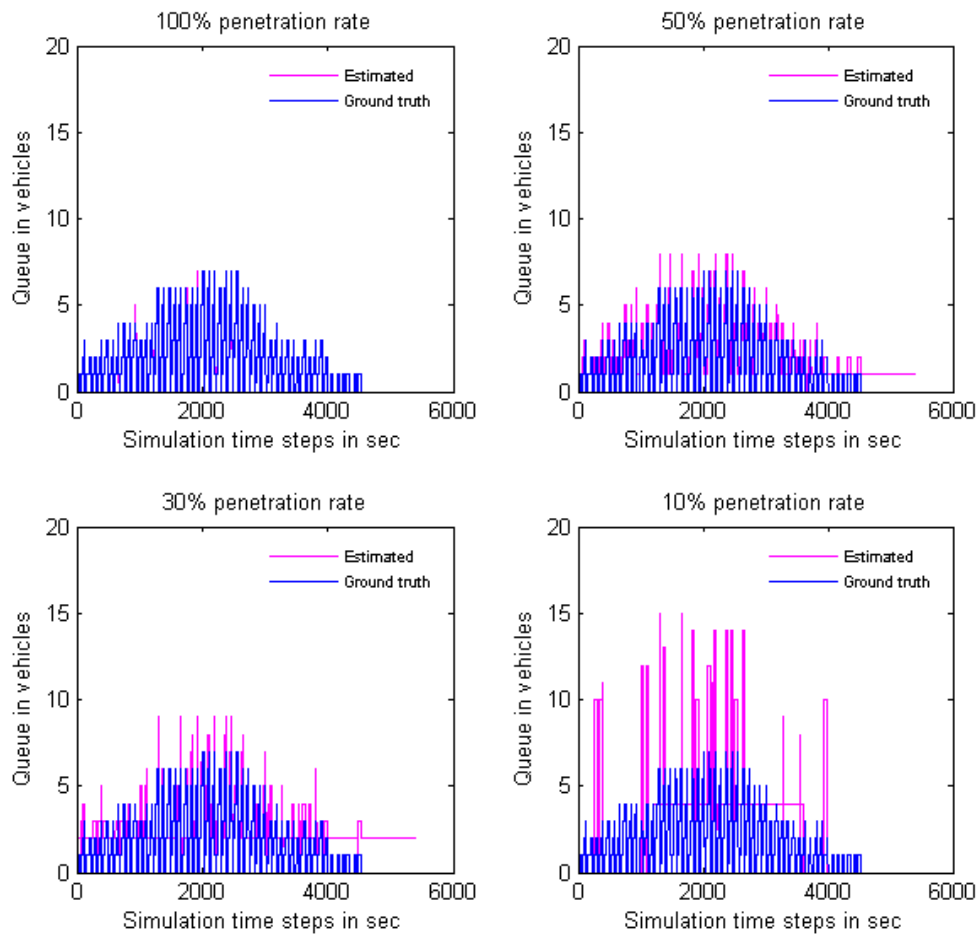


Figure A.35: Difference of queue estimation and real queue value for section O15, for different penetration rates

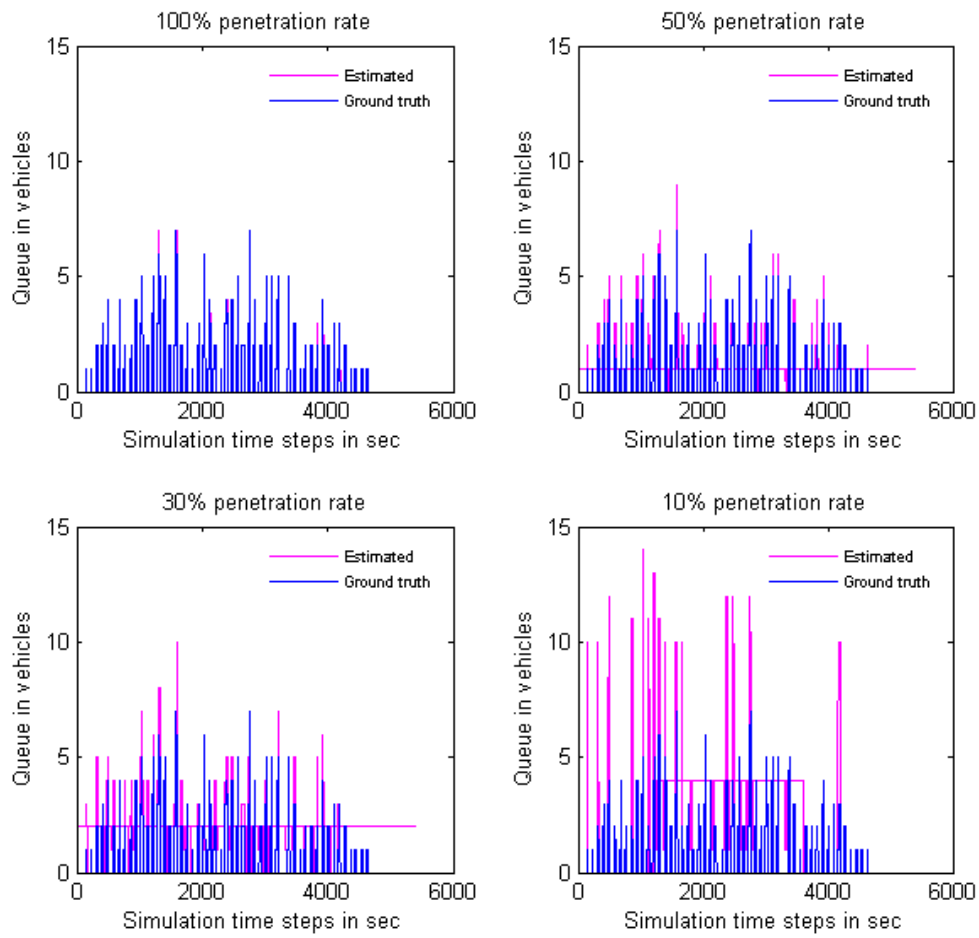


Figure A.36: Difference of queue estimation and real queue value for section L36, for different penetration rates

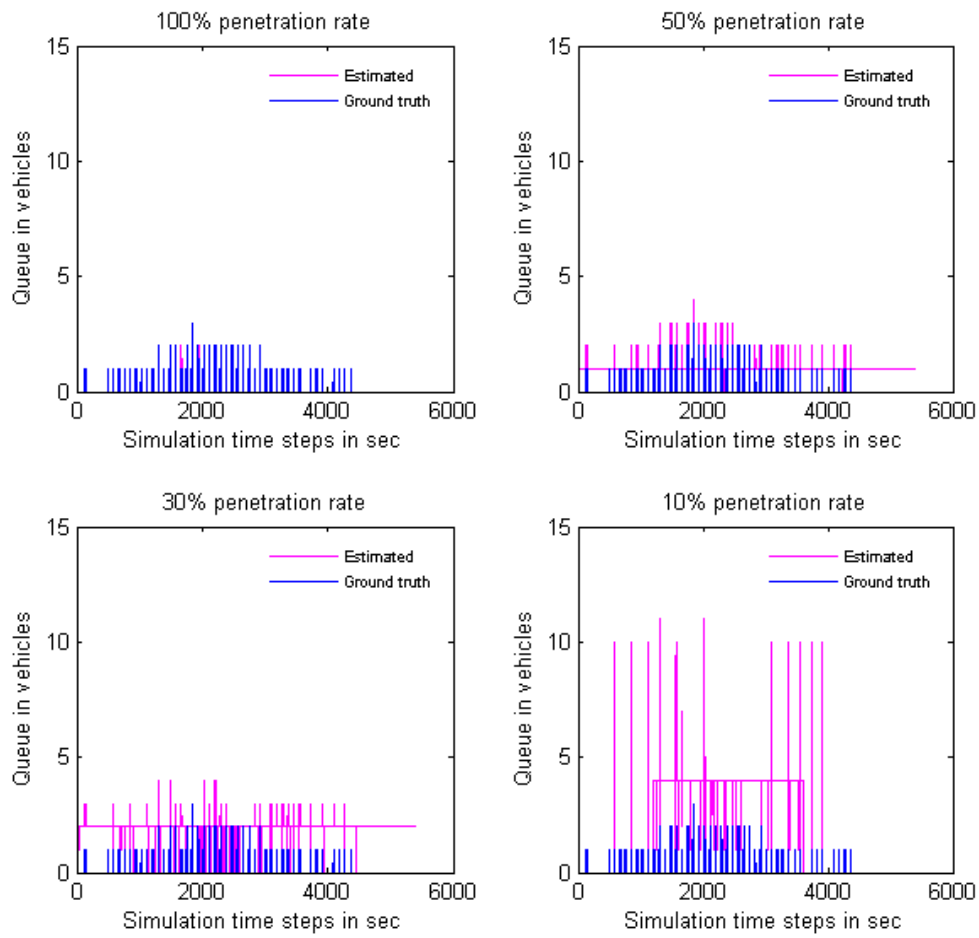


Figure A.37: Difference of queue estimation and real queue value for section O14, for different penetration rates

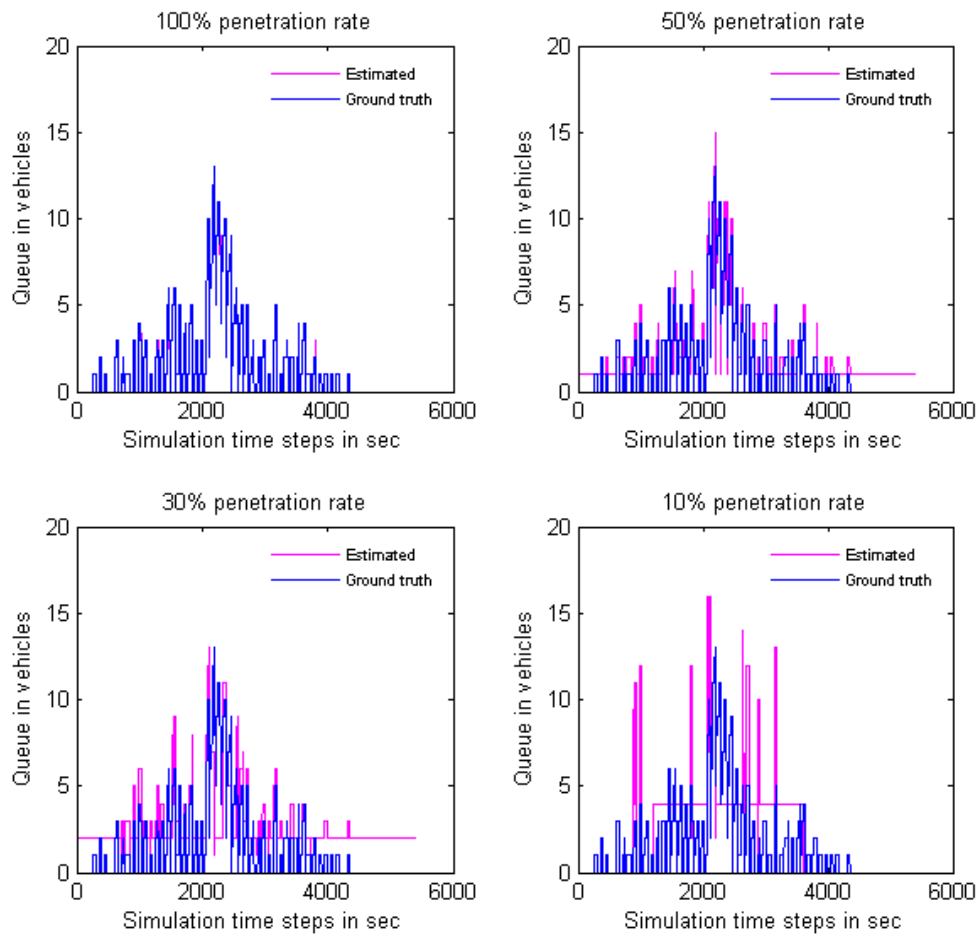


Figure A.38: Difference of queue estimation and real queue value for section O24, for different penetration rates

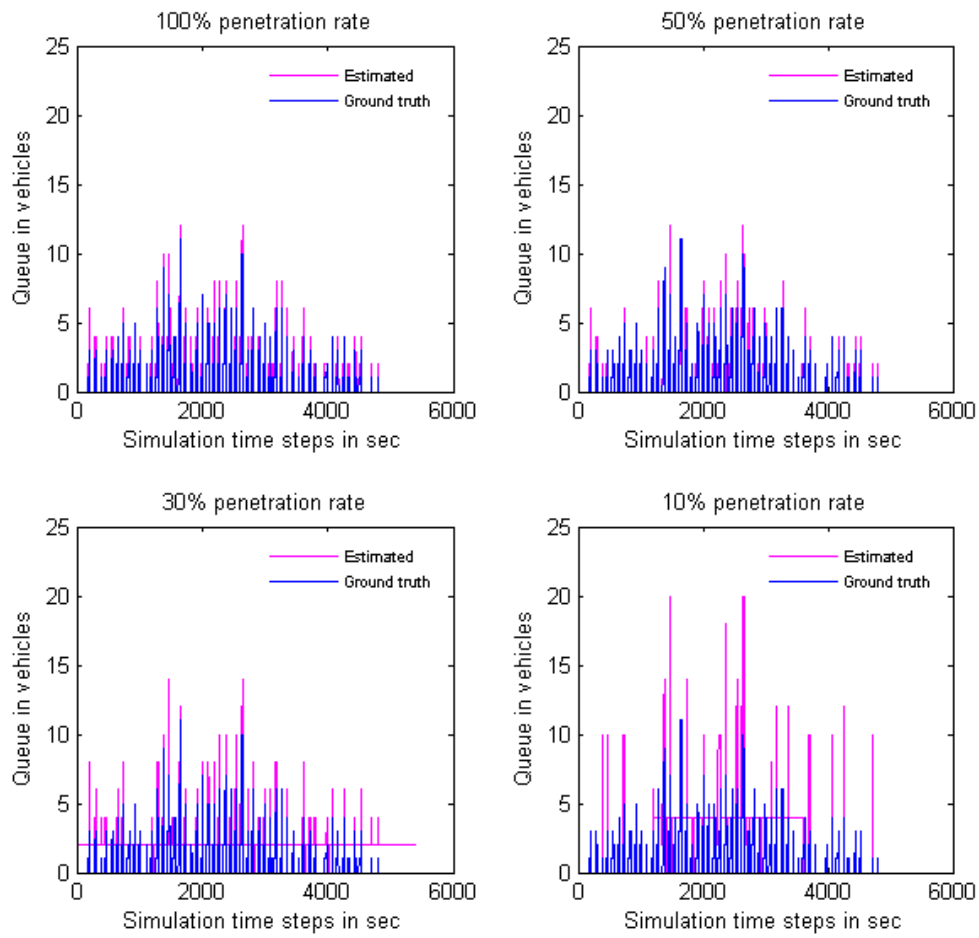


Figure A.39: Difference of queue estimation and real queue value for section L49, for different penetration rates

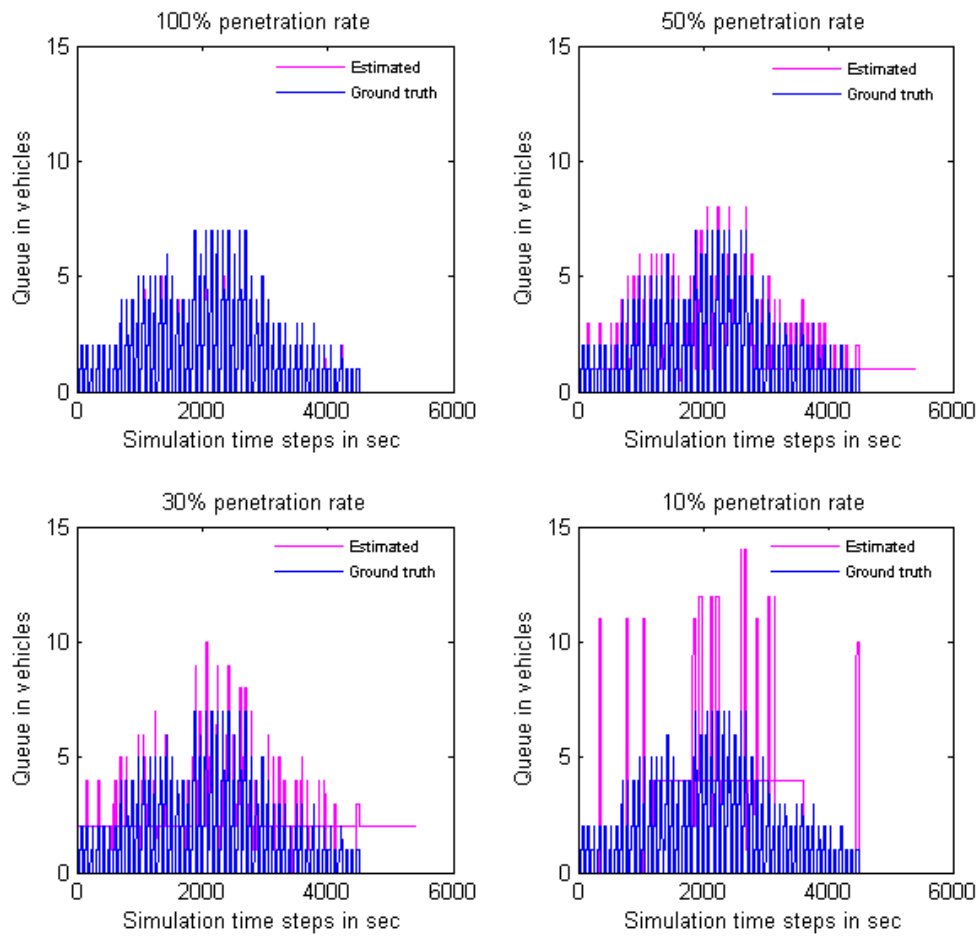


Figure A.40: Difference of queue estimation and real queue value for section O25, for different penetration rates

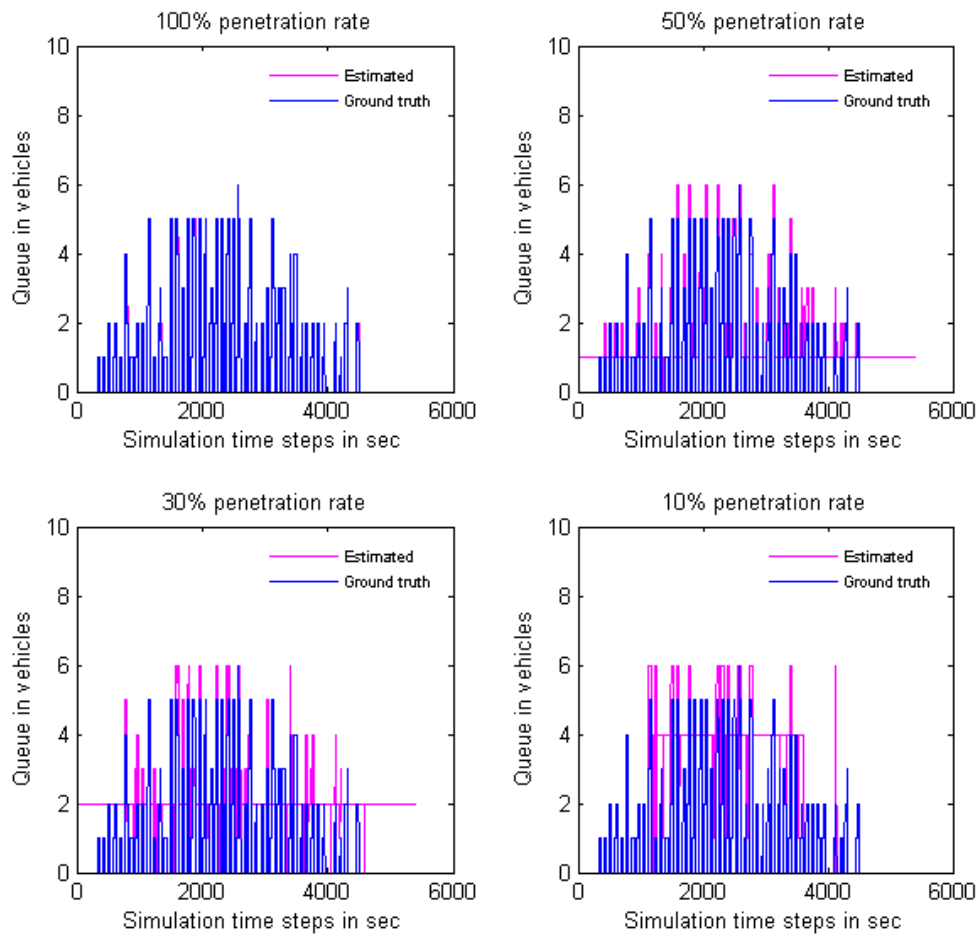


Figure A.41: Difference of queue estimation and real queue value for section L58, for different penetration rates

# Appendix B

The t-Test is used to test the null hypothesis that the means of two populations are equal. In our case, t-test was used for TUC and Max-pressure delay results for all connected vehicles cases, assuming unequal variances for each two-sample.

To determine whether the difference is statistically significant, the t-test calculates a t-value. If  $t \text{ Stat} < -t \text{ Critical two-tail}$  or  $t \text{ Stat} > t \text{ Critical two-tail}$ , we reject the null hypothesis. In all cases of TUC strategy, we accept the null hypothesis hence there is no statistical significance in different average delay values for different penetration rates. However in all Max-pressure cases we reject the null hypothesis hence there is statistical significance in average delay values for different penetration rates.

	100%	50%
Mean	125.9460576	124.2759381
Variance	10.87413209	48.13074194
Observations	10	10
Hypothesized Mean Difference	0	
df	13	
t Stat	0.687548918	
P(T<=t) one-tail	0.251909817	
t Critical one-tail	1.770933396	
P(T<=t) two-tail	0.503819634	
t Critical two-tail	2.160368656	

Table B.1: t-Test for 100% penetration rate and 50% penetration rate TUC delay results

t-Test for Max-pressure algorithm connected vehicles cases: Two-Sample Assuming Unequal Variances

	100%	30%
Mean	125.9460576	122.6429432
Variance	10.87413209	37.04682817
Observations	10	10
Hypothesized Mean Difference	0	
df	14	
t Stat	1.508901392	
P(T<=t) one-tail	0.076778949	
t Critical one-tail	1.761310136	
P(T<=t) two-tail	0.153557898	
t Critical two-tail	2.144786688	

Table B.2: t-Test for 100% penetration rate and 30% penetration rate TUC delay results

	100%	10%
Mean	125.9460576	122.6429432
Variance	10.87413209	37.04682817
Observations	10	10
Hypothesized Mean Difference	0	
df	14	
t Stat	1.508901392	
P(T<=t) one-tail	0.076778949	
t Critical one-tail	1.761310136	
P(T<=t) two-tail	0.153557898	
t Critical two-tail	2.144786688	

Table B.3: t-Test for 100% penetration rate and 10% penetration rate TUC delay results

	50%	30%
Mean	124.2759381	122.6429432
Variance	48.13074194	37.04682817
Observations	10	10
Hypothesized Mean Difference	0	
df	18	
t Stat	0.55952849	
P(T<=t) one-tail	0.291348645	
t Critical one-tail	1.734063607	
P(T<=t) two-tail	0.582697291	
t Critical two-tail	2.10092204	

Table B.4: t-Test for 50% penetration rate and 30% penetration rate TUC delay results

	30%	10%
Mean	122.6429432	126.809458
Variance	37.04682817	57.57429454
Observations	10	10
Hypothesized Mean Difference	0	
df	17	
t Stat	-1.354499598	
P(T<=t) one-tail	0.09665367	
t Critical one-tail	1.739606726	
P(T<=t) two-tail	0.193307341	
t Critical two-tail	2.109815578	

Table B.5: t-Test for 30% penetration rate and 10% penetration rate TUC delay results

	100%	50%
Mean	106.9372533	115.1901893
Variance	36.04583141	36.67937381
Observations	10	10
Hypothesized Mean Difference	0	
df	18	
t Stat	-3.060314074	
P(T<=t) one-tail	0.003369535	
t Critical one-tail	1.734063607	
P(T<=t) two-tail	0.00673907	
t Critical two-tail	2.10092204	

Table B.6: t-Test for 100% penetration rate and 50% penetration rate Max-pressure delay results

	100%	30%
Mean	106.9372533	129.10349
Variance	36.04583141	106.4732118
Observations	10	10
Hypothesized Mean Difference	0	
df	14	
t Stat	-5.871587233	
P(T<=t) one-tail	2.03176E-05	
t Critical one-tail	1.761310136	
P(T<=t) two-tail	4.06352E-05	
t Critical two-tail	2.144786688	

Table B.7: t-Test for 100% penetration rate and 30% penetration rate Max-pressure delay results

	100%	10%
Mean	106.9372533	180.9145764
Variance	36.04583141	444.4614263
Observations	10	10
Hypothesized Mean Difference	0	
df	10	
t Stat	-10.67206929	
P(T<=t) one-tail	4.36496E-07	
t Critical one-tail	1.812461123	
P(T<=t) two-tail	8.72991E-07	
t Critical two-tail	2.228138852	

Table B.8: t-Test for 100% penetration rate and 10% penetration rate Max-pressure delay results

	50%	30%
Mean	115.1901893	129.10349
Variance	36.67937381	106.4732118
Observations	10	10
Hypothesized Mean Difference	0	
df	15	
t Stat	-3.677312797	
P(T<=t) one-tail	0.001120424	
t Critical one-tail	1.753050356	
P(T<=t) two-tail	0.002240849	
t Critical two-tail	2.131449546	

Table B.9: t-Test for 50% penetration rate and 30% penetration rate Max-pressure delay results

	50%	10%
Mean	115.1901893	180.9145764
Variance	36.67937381	444.4614263
Observations	10	10
Hypothesized Mean Difference	0	
df	10	
t Stat	-9.475245077	
P(T<=t) one-tail	1.29964E-06	
t Critical one-tail	1.812461123	
P(T<=t) two-tail	2.59928E-06	
t Critical two-tail	2.228138852	

Table B.10: t-Test for 50% penetration rate and 10% penetration rate Max-pressure delay results

	30%	10%
Mean	129.10349	180.9145764
Variance	106.4732118	444.4614263
Observations	10	10
Hypothesized Mean Difference	0	
df	13	
t Stat	-6.980277043	
P(T<=t) one-tail	4.81028E-06	
t Critical one-tail	1.770933396	
P(T<=t) two-tail	9.62055E-06	
t Critical two-tail	2.160368656	

Table B.11: t-Test for 30% penetration rate and 10% penetration rate Max-pressure delay results